APPLIED COMPUTATIONAL ELECTROMAGNETICS SOCIETY (ACES)

NEWSLETTER

Vol. 12 No. 2 July 1997

TABLE OF CONTENTS

ACES NEWSLETTER STAFF

EDITORS

ACES JOURNAL

NEWSLETTER ARTICLES AND VOLUNTEERS WELCOME

The ACES Newsletter is always looking for articles, letters, and short communications of interest to ACES members. All individuals are encouraged to write, suggest, or solicit articles either on a one-time or continuing basis. Please contact a Newsletter Editor.

AUTHORSHIP AND BERNE COPYRIGHT CONVENTION

The opinions, statements and facts contained in this Newsletter are solely the opinions of the authors and/or sources identified with each article. Articles with no author can be attributed to the editors or to the committee head in the case of committee reports. The United States recently became part of the Berne Copyright Convention. Under the Berne Convention, the copyright for an article in this newsletter is legally held by the author(s) of the article since no explicit copyright notice appears in the newsletter.

NEEDED: ADVERTISING AND REPORTS EDITOR

If interested, please contact :

Ray Perez
Martin Marietta Astronautics
MS 58700, PO Box 179
Denver, CO 80201
Phone: 303-977-5845
Fax: 303-971-4306
email:ray.j.perez@ast.lmco.com

Visit us on line at: www.emclab.umr.edu/aces

OFFICER'S REPORTS

SECRETARY'S REPORT

ACES BOARD OF DIRECTORS MEETING

1. The ACES Board of Directors met on Tuesday, 18 March 1997, in the Terrace Room of Herrmann Hall at the Naval Postgraduate School, Monterey, CA. ACES President Hal Sabbagh called the meeting to order at 11:45 AM.

2. Present were Directors Hal Sabbagh (HS), Pat Foster (PF), John Brauer (JB), Todd Hubing (TH), and Perry Wheless (PW), ACES Executive Officer Richard W. Adler (RWA), and others, including Andy Drozd, Keith Whites, Atef Elsherbeni, Eric Michielssen, Jianming Jin, Randy Haupt, Don Pflug, and Bob Bevensee.

3. Director Proxies: Andy Peterson (AP) to PW, Duncan Baker (DB) to PF, and Adalbert Konrad (AK) to JB)

4. Motion to approve the minutes of the last BoD meeting, as distributed earlier by ACES Secretary PW, by JB, second by PF. Motion passed.

5. Results of the BoD election were announced by HS, in accord with the e-mail report filed by Elections Committee Chair Ping Werner. Andreas Cangellaris, Ray Perez, and Noria Takahashi were elected to three-year terms March 1997 - March 2000.

6. Andy Peterson distributed a financial report by mail earlier. TH and RWA presented reports. ACES reserves decreased during the past year, due to reduced net conference income from 1996 and an artifact in membership renewals. RWA pointed out that ACES received a $10k grant/donation in connection with the1995 conference which it did not receive in 1996, and that partly accounts for the differences between the two years.

7. Eric Michielssen reported approximately 255 papers were accepted for the ACES '97 conference, and about 220 final papers are in the Proceedings.

8. RWA reported that ACES should only count on having three session rooms available for 1998, and so it is important that no more than three parallel sessions should be scheduled at any time for next year's conference.

9. Bob Bevensee reported that there are three papers in the new student paper competition initiated with ACES '97. Judging arrangements have been completed, and the winner will receive a cash prize as previously agreed. Bob announced that the present Conference Committee members are Jim Breakall, PF, PW, RWA, Bob Bevensee, Eric Michielssen, Jianming Jin, and Keith Whites. This committee composition is subject to revision. Don Pflug was added to the conference committee member list, for a total of nine members.

10. PW on behalf of AK: Is there any possibility that the ACES conference might be held in June after the end of the spring academic term? HS: This question is remanded to the Conference Committee for consideration.

11. PW of behalf of Rudy Anders: The BoD should be advised that I am not attending ACES '97 because of the format of the conference. ACES should consider how many long-time members are not attending because they strongly object to the multiple parallel sessions, spread out location of events, and the trend toward IEEE-like papers. HS: Rudys comments are well taken, but the BoD is not the appropriate forum for these considerations. This matter is also remanded to the Conference Committee.

12. RWA discussed, on behalf of Jim Breakall, the proposed ACES fall workshop at Penn State University. The main point was that PSU will guarantee that ACES will not lose money; they will cancel the workshop if advance registrations are insufficient to ensure the income will exceed expenses.

Motion by JB: Moved that ACES will sponsor a workshop/short course format meeting at Penn State University, 21 September 1997 - 24 September 1997, provided that the terms and conditions with Penn State preclude any possible financial loss to ACES. Seconded by PF. Motion passed.

13. HS charged the Conference Committee to conduct a thorough review of annual conference structure and activities, and adopt policies, as necessary, that will ensure smooth and successful conferences into the future. This charge includes work with RWA and PSU regarding details of the September workshop at Penn State.

14. PW: Many members of the ACES Journal Editorial board have previously been non-members of ACES. We have been working to improve that situation, and now only about eight editors are non-members. ACES Publications would like to give non-member editors an incentive to join. Therefore, it is moved that non-member editors may join ACES for the regular dues. The special rate will only apply once, to their first year of ACES membership. Second: PF. Motion passed.

15. RWA discussed inactive committees. Three committees, in particular, were discussed. These are all Membership Activity Committees, so they can be activated by the President and/or Executive Committee at any time. The Code User Group has been inactive for several years. It was decided, that this Code User Group, should be deactivated at this time. Don Pflug discussed the Software Performance Standards Committee; this committee has some ongoing activity, and Don recommend that we should defer action on this committee until 1998. The following note has been appended: Bob Bevensee, ACES Historian, mentioned his intention to write the next ACES history update based primarily on information in the Newsletters.

Finally, Atef Elsherbeni discussed the Software Exchange Committee; the decision was to similarly review the status of this committee at ACES'98. Atef suggested that ACES Publications could start appealing to authors to submit software with their papers to reinvigorate interest in software exchange.

16. Further, Atef Elsherbeni reported that progress on the Software Sourcebook has ground to a standstill. Completion of the project is in doubt, but still possible.

17. PF gave an ACES U.K. report. ACES U.K. is financially sound, their technical paper meeting was a success, and other activities such as an Adler/Breakall NEC course in April are planned.

18. TH reported on the ACES Web site. Institutional links are now allowed, but there are none yet. ACES '98 should utilize the Web Site to distribute conference information and registration forms, the agenda, hotel details, etc. It was recommended that the Newsletter should conspicuously note the Website in future issues.

19. AK submitted a Nominations Committee report by email, basically indicating that he is operating basically as a committee of one. HS expressed appreciated for AK's good works in securing an outstanding slate of candidates for this years BoD election.

20. PW made a report on the status of ACES Publications. The ACES Journal editorial board has just been reviewed and renewed. Planning has started for anticipated turnover in 1998 in the Editor-in-Chief and Associate positions, both Journal and Newsletter. Study of new electronic methods is now underway. RWA added that color printing is now a loose cannon issue, and that ACES Publications need to come up with a policy. The present printer has learned how to apply his digital machines successfully to grey scale reproduction.

21. JB gave an Awards Committee Report. Recipients of awards at ACES '97 include Richard Gordon, Keith Whites, and J.P.A. Bastos in addition to the Journal 1996 Best Paper and Student Best Paper awards. Perhaps we should give a few more awards in 1998.

22. RWA reported the need for a new photocopy machine. JB: Moved that ACES purchase a new photocopy machine for use by the ACES Executive Officer in the performance of his duties. Second by PF. Motion passed.

The meeting was adjourned at 1:08 PM.

SUPPLEMENTAL MINUTES
ACES EXECUTIVE COMMITTEE ACTION
19 MARCH 1997

ACES Executive Committee members HS. PF, RWA and PW met at 11:45 AM on Wednesday, 19 March 1997, in the conference registration area in Glasgow Hall at NPS, to act on a problem with conference vendors which arose the previous afternoon. RWA summarized the problem:

Eight (8) vendors are upset because they have a contract which states that they will have ACES97 attendees available for visiting their displays from 1300-1800 on Tuesday, 18 March 1997, WITH NO CONFLICTING ACES ACTIVITIES. In reality, they did not visitors until 1520, missing approximately 2 hours, 20 minutes of activity.

The conflict occurred because additional conference papers were added into the Tuesday afternoon time slot AFTER the vendors had signed up. The problem continued because the Wine and Cheese Social began shortly after 1520 and many people then migrated away from the vendor area and posters. On recommendation of RWA, the Executive Committee voted unanimously to refund 60% of the fee paid by these vendors because of the problems.

Additional note: RWA noted that the Conference Committee may have to exercise more rigid controls over the scheduling for ACES98, starting with an imposed cap on the number of sessions and/or papers, so that this does not recur.

Submitted by
W. Perry Wheless, Jr.
ACES Secretary

PERMANENT STANDING COMMITTEES OF ACES INC.

COMMITTEE	CHAIRMAN	ADDRESS
NOMINATIONS	Adalbert Konrad	University of Toronto ECE Department 10 King's College Road Toronto, ON, CANADA M5S 1A4
ELECTIONS	Pingjuan Werner	Penn State University 321 Oakley Drive State College, PA 16803
FINANCE	Andrew Peterson	Georgia Institute of Technology School of ECE Atlanta, GA 30332-0250
WAYS & MEANS	Pat Foster	Microwaves & Antenna System 16 Peachfield Road Great Malvern, Worc, UK WR14 4AP
PUBLICATIONS	Perry Wheless	University of Alabama P.O. Box 11134 Tuscaloosa, AL 35486-3008
CONFERENCE	Robert Bevensee	BOMA Enterprises PO Box 812 Alamo, CA 94507-0812
AWARDS	John Brauer	Ansoft Corporation 4300 W. Brown Deer Rd., Suite 300 Milwaukee, WI 53223-2465

MEMBERSHIP ACTIVITY COMMITTEES OF ACES INC.

COMMITTEE	CHAIRMAN	ADDRESS
SOFTWARE EXCHANGE	Atef Elsherbeni	Univ of Mississippi Anderson Hall, Box #13 University, MS 38677
SOFTWARE PERFORMANCE STANDARDS	Donald Pflug	Rome Laboratory/ERST 525 Brooks Rd. Griffiss AFB, NY 13441-4505
HISTORICAL	Robert Bevensee	BOMA Enterprises PO Box 812 Alamo, CA 94507-0812

COMMITTEE REPORTS

ACES PUBLICATIONS

Appointments to the ACES Journal Editorial Board are usually for a term of three years. The cycle of new appointments has been essentially completed during the past ninety days. Because this cycle was initiated late, these Editor appointments were made effective through the end of March, 1999. Completion of an Editorial Board Areas-of-Interest Questionnaire was required by June 1 as an indication of appointment acceptance. As of this writing (26 May 1997), the following appointments have been confirmed: Dick Adler, Rudy Anders, Brian Austin, Duncan Baker, Joao Bastos, John Beggs, Bob Bevensee, John Brauer, Pat Foster, Allen Glisson, Christian Hafner, Kueichien C. Hill, Nathan Ida, Ahmed Kishk, Adalbert Konrad, Ron Marhefka, Gerard Meunier, Ed Miller, Giorgio Molinari, Gerrit Mur, Giuseppe Pelosi, Andy Peterson, Kurt Richter, Harold Sabbagh, Norio Takahashi, Perry Wheless, Keith Whites, and Wes Williams. Three additional appointments are in process.

There is no magic, or fixed, number of Editorial Board members. At this time, we could consider the addition of a few more Editors. If you would like to nominate a colleague or yourself for service to ACES in this capacity, please contact me at your earliest convenience. If you already received an appointment invitation letter, but your name is not on the list above, you either have not returned your Questionnaire or I did not receive it; in either event, you also need to contact me as soon as possible.

Also, planning is underway toward orderly changes in 1998 in the positions of ACES Publications Chair and Editor-in-Chief, ACES Journal Editor-in-Chief and Associate Editor-in-Chief, and ACES Newsletter Editor-in-Chief and Associate Editor-in-Chief. New appointments for these positions may be expected at the 1998 conference in Monterey. Comments from the membership in this matter are invited and welcome.

Major issues before ACES Publications now include (a) attraction of high-quality papers for the ACES Journal in greater quantity, (b) initiation of new Special Issue projects, (c) planning for an eventual transition to electronic publishing, and (d) the best means for accommodation of color figures for both the Journal and Newsletter. If you have special interest or expertise in any of these areas, we will find a way to involve you productively in the deliberations.

ACES Journal Special Issues have been very successful in recent years, and we should keep our innovation and energy level high in that area. We need ideas and Guest Editors for 1998 and 1999 Special Issues now! Let us hear from you if you wish to contribute a topic concept or volunteer as an Editor.

Submitted by
Perry Wheless
ACES Publications Chairman

ACTIVITIES RELATED TO CEM IN FRANCE

Professor Michel M. Ney*

Various national symposia on topics related to CEM are organized every year or two years in France. The most popular is the National Microwave Conference (JNM) that takes place every two years and each time in a different city in France. It is generally the opportunity for graduate students to have their first experience in attending a relatively large conference and presenting a paper. It gathers approximately 800 people and includes an industrial exposition. Many sessions are devoted to topics closely related to CEM. Exclusively in French language, the JNM is a typical illustration of research activities related to microwaves and millimeter-wave circuits, antenna and numerical modeling in France. This year, the JNM will take place in the charming town of Saint Malo in May, near Mount Saint-Michel. The 2d European Conference on Numerical Methods in Electromagnetics (NUMELEC'97) will be organized in Lyon next September. This meeting involves about 100 papers on topics closely related to CEM. It emphasizes on the development of new numerical procedures or formulations applied to field computation. Although the conference is organized in French, papers can be presented either in French or English. Finally, another bilingual meeting (Hertzian Optics and Dielectrics) will be held in Clermond-Ferrand at the Blaise Pascal's university next September Many topics will be related to computational electromagnetics [1].

Last year was also very busy in France for meetings related to CEM topics. The International Conference on Antenna (JINA) organized every two years took place in Nice last November. Two months before, the URSI XXVth General Assembly was held in Lille. Near to 200 papers were presented in Commission B Fields and Waves, among which 28 by various French laboratories. Organized jointly with URSI, the 8th Colloquium on Electromagnetic Compatibility attracted about 400 people and 45 industrial exhibitors. One could notice a growing importance (6 sessions over 20) with topics related to field numerical modeling. Held every two years and organized in French, more than 90 percents of the speakers were from France. Others were coming from Switzerland, Belgium, Italy, Canada and North African countries. It will be organized again in the city of Brest in 1998.

Finally, PIERS 1998 will be held in France (in the city of Nantes) for the first time. There will be one full session devoted to computer techniques for field computations. The above involvement of research centers in organizing major national and international meetings shows their true commitment to develop activities related to CEM in France.

RESEARCH ACTIVITIES RELATED TO CEM

Research in Computational Electromagnetics, is active in France. It is carried out in many research labs either in Graduate Engineering Schools [2] or labs related to universities, industries and national research centers. Generally, laboratories have established their expertise in a specific domain related to CEM. It would be a too exhaustive job to list all laboratories that carry out research related to CEM and that really contribute to maintain this activity in France at a dynamic level. One can, however, mention the major research centers and laboratories that have established an international recognition in the area of electromagnetic field modeling. Most of them belong to the CNRS [3].

In the area of time-domain methods, some intensive research is being carried out on the development of the Finite-Difference Time-Domain (FDTD) method at the Research Institute on Microwave and Optical Communications (IRCOM) of the University of Limoges. The research team is developing New procedures to extend the FDTD to a wider range of applications. This includes, modeling of dispersive media, non-linear media and coupling with geometrical optics. Commercially available software for planar antenna and a version dedicated to educational purposes were also developed [4]. The CNET [5] near Paris also does some active research on FDTD with applications to planar microwave and millimeter-wave circuits [6].

Continuing with time-domain methods, the Transmission-Line Matrix (TLM) method is subject to some intensive research and development in three laboratories in France. At the Graduate Engineering School of Grenobles, the laboratory for Microwaves and Optronics (LEMO) was the first to develop a new condensed TLM node. The first variable mesh technique was also originally

proposed by researchers at the LEMO. They are currently developing software for applications in Electromagnetic Compatibility (EMC) and are working on the development of new cells to account for anisotropic dispersive media [7]. At the University of Nice Sophia-Antipolis, the laboratory of microwave and optical communications does also research on TLM with emphases on implementing the algorithm on parallel processors and developing prediction procedures in order to limit the number of time iterations. Major applications are in the characterization of antenna in planar technology [8].

Finally, active research on TLM is carried out at the Laboratory for Electronics and Communication Systems (LEST) at the Graduate Engineering School in Telecommunications of Brittany (ENST-Br). New TLM cells are developed to decrease the number of operations per iteration and some substantial contributions have been produced on the development of super absorbing conditions for field computation in open structures. Also, new TLM schemes are being developed for structures of revolution and new algorithms for interface with lumped elements are being investigated. Applications are in antenna and characterization of planar millimeter-circuits as the center is well recognized in the development of new technologies for the fabrication of miniaturized components [9].

Regarding frequency domain techniques, another research group at the IRCOM has had significant contributions in the development of numerical schemes for the Finite-Element Method (FEM). Applications are mainly on three-dimensional filter structures and planar circuit characterization. They are doing research on hybrid procedures using modal decomposition for the characterization of discontinuities and on interfacing discrete components (active or passive) with the FEM algorithm [10].

Major activities are carried out on integral equation techniques. A pioneer work was done in France on the surface element technique. Based on the work by Ndelec [11], a surface integral formulation is solved by the Moment Method (MoM). A commercially available program is being developed at the CNET La Turbie. This research center, which is located in a magnificent site overhanging Monaco, possesses one of the most modern and convenient measurement facilities for antenna testing and characterisation. The software developed there is mostly applied to antenna problems, although it can be used for arbitrary geometry [12]. Another version treats structures with symmetry of revolution. Other software based on the same approach were also developed at Thomson CSF [13] for antenna design and at Aerospatiale [14] for EMC applications. Integral equation solved with MoM is also an area of interest in the research carried out in Rennes (Brittany), where a commercial software for planar structures was developed. This center, that includes the INSA (National Institute of Applied Sciences) and the University of Rennes, carries out some intensive research on planar antenna, including active antenna with applications to microwave and millimeter-wave systems [15]. Other CEM activities are present in the domain of imaging. Some pioneer work was done at the Microwave Laboratory of the National Superior Engineering School of Electricity (SUPELEC) on developing algorithms for microwave tomography applications. Near-field measurement techniques were also developed with current applications in antenna characterization [16].

Finally, research units in major CNRS or university laboratories are also contributing to some research in computational electromagnetics. This is the case at the North Institute for electronics and microelectronics (IEMN) at Lille. The Semiconductor and Microwave Department develops numerical tools for field computation in planar lines taking into account various aspects such as metallic losses and nonlinear loading [17]. At the Graduate National Engineering School of Toulouse (ENSEEIHT), the research group in Microwaves does some research on numerical procedures applied to field computation such as MoM applied to integral equation formulation, spectral domain and transverse resonance techniques [18].

CONCLUSION

The above brief survey on the research activities related to CEM illustrates the vitality of French laboratories in this discipline. Like probably in other countries, there is some great financial pressure on granting agencies that has resulted in budget cuts. This has contributed to intensify cooperative research with the industry. However, it is the feeling of the majority of the research labs that effort

must be devoted to maintain activities on fundamental and long-term research which is the only way to remain at the leading edge. As a result, some true effort to develop synergy between labs has been observed. This is concretized by joint research program and Ph.D supervision, and exchange of graduate students

[1] For inquiries contact <OHD@lasmea.univ-bpclermont.fr>
[2] Three-year program engineering schools. Before entering the so-called Grandes Ecoles" students must take intensive full-time maths and physics courses at dedicated colleges for a two-year period. They prepare students for a national entrance examination to the graduate engineering schools. These engineering schools are generally separated from the French National Education System.
[3] National Scientific Research Center. Laboratories can become a member of the CNRS when they are recognized by a scientific committee as having research activities of national importance.
[4] Contact: Prof. Jecko <jecko@unilim.fr>
[5] National Center for Research in Communications that belongs to a network of laboratories owned by France Telecom (the French, recently privatized, telephone company).
[6] Contact: Dr. Fouad-Hanna. Fax: +33 1.45.29.45 34
[7] Contact: Prof. Saguet <saguet@enserg.fr>
[8] Contact: Prof. Pompei <pompei@mimosa.unice.fr>
[9] Contact: Prof. Ney <michel.ney@enst-bretagne.fr>
[10] Contact: Prof. Guillon <dir@ircom.unilim.fr>
[11] J. N. Ndelec, "Mixed finite elements in R3", Numeric. Math., vol. 35, pp. 315-341, 1980.
[12] Contact: Dr. Dedeban. Fax: +33 4.93.41.02.29
[13] Contact: Mrs. Perpere. Fax: +33 1 34 59 62 90
[14] Contact: M. Lonard <as-soft@espace.aerospatiale.fr>
[15] Contact: Prof. Citerne <citerne@insa.fr>
[16] Contact: Prof. Bolomey <bolomey@supelec.fr>
[17] Contact: Prof. Kennis <Patrick.kennis@IEMN.Univ-Lille1.fr>
[18] Contact: Prof. Baudrand. Fax +33 5 6158 83 77

* Michel M. Ney, Professeur
Ecole Nationale Superieure des Telecommunications de Bretagne
Laboratoire d'Electronique et des Systemes de Telecommunications (LEST),
(UMR CNRS no. 1329)
BP 832
29285 BREST Cedex, FRANCE
Phone: +33.2.98.00.13.09/13.41
FAX: +33.2.98.00.13.43
E-mail: michel.ney@enst-bretagne.fr

MODELER'S NOTES

Gerald J. Burke

This column includes some new PC benchmark results from Larry Laitinen, updating his results from the March 1996 Newsletter [1], and a NEC-4 patch to fix a glitch that may occur in the near magnetic field over ground. This time Larry is busy with work and buying a new house, and did not have time to write much about his results, so I will present his data and include some comments and explanations from e-mail that we have been exchanging. It is immediately apparent from Larry's data that there has been a significant increase in processor speed over the boards available for testing a little over a year ago, when the fastest board tested had a clock speed of 120 MHz. A similar clock speed increase has taken place on the Macintosh side, and seems fairly substantial for this short period.

Enn Vinnal at Telstra Research Labs in Melbourne, Australia sent some interesting information on a Mac application called PowerTap that he saw in the January MacTech magazine that offers still more speed if you have access to several Macs. The advertisement says that PowerTap, from Fortner Research, "adds multiprocessing and cross-network processing speed to your applications today... [It] is a robust, easy to use software library used by Macintosh software developers to make their applications lightning fast..." He says there is a free demo at www.fortner.com/PowerTap_demo. I have not had a chance to check out this, or any of the other communication packages for running on multiple processors, but it sounds like an inexpensive way to get still faster processing speed if you have access to several PCs. I just hope it does not require rewriting code in C++.

As usual, if anyone can contribute material on modeling, NEC or otherwise, they are encouraged to submit it to our editor Ray Perez or to Gerald J. Burke, Lawrence Livermore National Lab., P.O. Box 808, L-156, Livermore, CA 94550, phone: 510-422-8414, FAX: 510-422-3013, e-mail: burke2@llnl.gov. Note the change in P.O. Box, since EE no longer has their own box.

PC benchmarks running NEC-4.1 on various Pentium motherboards, from L. H. Laitinen, W7JYJ, University of Oregon, laitinen@oregon.uoregon.edu.

Table 1 shows Larry's results for matrix-fill, -factor and total execution time running double precision NEC-4.1 on the 299-segment data set shown at the end of this section. Larry was surprised at the relatively poor performance of the HP Vectra with 200 MHz Pentium-Pro processor. He suspects that the slow fill time indicates a generally slow motherboard, while the factor time is good because the L2 cache is on the Pentium-Pro chip carrier, rather than on the motherboard as with the 586 Pentium. Matrix factoring benefits more from the cache than the less memory-intensive fill operation, and since it dominates as the number of segments is increased, the Pentium-Pro would probably win out for really large problems. Larry was impressed with the Hitachi MX-166T Notebook PC, which is almost as fast as the Gigabyte 586HX desktop.

The non-parity EDO memory used with the HP Vectra should be somewhat faster than the check-and-correct ECC memory used on all the Gigabyte boards, but Larry said that he favors the slightly slower but safer ECC memory. The issue of memory parity checking was discussed recently by W. D. Swift in the IEEE AP Magazine [2].

Table 1. Execution times in seconds for the TEST299.NEC input file run in double-precision NEC4.1 on various processors.

	CPU/Motherboard	L2 Cache	RAM	Matrix Fill	Matrix Factor	Total Exec.
1.	Pentium 200-MHz MMX Gigabyte 586HX	512KB pburst	64MB FPM	8.430	4.342	13.07
2.	Pentium-Pro 200-MHz HP Vectra XU 6/200	256KB CPU	64MB EDO	11.530	2.843	14.67
3.	Pentium 166-MHz MMX Gigabyte 586HX	512KB pburst	64MB FPM	9.738	5.087	15.22
4.	Pentium 166-MHz MMX Hitachi MX-166T Notebook	256KB pburst	80MB EDO	9.729	5.242	15.37
5.	Pentium 166-MHz Gigabyte 586HX	512KB pburst	64MB FPM	10.830	6.086	17.36
6.	Pentium 133-MHz Gigabyte 586HX	512KB pburst	32MB FPM	12.630	6.731	20.10
7.	Pentium 133-MHz Shuttle	512KB pburst	32MB FPM	12.730	6.986	20.46
8.	Pentium 133-MHz Hitachi MX-133T Notebook	256KB pburst	48MB EDO	12.573	7.286	20.46
9.	Pentium 133-MHz Epox	512KB pburst	32MB FPM	12.730	8.530	22.10
10.	Pentium 100-MHz Gigabyte 586HX	512KB pburst	64MB FPM	15.860	8.385	24.96
11.	Pentium 133-MHz Hitachi M-134T NoteBook	none	32MB EDO	15.470	10.970	27.20
12.	Pentium 90-MHz Gigabyte 586HX	512KB pburst	64MB FPM	17.610	9.384	27.74
13.	Pentium 100-MHz Dell Optiplex GXM-5100	256KB ??	16MB EDO	18.660	8.685	28.89
14.	Pentium 90-MHz Intel Neptune P54C-PCI	256KB SRAM	16MB FPM	18.800	10.600	30.23
15.	Pentium 100-MHz Hitachi M-100T Notebook	none	40MB EDO	18.260	11.230	30.29

Notes: FPM = Fast Page Mode; pburst = Pipeline Burst cache; EDO = Extended Data Output; SRAM = Static RAM cache.

Table 2 shows the performance ratios relative to the 90 MHz Intel Neptune P54C-PCI that was also included in the tables in [1]. The performance ratios normalized by clock speed demonstrate improved performance of the MMX chips due to the larger level-1 cache internal to the CPU. The MMX processors include 32 KB of L1 cache internal to the CPU, up from 16 KB on standard Pentiums. Even with a large L2 cache on the board, the faster

Table 2. Comparison of performance ratios for NEC4.1 on various CPU chip and motherboard configurations.

	CPU/Motherboard	Clock Ratio	M-Fill Ratio	M-Fact Ratio	Exec Ratio	Norm. by CPU clock M-Fill	M-Fact	T-Exec
1.	Pentium 200-MHz MMX Gigabyte 586HX	2.22	2.230	2.440	2.313	1.004	1.099	1.041
2.	Pentium-Pro 200-MHz HP Vectra XU 6/200	2.22	1.631	3.728	2.061	0.735	1.679	0.928
3.	Pentium 166-MHz MMX Gigabyte 586HX	1.84	1.931	2.084	1.986	1.049	1.132	1.079
4.	Pentium 166-MHz MMX Hitachi MX-166T Notebook PC	1.84	1.932	2.022	1.967	1.048	1.096	1.066
5.	Pentium 166-MHz Gigabyte 586HX	1.84	1.736	1.742	1.741	0.943	0.947	0.946
6.	Pentium 133-MHz Gigabyte 586HX	1.48	1.489	1.575	1.504	1.006	1.064	1.016
7.	Pentium 133-MHz Shuttle	1.48	1.477	1.517	1.478	0.998	1.025	0.998
8.	Pentium 133-MHz Hitachi MX-133T Notebook PC	1.48	1.495	1.455	1.478	1.012	0.984	1.000
9.	Pentium 133-MHz Epox	1.48	1.477	1.243	1.368	0.998	0.840	0.924
10.	Pentium 100-MHz Gigabyte 586HX	1.11	1.186	1.264	1.211	1.067	1.138	1.090
11.	Pentium 133-MHz Hitachi M-134T Notebook PC	1.48	1.215	0.966	1.111	0.821	0.653	0.751
12.	Pentium 90-MHz Gigabyte 586HX	1.00	1.067	1.130	1.090	1.067	1.130	1.090
13.	Pentium 100-MHz Dell Optiplex GXM-5100	1.11	1.008	1.221	1.046	0.907	1.098	0.942
14.	Pentium 90-MHz Intel Neptune P54C-PCI	1.00	1.000	1.000	1.000	1.000	1.000	1.000
15.	Pentium 100-MHz Hitachi M-100T Notebook PC	1.11	1.030	0.944	0.998	0.927	0.850	0.898

access of the L1 cache offers a significant increase in speed for operations such as matrix factoring. The advantage of the larger L1 cache is illustrated in Table 3, where the Gigabyte motherboards are compared for performance ratio in factoring the matrix. The reference is now the non-MMX 90-MHz Gigabyte 586HX board, which is a good performer for its clock speed. At 166-MHz the effect of the low-bandwidth bottleneck to the L2 cache is clearly

Table 3. Performance ratios of the Gigabyte motherboards and CPU chips for NEC-4.1 matrix factorization. The reference is the Gigabyte 586HX motherboard with 512KB pipeline burst cache, 64 MB of RAM and Intel 90-MHz Pentium CPU chip.

Gigabyte 586HX CPU & speed	L1 cache	Clock Ratio	M-fact. ratio	M-fact. ratio clock normalized
200-MHz MMX	32KB	2.22	2.161	0.973
166-MHz MMX	32KB	1.84	1.845	1.003
166-MHz	16KB	1.84	1.542	0.838
133-MHz	16KB	1.48	1.394	0.942
100-MHz	16KB	1.11	1.119	1.007
90-MHz	16KB	1.00	1.000	1.000

Table 4. Effects of the CPU L1 (internal) and L2 (external) caches on performance for the P-166 MMX and P-166 standard CPUs on the Gigabyte 586HX motherboard. Execution times are in seconds.

CPU L1 cache	L2 cache	Fill		Factor		Total	
		MMX	std.	MMX	std.	MMX	std.
on	on	9.74	10.84	5.087	6.086	15.22	17.36
on	off	11.03	16.03	8.130	10.62	19.72	27.19
off	on	44.76	51.20	30.93	39.66	78.29	93.86
off	off	151.38	158.97	107.98	129.63	268.29	298.03

seen, while the larger L1 cache with MMX allows only a small degradation at 200 MHz. Table 4, in which Larry has switched each of the caches on or off, demonstrates the critical importance of the L1 cache.

Larry hopes to be able to supply more data in the future. He says that a vendor has offered to loan a Pentium II board for evaluation, and would like to run some benchmarks with Linpack routines, but just needs the time to get things done. It would be interesting to see the results for a non-MMX processor at 200 MHz.

Input data for timing tests: David Pinion, P.E., submitted the following NEC data file TEST299.NEC used in these tests:

```
CE CENTER FED HORIZONTAL HALF-WAVE DIPOLE OVER EXCELLENT GROUND.
GW 1,299,-139.,0, 6.,+139.,0, 6., .001,
GE 0,
GN 1,
FR 0,0,0,0, 0.54,
EX 0, 1,150,0,1., 0.,
RP 1, 1, 1,0000, 1.5, 0., 0., 0., 1000.,
EN
```

NEC-4 matters. Roy Lewallen and people at the ARRL have found some glitches in the near-magnetic field on the ground while looking at field strengths of Ham antennas

for the issue of safety standards. This is another case of an old problem. All versions of NEC directly compute only the electric field due to ground, since that is all that is needed in the electric-field integral equation. Electric fields are obtained using numerical table-lookup and "parameter estimation" schemes to reduce evaluation times. The Sommerfeld-integral ground treatment is not implemented for the MFIE patch model which would require H. When near magnetic fields are requested by an NH command they are obtained from a central-difference evaluation of the curl of E. This differencing for H can magnify any numerical noise in the electric field evaluation. Problems that can occur at low frequencies were documented by Greg Haack and Tony Fleming ("Using the Numerical Electromagnetics Code (NEC) to calculate magnetic field strength close to a Sommerfeld ground," *7th Annual Review of Progress in Applied Computational Electromagnetics*, pp. 493-501, March 18-22, 1991.)

The problem that the ARRL ran into is the result of an attempt to save computation time. When the evaluation point is close to the source segment the Sommerfeld-integral Green's function is integrated over the current distribution using either adaptive or Gaussian integration schemes. At larger distances the integration is reduced to the value at the center of the segment times segment length. This switch in integration was made at a distance where it made a relatively small change in the electric field. However, the difference evaluation can turn the small step in E into a larger spike in H if you are unlucky in where the NH points land. The easiest way to fix this problem for now seems to be to comment out the code that does this switch in subroutine EFLD. Then 3-point Gaussian quadrature will be used at the larger distances. The four lines commented out in EFLD are at the bottom of the code below:

```
C     FOR SOMMERFELD GROUND EVALUATION, TEST IF DISTANCE IS GREAT ENOUGH
C     TO USE POINT SOURCE APPROXIMATION.  IF SO THE TOTAL REFLECTED
C     FIELD IS EVALUATED BY SOMMERFELD-INTERPOLATION CODE.
C
      IF(IPERF.EQ.2)THEN
        IMAGF=1
        RHO=SQRT(XIJ*XIJ+YIJ*YIJ)*GSCAL
        ZIJS=ZIJ*GSCAL
C         IF((ZIJS.GT.ZZMX1).OR.(-ZIJS.GT.ZPMX1).OR.(RHO.GT.RHMX1))THEN
C           IMAGF=2
C           GO TO 17
C         END IF
      END IF
```

With this change the evaluation may take a little longer, but should give a glitch-free result for H.

References

[1] L. Laitinen, "PC Processor and Motherboard Benchmarks Using the NEC Method of Moments Antenna Analysis Codes," *ACES Newsletter*, Vol. 11, No. 1, pp. 14-19, March 1996.

[2] W. D. Swift, "Threads," *IEEE Antennas and Propagation Magazine*, Vol. 38, No. 6, pp. 124-125, December 1996.

AN EXPERT SYSTEM TOOL TO AID CEM MODEL GENERATION

Andrew L.S. Drozd
ANDRO Consulting Services
P.O. Box 543
Rome, NY 13442-0543
andro1@aol.com

Timothy W. Blocher
Rome Laboratory/ERST
525 Brooks Road
Rome, NY 13441-4505
blochert@rl.af.mil

Kenneth R. Siarkiewicz
Rome Laboratory/ERST
525 Brooks Road
Rome, NY 13441-4505
kens@rl.af.mil

1.0 INTRODUCTION

This paper presents an update of ongoing research and development to apply Artificial Intelligence (AI) methodologies and Expert System (ES) software technologies in the design of a smart pre-processor for government, university, and industry Computational Electromagnetics (CEM) codes. The pre-processor is called the Intelligent Computational Electromagnetics Expert System (ICEMES). Its purpose is to enhance the analyst's efficiency in generating complex CEM models and in choosing appropriate electromagnetic physics and solution techniques within the constraints of selected codes. This ongoing effort builds upon the original research and findings previously reported on in the ACES literature.[1,2] Work in progress is being funded under the DoD SBIR Program, Contract F30602-96-C-0163, Phase II for the USAF Rome Laboratory.

The intelligent pre-processor invokes modeling rules-of-thumb based on an array of CEM physics formalisms and numerical solution techniques, and, in turn generates electromagnetic structure models for corresponding CEM codes and user modeling scenarios. Discussed in this technology update is the evolution of the pre-processor design, refinements to its framework and functionality, and particularly, how it will benefit the CEM code user community at large.

1.1 Background

For all practical purposes, the "resident electromagnetics expert" is the one relied upon to undertake complex CEM modeling and analyses tasks for his/her organization on behalf of a product or customer. At times however, even the "expert" can be overwhelmed by the complexity of a given problem let alone how to best approach the electromagnetics problem-solving task. An added complication arises when the analyst finds that his/her arsenal of tools may not be well suited to the task and/or may require a great deal of proficiency. This dilemma begs for a solution, one that assures the availability of a "resident expert" and a readily usable set of tools to address CEM requirements.

Recently, there has been a great deal of interest in identifying and implementing new, effective procedures for automating CEM modeling and analyses tasks to assess antenna performance and radiation scattering in the presence of complex structures, radar cross section (RCS), intrasystem Electromagnetic Compatibility (EMC), and so on. Techniques range from the use of simplified, graphical user interfaces to highly robust, software pre-processor frameworks employing expert system engines and rule-based methods. These approaches are intended to ease burdensome modeling tasks, assist in more rapidly generating valid CEM structure models and performing complex system analyses, and reduce associated modeling/analysis uncertainties.

This paper focuses on an approach using AI/ES technologies and knowledge/rule-basing techniques to develop a state-of-the-art pre-processor that automates the CEM modeling/analysis task, and, in turn assists the novice-to-experienced engineer in efficiently addressing CEM problems. The evolving, cutting-edge capability is discussed in terms of recent architecture design and functionality enhancements, and its application to CEM problem solving by way of illustration.

1.2 Intelligent Pre-processing Environment

The modular, flexible framework currently under construction will readily allow a number of CEM formalisms (MoM, GTD, SBR/PO/PTD, hybrids), software codes (GEMACS, NEC-MOM, NEC-BSC, Carlos-3D, Apatch, Xpatch, etc.), and associated constraints to be "plugged-in" or linked to the system in either a loosely- or tightly-coupled manner, as appropriate. The ability to accommodate a range of CEM physics is highly dependent upon properly generating a hierarchical and interlinked set of generic knowledge base reference objects. These consist of superior (parent) class objects, subordinate (child) class objects or items, nth-generation entities, and so on. These objects embody the essential "general" knowledge (characteristics, attributes, and parameters) common to all CEM formalisms, as well as code/data-specific knowledge (i.e., characteristics and constraints that are unique to selected CEM codes and Computer Aided Design or CAD data). Common attributes and relationships are established to "share" characteristics and eliminate superfluous parameter definitions within the knowledge base. Examples of common attributes include frequency, physical dimensions, electrical properties (conductivity, permitivitty, etc.), and a specified range of observable quantities. Fundamentally these parameters, variables, and quantities are applicable to all CEM formalisms and analysis methodologies.

2.0 ENHANCED SYSTEM FRAMEWORK AND FUNCTIONALITY

Refinements have been made to the baseline ICEMES architecture design to further enhance its modularity and functionality. These enhancements affect the configuration and integration of the following key components of the system: the CEM Knowledge Base (KB), its partitioned structure and associated rule sets; interactive geometry modeling and visualization packages; graphical user interfaces (GUIs); file/database management systems; discipline-specific data dictionary; CAD engine interface and built-in translators operating on shared, reusable data for a select range of CAD data types/formats; and other Commercial Off-the-Shelf/Non-Development Item (COTS/NDI) software used to support the system's functionality.

At the heart of the current ICEMES framework is a high-end, commercial Expert System and an Intelligent Manager operational and accessible through an interactive GUI. The Intelligent Manager provides the central link to/from all other essential components of the system. These include:

- Interactive Geometry Modeler (IGM) providing 3-D, color-rendered visualization and the ability to manipulate generated CEM structure models;
- CAD Engine Interface Translator to convert a subset of popular CAD package data formats into equivalent KB and corresponding CEM models;
- Relational Database Manager working with a discipline-specific Data Dictionary[3] to capture and store geometric as well as electromagnetic properties of a physical system; and
- File System and Support Utilities which support overall functionality, seamless data transactions and other data storage management operations.

The overall ICEMES framework showing its constituent components is illustrated in Figure 1. This figure also shows that the system can automatically launch the execution of external CEM codes, at the operator's request, under the control of the Intelligent Manager. These codes may be resident in parallelized form on a massively parallel processor or High Performance Computer (HPC, e.g., multi-node Paragon), or accessed from within a configuration of distributed workstations communicating through a central server. It is noted that ICEMES itself is being hosted on a platform running Windows NT 4.0.

The modularized design based on an Intelligent Manager allows the system functions that do not require the expert system to be performed by FORTRAN, PASCAL, C, and C++ programs. This includes a number of house-keeping functions such as user interface management, identifying authorized users, loading user profiles, object and data storage, data translation, on-line help systems, software interfacing, and calls to the various module calls. This allows the expert system to focus on tasks and functions that require the use of its inferencing/reasoning engine. This approach also limits the number of direct links between the expert system and external programs which in general alleviates potential "bottle necks" which would slow down system performance.

Further, the Intelligent Manager acts as the main controller for the entire system. It is being coded in C and C++ to maximize functionality and performance. The flexibility and portability of C/C++ enables the main controller to communicate with the GUI, Expert System Module, the IGM as well as any other C, FORTRAN or PASCAL programs. For example, it will work closely with the Expert System and GUI to develop "user profiles" whereby the system would collect statistics and information about an operator over time, establish a profile, and interact with the user in a highly meaningful way based on his/her level of expertise. Effectively, the expert system will "learn" from the operator how he/she typically approaches CEM modeling and analysis tasks, making the overall process more efficient and user friendly.

Next, consider the role of the IGM. Assuring the IGM's seamless interplay with the rest of the system is crucial to demonstrating ICEMES' full potential and utility for CEM modeling tasks. The present IGM design, based on a virtual reality visualization approach, is anticipated to provide two important capabilities to the operator: (1) allow the user to graphically display interim and final versions of the CEM structure model in 3-D space, and (2) permit the user to manipulate or institute modifications to the model (add, modify, delete, zoom in/out, or select regions of the overall structure model) and intelligently re-evaluate the impact of any changes through the expert engine. Modifications made interactively by the user to a baseline model via the IGM would be automatically reasoned upon, assessed for validity, and archived to establish a series of system-project files. These would be stored with the aid of the Relational Database Manager working in conjunction and in conformance with the Data Dictionary structure.

In order to facilitate rapid development and demonstration of the system, the current approach involves integrating a cost-effective commercial database package (e.g., MiniSQL, Microsoft Access) and implementing SQL-compatible calls, data transfers, and scripts that permit other modules to communicate with this database component. Sufficient flexibility is being instituted in the design and configuration management process to accommodate the insertion of any SQL-based data management package such as Oracle, Sybase, FoxPro, etc. with a minimum number of software interface modifications.

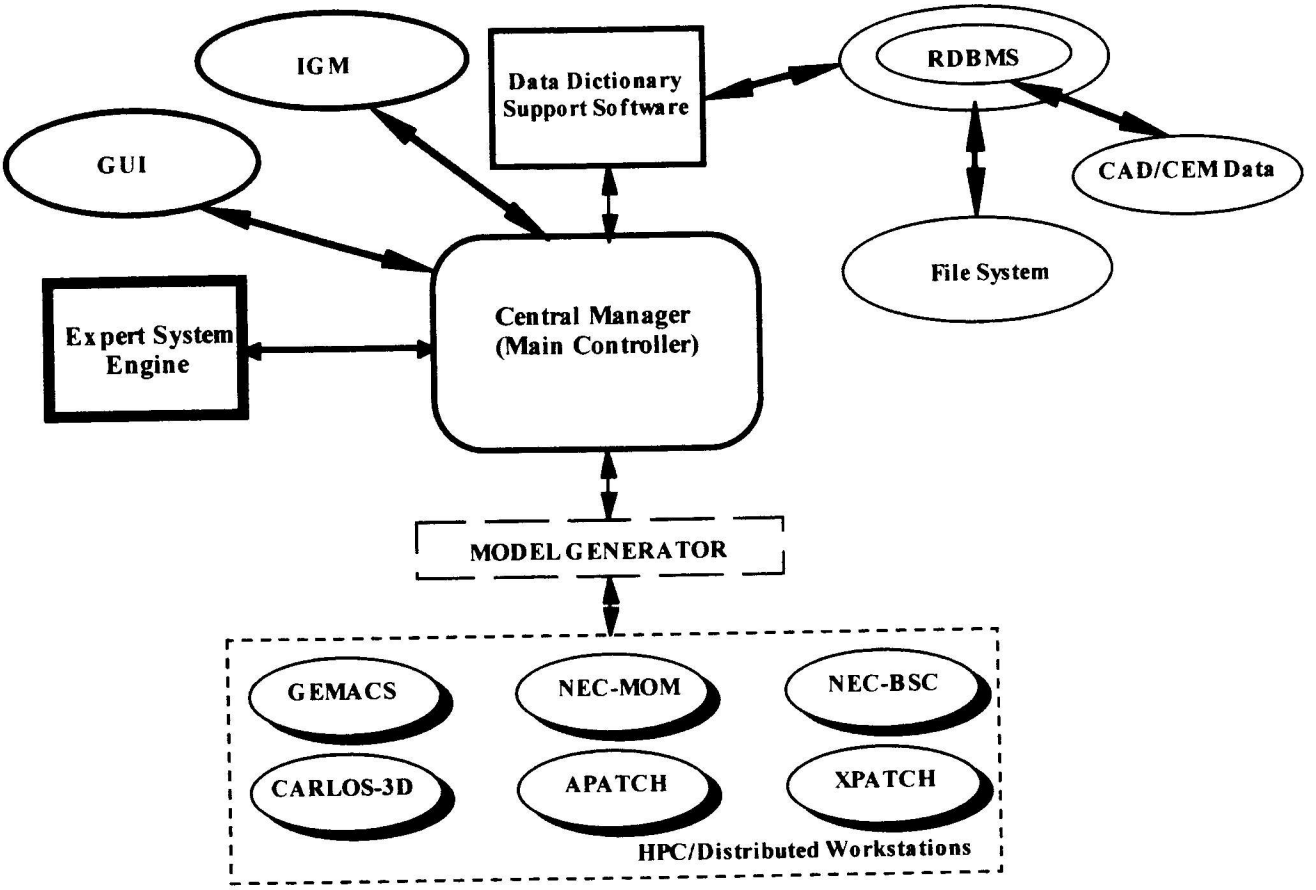

Figure 1. ICEMES Configuration Illustrating Component Framework and External CEM Code Communications

With regard to the CAD Engine component, current research and applications of CAD data are focusing on methods to read, parse, strip, and translate 3-D facet files; finite element data; subsets of the IGES (superset) standard; and associated spline functions and parameters. Research to investigate the possible translation of the STEP data standard is also anticipated as part of the capability's future expansion.

As in the prototype design previously reported upon, ICEMES will convert input data, whether CAD geometry or CEM, into a set of generic CEM objects in order to maximize the applicability of its inherent knowledge across the various CEM formalisms. Generic objects contained within the KB structure are intended to represent the basic building blocks that can be combined to form complex CEM geometries. The generic CEM objects include points, wires, plates, and cylinders as well as geometric variations on these. The generic CEM components permit the analyst to perform a number of data manipulations prior to selecting the analysis code or formalism type. This approach also provides a convenient method of sharing input data sets among CEM codes.

Figure 2 illustrates how the above functions work in unison to produce a valid CEM input model. This figure shows the general method of reading in all or a portion of a CAD model; converting the CAD data into an equivalent KB representation that conforms to the Data Dictionary definitions and structure; generating the CEM model; and performing (iterative) validations to arrive at the final model.

Per the original concept, the present ICEMES design and framework development approach will allow the individual software modules to be maintained and upgraded independently of each other. This means that the linking process does not fix the design to operate with a single version of any one of the components. Also, the use of Application Program Interfaces (APIs) simplifies the incorporation of additional tools as the system continues to grow in the future.

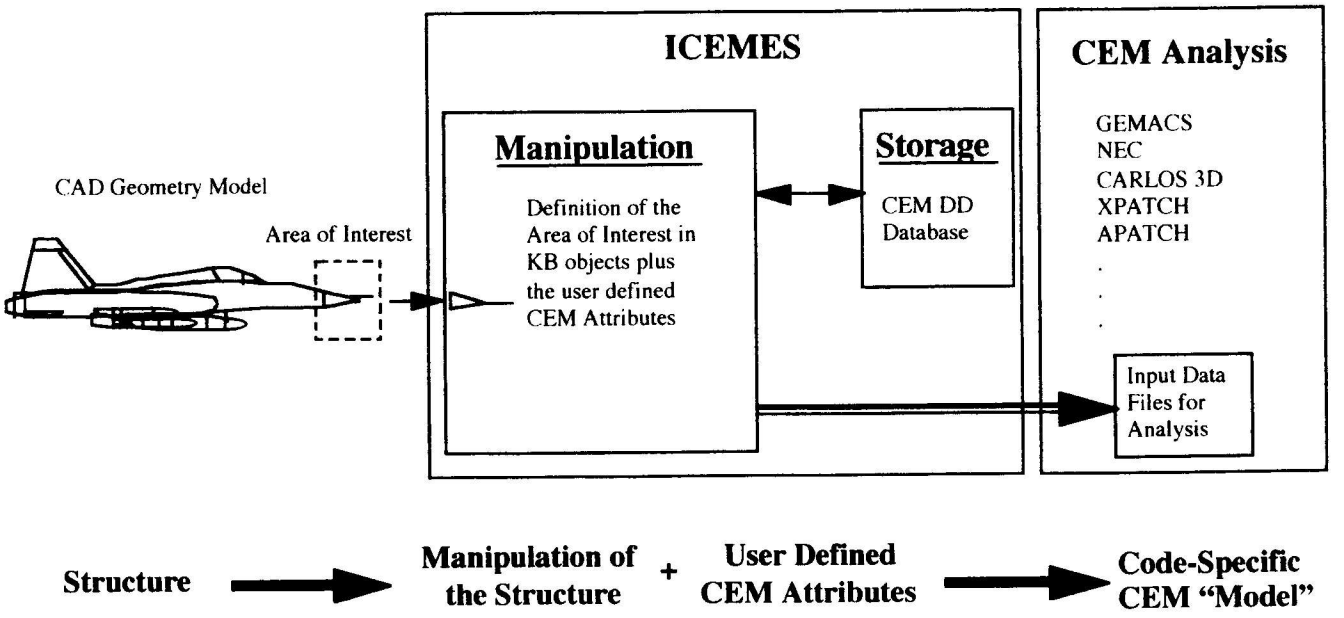

Figure 2. ICEMES and CEM Data Dictionary Functional Connection for CEM Input Model Generation

It is pointed out that a separate, Air Force sponsored research and development effort is anticipated to establish a Data Dictionary capability that is compliant with the government's Research and Engineering Framework (REF) technical requirements[3,4]. This will involve implementing an RDBMS and File System approach that is generally consistent with the methods and applications outlined above for ICEMES. This independent effort is expected to result in a capability that will complement the ICEMES concept and approach, and assist in enhancing its overall utility and functionality.

2.1 Knowledge Base Environment

In the present design, a "Master Knowledge Base" is established which consists of a series of separate, but interlinked KB partitions. The separate KBs are used to incorporate the knowledge and interfaces required for individual or unique CEM formalisms and processes, respective software packages, CEM codes, etc. Since each of these KBs shares the same basic structure, they can easily be duplicated and updated to accommodate new capabilities, including individual CEM formalisms and CEM code-specific modeling constraints. With this approach the end-user is not required to have all the modules or analysis programs in order to operate the system. The knowledge is incorporated into the partitioned KBs via objects, rules, procedures, and relations.

The updated block diagram of Figure 3 illustrates the individual, hierarchical nature of the internal KB partitions and their purpose. Specifically, the block diagram shows the partitioning of knowledge first as a function of CEM formalism (i.e., "general" knowledge), and then by individual CEM codes and their peculiar modeling constraints (i.e., "specific" knowledge). This approach supports modularity, portability, and expansion to include other formalisms and code constraints.

3.0 MODELING METHOD AND USER SCENARIO

The reader may recall from previously published literature on this subject that a viable user interface which facilitates automated CEM structure model generation was initially developed and demonstrated[1,2]. This was defined in the technical literature as the "User Modeling Scenario" or UMS. The UMS is a methodology or roadmap which describes the general procedures involved in a typical ICEMES model development session, with the GUI as its infrastructure. At the time of this writing, a fairly comprehensive query-response system was in the initial stages of detailed design. This system will eventually provide varying degrees of user interaction depending upon the analyst's modeling and simulation goals, and CEM domain expertise.

The analyst will have the option of using a standard set of pull-down menus, tool bars, and an automated Assistant to navigate through the system during a modeling session. The Assistant consists of menus that lead the analyst through each step of the modeling task, and it provides recommendations along the way regarding the use of various modeling parameters as requested by the user or as determined by ICEMES' internal inferencing/reasoning engine.

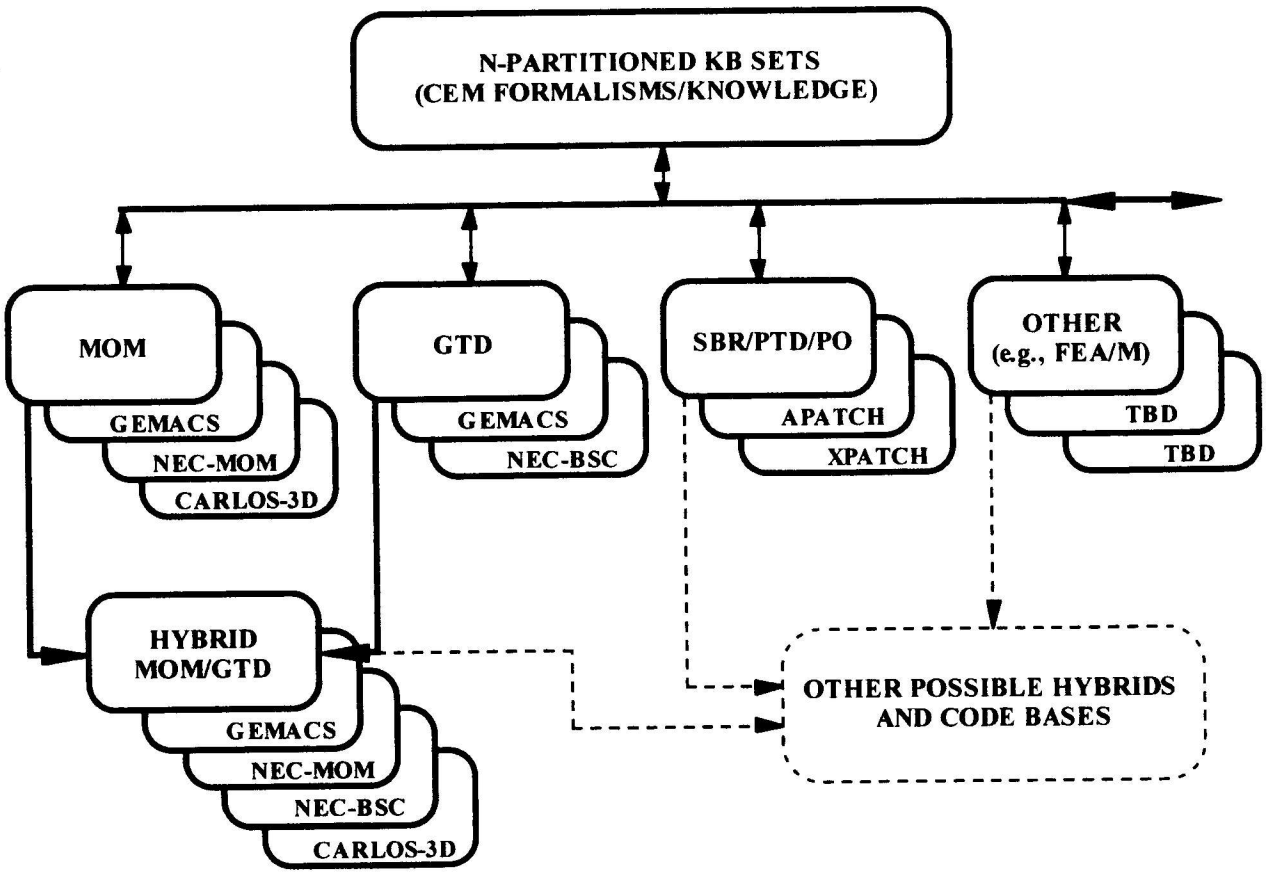

Figure 3. Hierarchical Knowledge Base Structure

3.1 Example Illustration

Consider the generalized system geometry illustrated in Figure 4. A "typical" albeit simplified modeling scenario may involve a situation in which the analyst is interested in (a) performing antenna siting on a complex structure such as the aircraft system of Figure 4 and (b) generating a corresponding CEM structure model as a function of antenna location, frequency and some observable quantity (e.g., electric field). Let us also assume that the analyst is attempting to concentrate his/her investigation on a "local" region (e.g., forward conical radome) of the total geometry based on some performance or safety-critical criterion. Finally, assume that the analyst is also looking for ways to achieve a simplified, yet valid CEM structure model, i.e., one which does not require significant computational resources or time to analyze.

In this case, the analyst may display the complete model via the IGM and interactively select a region to be emphasized for which a corresponding CEM structure model will be generated. This is shown via the 2-D "clip box" centered about the nose cone geometry of Figure 4. The result will be the generation of a complete, valid CEM structure model which exhibits high fidelity or which is more accurately defined in the subregion of interest (e.g., using a series of contiguous, discrete patches or wire gridded surface), and less detail (e.g., properly-sized GTD objects) beyond some $n\lambda$ boundary limit possibly dictated by the extent of the clip box area where λ is the wavelength of interest. The region of interest is highlighted in Figure 5.

The method of successfully accomplishing the above is currently under detailed investigation and initial implementation. The validity of this highlighting method is dependent upon the following: the manner in which selected objects (subregions) are grouped or tagged; determining the 2-D to 3-D transfer function or extent to which the 2-D clip box area relates to a 3-D volume; and assuring valid boundary conditions at the interface between the higher- and lower-fidelity regions of a model.

It is reiterated that the ICEMES model validation and correction measures ultimately act upon the generic CEM objects resident in the KB. Any size adjustments, position changes, connectivity modifications, etc. are applied directly to the generic CEM model components.

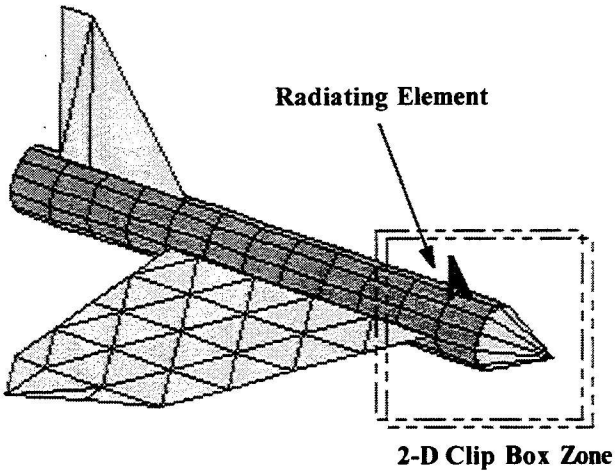

Figure 4. Generalized System Geometry Illustrating Interactive Display and Region Selection

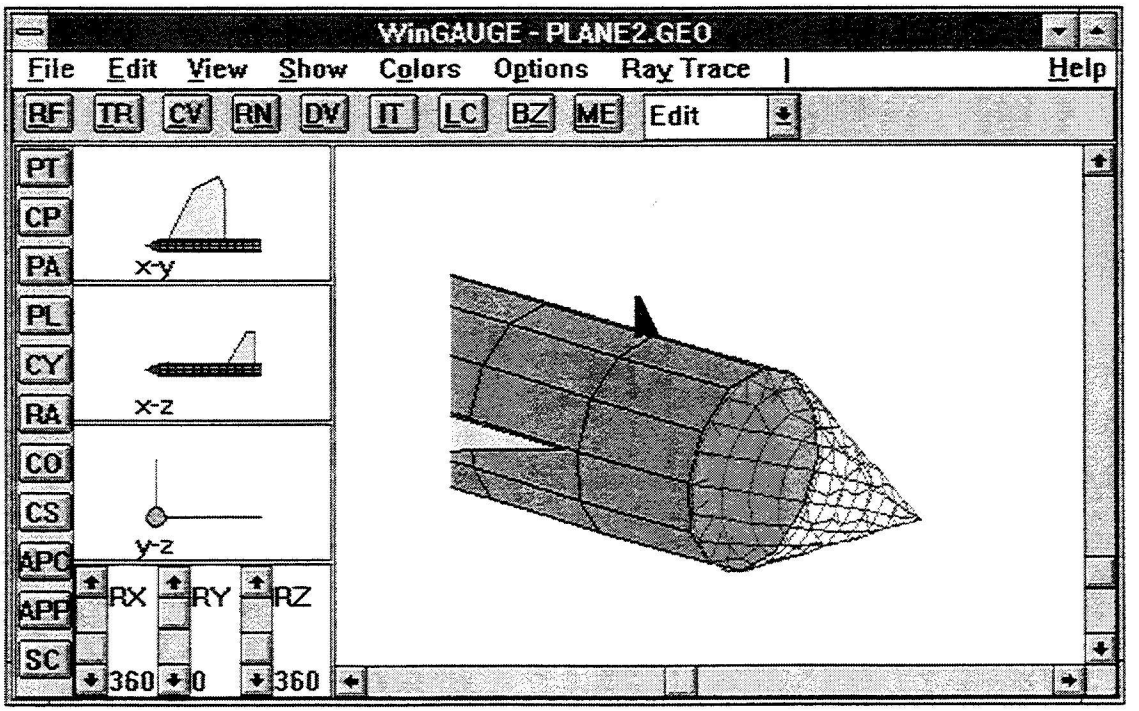

Figure 5. View of Aircraft Nose Cone Region of Interest Using WinGAUGE

Also, other validations that will be performed during the model generation process include: finite-element resizing (plate sizing), connectivity/misalignment checking (MoM wire segments to GTD objects, GTD plates to GTD cylinder), incomplete definitions, and MoM element sizing and connection angles. Again, each of these validations is based upon assessing the relevant electromagnetic conditions and "physical" parameters defined for the given problem such as: frequency, object dimensions, relative location of source(s) with respect to the system geometry, specified observables (e.g., field points, wire currents, patch current densities, etc.), and any specified accuracy constraints.

Once the geometry model complies with the set of applicable CEM rules, it passes through a "filter" for the application code selected; and the filter converts the generic parameters into a specific format required by the CEM code.

4.0 CONCLUSIONS AND FUTURE DIRECTIONS

The evolving ICEMES capability is an innovative, significant step forward in the successful adaptation and integration of next-generation software technologies with existing CEM codes. The present stage in ICEMES' development cycle is focusing on expanding its framework to encompass additional CEM formalisms, codes and associated data formats, and algorithms. Ancillary features and capabilities are also being adapted to ICEMES' architecture. These include a database management system, CEM model libraries and data dictionary, interactive geometry modeling and visualization tools, and tailored graphical user interfaces.

ICEMES exhibits the potential to support the goals and objectives of broader modeling and simulation computational engineering environments. One example is the Air Force's Integrated Computational Environment/Research and Engineering Framework (ICE/REF)[4] which stresses Concurrent Engineering applications, the use of common-type data, and a "global" modeling/simulation environment. The current ICEMES concept and design continues to be generally in conformance with architectural and functional features of the ICE/REF that include code wrappers, Applications Program Interface (API) routines, CAD file data extraction, library structures generated via database managers, and use of the CEM Data Dictionary.

The ICEMES capability continues to offer opportunities for government and commercial sectors to benefit from advanced AI/ES-based tools for product value added. It is expected to also benefit academia by providing a learning tool for student and journeyman-level engineers who may be tasked with investigating CEM concerns in the professional job market.

Eventually, the AI/ES approach discussed herein is expected to support synthesis modeling whereby an item (e.g., antenna radiator) can effectively be "built" from a pallet library of "standard" elements and characteristics of commercially-manufactured hardware, and integrated with the host system using an incremental or building block approach. The synthesis method would be driven by operational, electrical and physical characteristics in conjunction with user-specific options all under the control of an expert engine.

REFERENCES

[1] A. Drozd, T. Blocher, et. al., "The Intelligent Computational Electromagnetics Expert System (ICEMES)", Conference Proceedings of the 12th Annual Review of Progress in Applied Computational Electromagnetics at the Naval Postgraduate School, Monterey, CA, 18-22 March 1996, pp. 1158-1165 (Research and Development sponsored under the DoD SBIR Program, Contract No. F30602-95-C-0198, Phase I for the US Air Force Rome Laboratory).

[2] A. Drozd, T. Blocher, et. al., "The Intelligent Computational Electromagnetics Expert System (ICEMES)", Applied Computational Electromagnetics Society Newsletter, Vol. 11, No. 2, ISSN 1056-9170, July 1996, pp. 28-40.

[3] J. Evans, "Research and Engineering Framework (REF) Data Dictionary Specification for Computational Electromagnetics", Conference Proceedings of the 12th Annual Review of Progress in Applied Computational Electromagnetics at the Naval Postgraduate School, Monterey, CA, 18-22 March 1996, pp. 340-346.

[4] L.W. Woo,. B. Hantman, et. al., "Continuing Development of the Research and Engineering Framework (REF) for Computational Electromagnetics", Conference Proceedings of the 12th Annual Review of Progress in Applied Computational Electromagnetics at the Naval Postgraduate School, Monterey, CA, 18-22 March 1996, pp. 383-390.

ACKNOWLEDGMENTS

The authors wish to acknowledge the ongoing support and contributions made on behalf of the ICEMES development program by Clifford E. Carroll, Jr. of ANDRO, Dr. Edgar L. Coffey III of Advanced Electromagnetics, Dr. Ronald J. Marhefka of The Ohio State University, Jeffrey A. Evans of Decision-Science Applications, Inc., and James B. McCreary of Innovation Strategy Group, Inc.

ABOUT THE AUTHORS

Andrew L. S. Drozd is President of and Chief Research Engineer for ANDRO Consulting Services. He has nearly 20 years of experience in the field of Electromagnetic Environmental Effects (E^3), Electromagnetic Compatibility (EMC) and Computational Electromagnetics (CEM). He holds a B.S. in Physics and Mathematics (1977) and an M.S. in Electrical Engineering (1983), both from Syracuse University. In recent years, he has focused his research on applying AI and expert systems to CEM applications. Mr. Drozd is also a Senior Member of the IEEE and is currently a Member of the IEEE EMC Society Board of Directors.

Timothy W. Blocher also conducts CEM research at the Rome Laboratory. He holds a B.S. in Physics and Electrical Engineering from the State University of New York and Clarkson University, respectively, and an M.S. in Electrical Engineering from Syracuse University.

Kenneth R. Siarkiewicz has over 30 years experience in the field of CEM at the Rome Laboratory. He holds a B.S. and M.S. in Electrical Engineering, respectively, from the University of Detroit and the University of Michigan. Mr. Siarkiewicz is a Rome Laboratory Fellow for his work in CEM, and he has been named IEEE Fellow for his work in developing and promoting computational models.

The Basic Scattering Code Viewer: A GUI for the NEC Basic Scattering Code

Donald Davis, Robert Paknys and Stanley J. Kubina *

Abstract— **The Numerical Electromagnetic Code Basic Scattering Code, NECBSC, is a computer code, written in FORTRAN, that uses the Uniform Theory of Diffraction to calculate the electromagnetic fields around scattering structures. Version 2 of the code has no user interface and no capability to produce graphics for output. To remedy this, a companion code for the NECBSC code was developed. The Basic Scattering Code Viewer, BSCV, is a pre and post processor with a GUI and ray tracing capability. The BSCV code runs within the MATLAB environment and uses some FORTRAN routines.**

1.0 INTRODUCTION

The increasing interest in electromagnetic compatibility has encouraged the development of many techniques for assessing the interaction of different devices in the presence of electromagnetic fields. The use of computational techniques, to simulate the behavior of the fields, is a cost effective way of modeling those interactions.

The Numerical Electromagnetic Code Basic Scattering Code, NECBSC, is a well known computational electromagnetic tool [1]. It uses ray tracing techniques and the Uniform Theory of Diffraction, UTD, to model and analyze the effects that scattering appendages have on the electromagnetic fields that are incident on the structure [2]. The NECBSC code is written in FORTRAN and uses ASCII text files as input. The text file contains the geometry of the structure and other relevant information, such as the source type and the pattern to be computed. The NECBSC code provides output in the form of text files that contain information about the field strength and phase for each polarization. The power density of the field is also written to the output file.

The presence of the raw data in column form does not provide necessary insight into the behavior of the field or the effect of the scattering geometry. There is a need for an interface that would provide both an easy command structure and more meaningful output. To this end, the Basic Scattering Code Viewer BSCV [3] was developed.

BSCV reads the NECBSC input and output files, enabling the user to view the input geometry and plot the computed fields. In addition, NECBSC was modified to write files that contain information on the ray path trajectories used to compute the fields. Using this data, BSCV allows us to view the rays.

BSCV is controlled from a series of nested menus that allow the code user to choose the feature required. The use of the associated MATLAB functions is largely transparent to the user.

2.0 USING THE VIEWER

The BSCV code can be used to preview the input files of the NECBSC code as well as process the output of the NECBSC code. The output of the code presents radiation patterns and ray pictures.

*The authors are with the Department of Electrical and Computer Engineering, Concordia University, Montreal, PQ, Canada H3G-1M8. This work was supported by the National Sciences and Engineering Research Council of Canada, Grant OGP0046227.

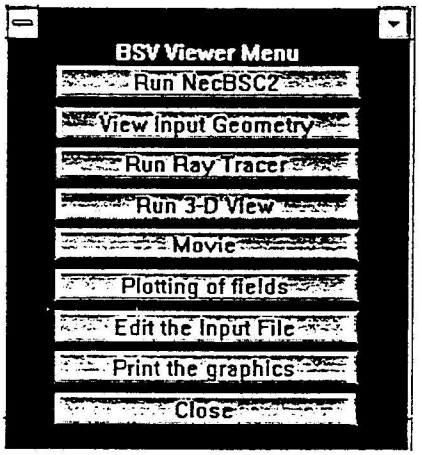

Figure 1 BSCV Main Menu.

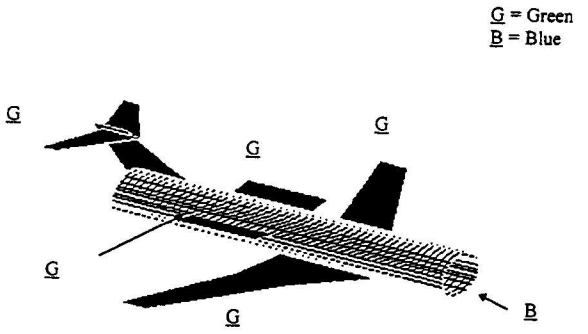

Figure 2 Preview Output from BSCV.

2.1 Previewer Operation

The previewer section uses the geometry described in the input file to produce a three dimensional image of the structure. This feature is useful in debugging the input file model and for comparing the input geometry with the actual structure being modeled.

To start up the session for the BSCV code, the user performs the following steps

- Start MATLAB
- type `bscv` (Enter)
- Select *Run Viewer* from the menu

The user is then be given the set of options shown in Figure 1.

The option *View Input Geometry* calls the previewer functions of the BSCV code. This operation reads the geometry from the input file and displays it as a three dimensional image. Figure 2 shows an example of the BSCV previewer output. The model is that of a Challenger Jet [4]. The figure shows a typical color scheme for the various geometrical objects.[1] The fuselage is modeled as a circular cylinder, while the rest of the aircraft is modeled as flat plates. The notch antenna in the tail assembly is approximated by a dipole placed above the tail. This model will be discussed in more detail in Section 2.2.2.

The previewed image may also have axes plotted if the user wishes to verify the exact coordinates of the geometry under study. If the user is satisfied with the input geometry, the next step would be to use the NECBSC code to perform the analysis of the geometry.

2.2 Analysis Using BSCV

The BSCV code can be used to generate radiation pattern plots as well as ray tracing plots. To make the radiation pattern plots, field strength data computed by NECBSC are read from files. Also, the ray tracing feature allows the user to see a three dimensional image of the geometry under study with all the UTD mechanisms, in the form of the ray paths, shown with color coding. The color coding can take two forms. The rays can be color coded according to UTD mechanism type. These color codes are: yellow for the direct ray, cyan for surface diffracted rays, magenta for edge diffracted rays, white for corner diffracted rays, and red for higher order rays that result from multiple UTD mechanisms. The

[1]Note that due to the black and white images used in the Newsletter, the figures have labels indicating the colors of the objects and rays. We have denoted R=red, Y=yellow, G=green, C=cyan, B=blue, M=magenta, K=black.

second form of color coding refers to the ray's relative magnitude with respect to a reference level of 1 V/m for the electric field and 1 A/m for the magnetic field. The absolute maximum and minimum levels for the ray magnitude are shown alongside a magnitude color bar. This feature identifies the rays according to their strength. The color coded magnitude option has the input geometry colored white for easier viewing and ray identification.

The next stage of the discussion presents typical output that can be obtained from the BSCV viewer, when used to analyze a scattering structure. A number of examples are shown, to illustrate the features of BSCV.

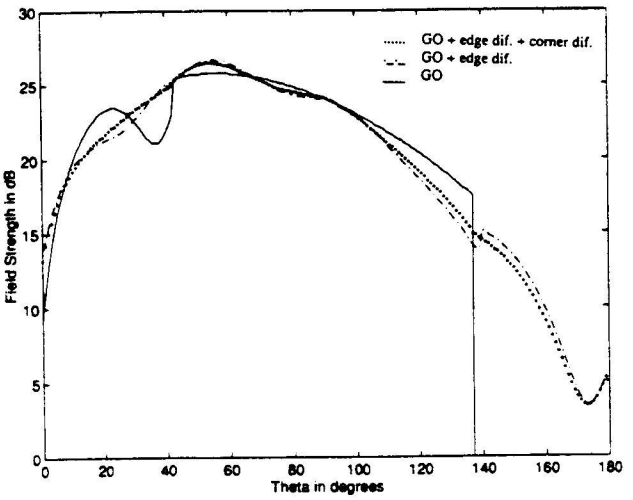

Figure 3 Radiation pattern comparison for GO and GO+UTD.

2.2.1 Sample Output 1: Flat Plate and Dipole

The first example geometry is that of a square flat plate with a side length of one wavelength [5]. The source is a dipole located above and off center from the plate. The frequency of the excitation is 300 MHz. Thus, one wavelength is equivalent to one meter. The source excitation is a one ampere current with a zero phase on a $\lambda/2$ dipole.

This geometry was analyzed by the NECBSC code using three different sets of UTD mechanisms. The selection of UTD mechanisms was accomplished by using the "TO", the test option command in the input file. The running of the NECBSC code is done by selecting the first option *Run NECBSC* from the main menu shown in Figure 1.

2.2.1.1 Radiation Pattern

First, the field was constructed using only the GO terms. Next, the field was computed from the GO + edge diffracted terms. Finally, the field was determined from the sum of the GO + edge diffracted + corner diffracted terms. GO refers to the Geometrical Optics field contributions, i.e. a direct ray from source to observer, plus a ray that leaves the source, reflects from the surface, and proceeds to the observer. The radiation pattern for each of these fields is plotted in Figure 3. The field point is in the near field at r=20 meters, $\phi = 0$ and $0 \leq \theta \leq 180$ degrees. The source is located at the point (0.2,0,1.0) meters in Cartesian coordinates. The plate is 1 by 1 meters in size, lies in the x-y plane, and is centered about the origin, as shown in Figures 4–6. The radiation pattern follows an arc which is perpendicular to the plane of the plate. The radiation patterns were made using the *Plotting of Fields* option from the main menu in Figure 1. The user would then specify what pattern was desired, using the BSCV radiation pattern functions. After the pattern is selected, the user would obtain the plot in Figure 3.

It is interesting to note that the plot of the GO field, shown as a solid line in Figure 3, exhibits a discontinuity at 43 degrees and another discontinuity at 139 degrees. The first discontinuity occurs at the reflection shadow boundary and is associated with the disappearance of the reflected ray. The second discontinuity is associated with the disappearance of the direct ray and occurs at the incident shadow boundary. The plot of the GO + edge diffracted field, shown as a dot-dash line in Figure 3, illustrates the effect of the edge diffracted ray. The discontinuities, occurring at the incident and reflection shadow boundaries, are smoothed out at the positions

43 degrees and 139 degrees by the addition of the edge diffracted rays. The radiation pattern has two other discontinuities, one at 40 degrees and the other at 140 degrees. These are smaller in magnitude than the previous discontinuities, but are still evident. The dotted line in Figure 3 shows how the addition of corner diffraction further smoothes out the plot. The compensation by corner diffraction is further discussed in the next section.

The radiation pattern, although instructive, does not impart any information about what particular UTD mechanism is dominant or the effect geometry has on the radiation pattern. To gather this type of information, the user must view the rays. The option to run the ray tracer can be selected from the main menu in Figure 1.

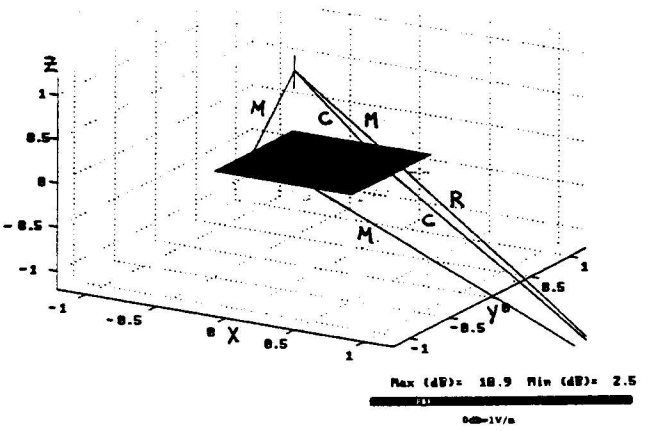

Figure 4 GO + edge diffracted rays, well before ISB. (0dB = 1 V/m, Red= 18.9 dB, Magenta=2.5 dB)

2.2.1.2 Ray Tracing

This section deals with the information extracted from the ray picture. The images in Figures 4, 5 and 6 represent the output of the ray tracing routine when color coded magnitudes of the rays are selected. The viewer draws all of the rays used to construct the field at the point of interest. The rays are drawn with a color representing the magnitude of the ray measured in dB with respect to 1 V/m.

The images shown in Figures 4–6 allow the observer to see how the direct ray is shadowed by the plate and how the edge diffracted ray increases in magnitude to compensate for the shadowing of the incident field. The same series of images also verify the appearance of edge diffracted rays which caused the discontinuity noticed in Figure 3. In these images the GO + edge diffracted rays are used to generate the dash-dot radiation pattern.

The ray picture on the lit side of the incident shadow boundary is shown in Figure 4. In this image there is a direct ray and two edge diffracted rays. The direct ray, which is dominant, is labelled as red.[2] The blue edge diffracted ray is the next in strength and the magenta edge diffracted ray is the weakest contributor to the field at the observation point. The receiver is then moved to a location just before the incident shadow boundary, as shown in Figure 5. The observation point is r=20 meters, $\phi = 0$, and $\theta = 136$ degrees. Here there are no changes in the number or type of rays, but the magnitude of the closer edge diffracted ray has increased. This is due to the fact that the edge diffracted ray becomes dominant in order to compensate for the disappearance of the direct ray after the incident shadow boundary has been crossed. The image shown in Figure 6 shows the ray picture when the observation point is past the incident shadow boundary (r=20 meters, $\phi = 0$, and $\theta = 147$ degrees). In this case, two additional rays, which *appear* to emanate from the corners, are actually edge diffracted rays with the diffraction point very close to the corner. Also, the direct ray has vanished. The color coded magnitudes allow the user to identify the strongest edge diffracted ray, labelled as red, which is now the dominant ray.

The above result also tells us that some of the edge diffracted rays are appearing and disappearing. This is precisely when corner diffraction is important, and explains why corner diffraction

[2]When colors are used to represent the field strength of the rays, the order from strongest to weakest is: R=red, Y=yellow, G=green, C=cyan, B=blue, M=magenta.

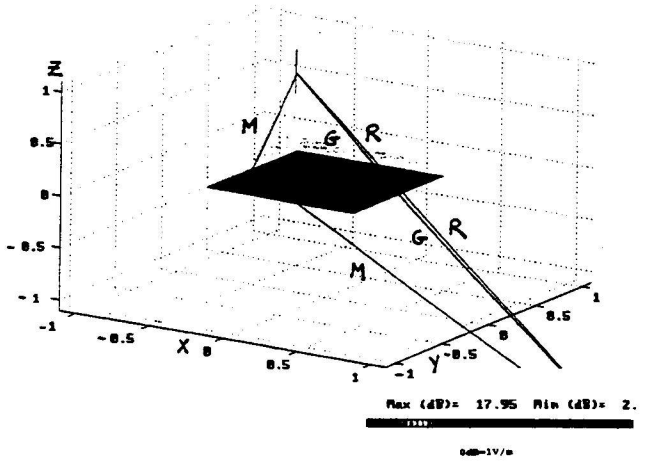

Figure 5 GO + edge diffracted rays, immediately before the ISB. $(r, \theta, \phi) = (20m, 136°, 0)$. (0dB = 1 V/m, Red= 17.95 dB, Magenta=2.0 dB)

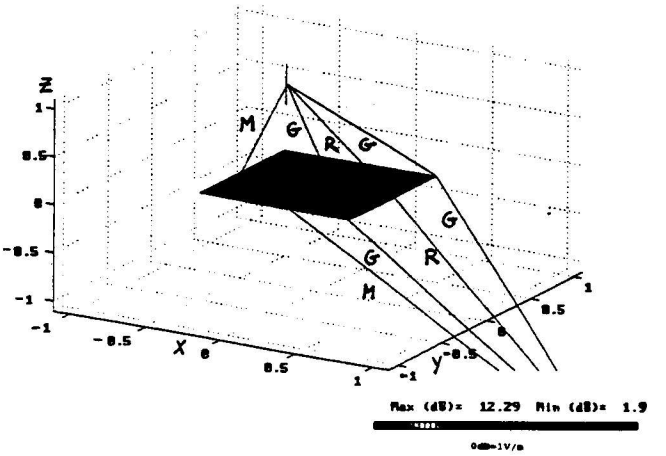

Figure 6 GO + edge diffracted rays, after ISB. $(r, \theta, \phi) = (20m, 147°, 0)$. (0dB = 1 V/m, Red= 12.29 dB, Magenta=1.9 dB)

was needed to get the smooth result seen earlier in Figure 3.

From such a ray picture, the effect of the geometry becomes clear. The sudden appearance of edge diffracted rays is confirmed and the need for the corner diffracted rays is validated. The ray pictures also identify the UTD mechanism of consequence in each of the observation positions. Thus the knowledge of both the effect of the shape of the structure as well as the relative strengths of each ray can be gathered using the ray tracing features.

2.2.2 Sample Output 2: Challenger Jet Model

The Canadair Challenger Jet is a 19.7 meter long business jet with a notch antenna mounted on the tail assembly. The aircraft is modeled by a circular cylinder, diameter of 2.7 meters and length of 15 meters for the body of the aircraft and flat plates for the tail fin assembly, wings and the engine pods to match the dimensions of the actual components. The notch antenna was modeled as a dipole [5]. A more complete discussion on the modeling of the Challenger Jet can be found in references [4],[5].

The model was analyzed using the NECBSC code. The near field pattern was calculated and plotted to see how the fields were behaving around the aircraft. The patterns were taken as a series of circumferential cuts about different yaw plane angles. The yaw plane z=0 is shown in Figure 7. The cuts are circles of constant radius and constant ϕ, with θ varying. These circular cuts range from $\phi = 0$ degrees to $\phi = 90$ degrees. When the radiation pattern is plotted for these cuts, a discontinuity in intensity was noticed. The next section discusses the results of the pattern plots.

2.2.2.1 Radiation Pattern

The radiation pattern plots for the θ -polarized electric field are presented in Figures 8–10. The elevation plane cut in Figure 8 in which $\phi = 5$ degrees shows a discontinuity at $\theta = 180$ degrees. The elevation plane cut in Figure 9 in which $\phi =$ 45 degrees also has a discontinuity at $\theta = 180$ degrees. The third radiation pattern which has $\phi = 90$ degrees (roll plane) has no discontinuity. Recalling our earlier results (in Sections 2.2.1.1 and 2.2.1.2), we speculate that the presence of discontinuities in Figures 8–10 may indicate an uncompensated sudden change in the number of

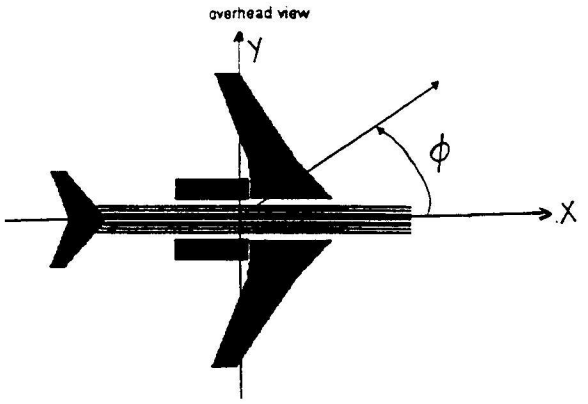

Figure 7 Coordinates for aircraft yaw plane, z=0.

UTD mechanisms used to calculate the field.

2.2.2.2 Ray Tracing

The ray tracing feature was used to further examine the discontinuity noticed in the radiation pattern. In this instance, we selected color coding according to mechanism type, i.e. incident, reflected, diffracted, and creeping waves. With this option, the geometrical bodies are colored black.

The images in Figures 11–13 represent the ray pictures for positions before and after the discontinuity. Figure 11 shows the rays that are used for the field point at $\phi = 5$ degrees, $\theta = 179$ degrees. The next image, shown in the Figure 12, is at $\phi = 5$ degrees with $\theta = 180$ degrees. The image in Figure 13 has the value of $\phi = 5$ degrees with $\theta = 181$ degrees. In all cases, the number and type of rays remained unchanged. This implies that the discontinuity was not caused by the appearance or disappearance of a UTD mechanism, as originally speculated, but by some other reason that has not yet been identified.

3.0 CONCLUSIONS

The BSCV code allows the users of the NECBSC code to perform pre and post processing of data. The menu driven system allows for ease of use and minimal memorization of commands. The code uses the MATLAB environment to produce three dimensional graphics that can be viewed from any position in space that the code user desires. The ray tracing features allow the user to identify the particular elements of the geometry responsible for the field at any point since the ray magnitude and type may be identified.

The BSCV code is in "m-file" form. The code does not require special toolboxes and can be run even with the relatively inexpensive student version of MATLAB. The BSCV code will allow the user to produce presentation level graphics and to run NECBSC all within the same environment. This allows for the seamless operation of the code and for an integrated package useful for electromagnetic compatibility studies.

4.0 AVAILABILITY OF BSCV

Authorized users of NECBSC-2 can obtain BSCV by contacting Dr. Robert Paknys at Concordia University. tel: (514) 848-3013, fax: (514) 848-2802, E-mail: paknys@ece.concordia.ca.

A paper or microfiche copy of the supporting thesis [5] is available from Micromedia Ltd., 165 Hotel de Ville, Place du Portage, Hull, Quebec, Canada J8X-3X2. Telephone: 1-800-567-1914, inside Canada toll free (819) 770-9928, otherwise fax (819) 770-9265.

BSCV is only available to authorized users of The Ohio State University NECBSC-2 code; our distribution of BSCV is contingent upon the prior consent of The Ohio State University.

References

[1] R.J.Marhefka and W.D.Burnside, "Numerical Electromagnetic Code- Basic Scattering Code (version 2), part I: User's Manual, Department of Electrical Engineering, The Ohio State University ElectroScience Laboratory, Tech. Rept. 712242-14, Dec. 1982. Also: R.J.Marhefka, "Numerical Electromagnetic Code- Basic Scattering Code (version 2), part II: Code Manual, Department of Electrical Engineering, The Ohio State University ElectroScience Laboratory, Tech. Rept. 712242-15, prepared under Contract N00123-79-C-1469 for Naval Regional Contracting Office, Dec. 1982.

[2] R.G. Kouyoumijian and P.H. Pathak, "A Uniform Geometrical Theory of Diffraction for an Edge in a Perfectly Conducting Surface," Proc. IEEE, vol. 62, pp. 1448-1461, Nov. 1974.

[3] D. Davis, S.J. Kubina, R. Paknys, "A Ray Tracer for the NEC Basic Scattering Code," ACES 10th Annual Review of Progress in Applied Computational Electromagnetics, vol. II, pp. 388-395, Monterey California, March 1994.

[4] Q.C. Luu, "Numerical Techniques for the Study of HF Coupling Modes on Large Aircraft," Master of Applied Science Thesis, Concordia University Department of Electrical and Computer Engineering, Montreal Quebec, H3G-1M8, March 1994, p. 13, p. 213.

[5] Don Davis, "The Development of a Graphical Pre- and Post Processor with Ray Tracing for the NEC-BSC Code Using a GUI," Master of Applied Science Thesis, Concordia University Department of Electrical and Computer Engineering, Montreal Quebec, H3G-1M8, April 1995, pp. 93-95. ISBN 0-315-013-47-2.

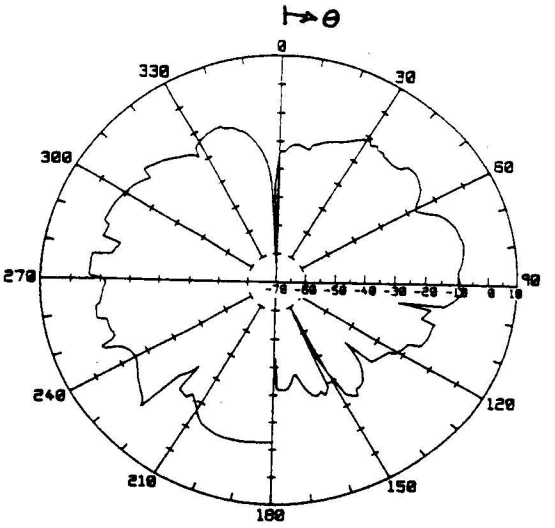

Figure 8 Elevation plane cut of electric field at $\phi = 5$ degrees. (dB scale)

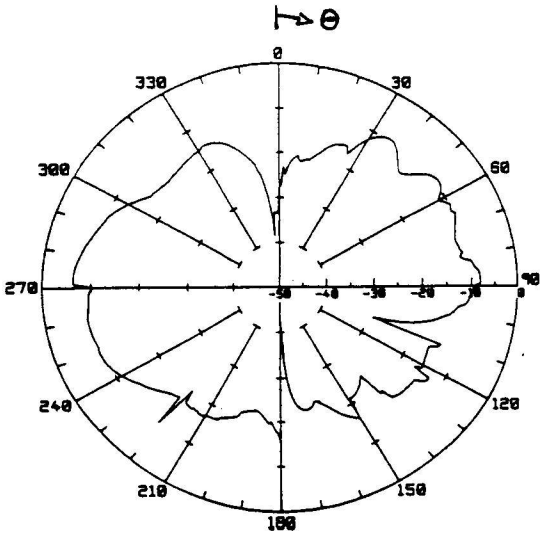

Figure 9 Elevation plane cut of electric field at $\phi = 45$ degrees. (dB scale)

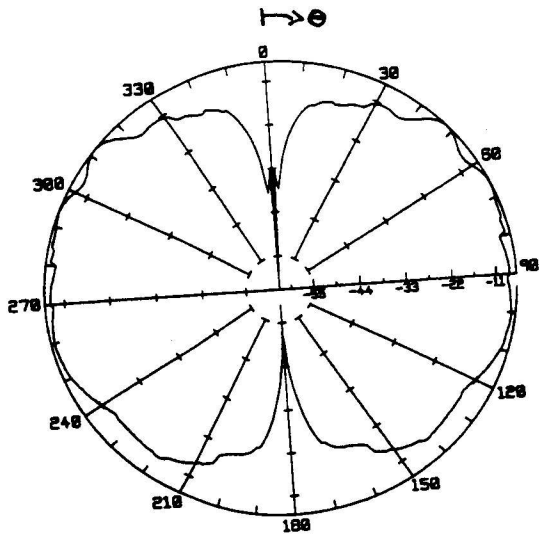

Figure 10 Roll plane cut of electric field at $\phi =$ 90 degrees. (dB scale)

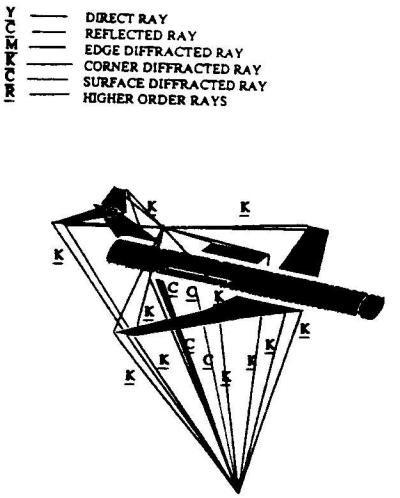

Figure 12 Ray picture at $\phi = 5$ degrees, $\theta = 180$ degrees.

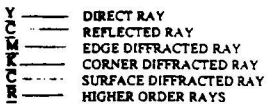

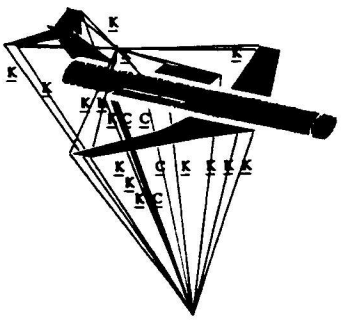

Figure 11 Ray picture at $\phi = 5$ degrees, $\theta = 179$ degrees.

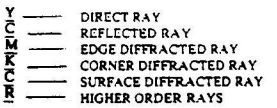

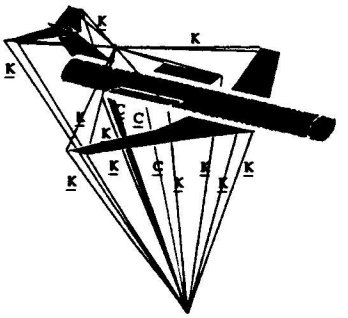

Figure 13 Ray picture at $\phi = 5$ degrees, $\theta = 181$ degrees.

PERSPECTIVES IN CEM

I was happy to be asked to edit the "Perspectives in CEM" column. I plan to bring you a series of interesting points of view from a broad spectrum of electromagnetic issues.

The following is a brief list of issues that I am interested in. If you feel that you could give a useful perspective on any of the issues, especially in relation to your specific area of research, please contact me. I am interested in exploring why so many people only report the possibilities of their work and not the limitations. The limitations are so important as the possibilities and only with a proper perspective of both can you make good decisions about which method/technique you might choose for a specific problem. It seems like we are encouraged to write about how wonderful our research is and to limit any "negative" conclusions or limitations to our work. The reader is left to rediscover limitations on his or her own, even though the author clearly understands the issues in depth.

I am also interested as to why I see so many publications but so little of the published work going into practice. It seems to me there is a void in computational CEM. Industry does not want to generalize algorithms, they want to use them. In academia we invent/discover the algorithms but are not encouraged or rewarded for generalizing the algorithms for practical everyday use. I expect this will change as industry becomes a more significant sponsor of our work, but our journals need to reflect and accept this change.

With the amount of information available today, it seems almost impossible to keep up with all the new techniques. There is certainly not time to investigate all the exciting algorithms and techniques, I would like to see our journals move more towards accurate honest discussions of all of the results of our work, the successes and failures. If we report what we conclude, along with all the things we learned along the way, the journals will become more useful to all readers. With the availability of the world wide web we should be able to publish this information in a concise format for the journals and then encourage readers interested in more specifics to investigate a specific web site. There is obviously much more to be discussed but hopefully the previous comments have started you thinking. Please feel free to contact me with nominations for a "Perspectives in CEM" author or comments regarding a column.

Melinda Piket-May
Perspectives in CEM editor
Campus Box 425
Electrical and Computer Engineering
University of Colorado at Boulder
Boulder, CO 80309-0425

phone: 303-492-7448
fax: 303-492-2758
email: mjp@boulder.colorado.edu

For this issue I bring you the perspective of Richard C. Booton, Jr.. He has seen many changes in electrical engineering through the course of time. I always enjoy conversing with him on the topic of where CEM has been, where it is heading, and where he sees problems or roadblocks. The following is a concise editorial of sorts. Richard expects that some of these comments will inspire discussion. I hope the following perspective makes you think about the direction of CEM, even if you do not agree with the points made. Enjoy!

MY THOUGHTS ON PERSPECTIVES IN COMPUTATIONAL EM

by

Richard C. Booton, Jr.

Melinda asked me to write a few words to express my thoughts on perspectives in computational EM. Rather than write a technical overview, which would require many pages, I decided to concentrate on my personal feelings about several developments.

First, the most obvious thought is that this is a very vigorous field. The steadily increasing power of computers is matched by a steadily increasing attention to algorithms. Both of these increases have lead to increasing realism of the problems being solved. There is some bad news, however, in my opinion. One aspect of computational EM that bothers me is the unceasing introduction of new algorithms (together with their acronyms). The explosion of acronyms, of course, is not restricted to EM. I once tried to remember the meanings of the algorithms encountered in computational EM, but I have given up. The apparent need by many to make a slight change in an existing algorithm and then created a new name with its own acronym seems to me to be regrettable. There is matching good news in the development of new algorithms to remove deficiencies in existing algorithms. The use of vector basis functions in the development of the so-called edge-element version of the finite-element method is a good example. The trick of course is to distinguish between the good news and the bad news, and personal taste undoubtedly plays a part.

The estimated accuracy in computed results still is a largely neglected area, but at long last some attention is being given to statement of accuracy, a subject Ed Miller has pushed for many years. Although a few excellent theory-based error analyses have been carried out, I do not see this as a worthwhile area to pursue because of its lack of generality. Because most errors are quantization errors that should approach zero as the quantization level does. I believe that more useful results can be obtained from convergence studies. Solution of benchmark problems is beginning to offer hope of providing useful results.

Linked to error estimation, at least in my opinion, is the use of Richardson extrapolation. Even though first discussed by Richardson around the time of World War I, its use still seems to be confined to Romberg integration. I fail to see why more general use of this technique has not happened.

More and more engineers are using software packages written by someone else. A serious problem is the need to understand the limitations of software packages, both university-generated and commercial. My personal experiences with programs written by others are not very encouraging in this respect. It seems that the creator of a program is not eager to find and publicize its limitations. Perhaps evaluation by some neutral body would help, but discussions with others have raised ethical and legal questions.

I expect (and hope) that some of these comments are controversial and inspire a response. Discussion of these topics is desirable.

The Practical CEMist

- *practical topics in communications* -

Perry Wheless, K4CWW

My first experience with HF radio communications was in 1960 on the 75-meter (3.8 - 4.0 MHz) amateur radio band. The memory of the formidable summertime static levels remains vivid. The respites of the early morning hours, particularly around sunrise, turned many young radio operators with a penchant for the low bands into either diehard night owls or very early risers. When the quiet, comparatively 'civilized' conditions on 10 meters (28.5 MHz) were discovered a few years later, I quickly developed a preference for the higher bands over fighting the noise level on 75 and 160 meters.

I recently re-activated on 75 meters, and began casually searching for some of my old colleagues. Indeed, some were still at it after all these years! Tom McLees, W5FV, frequents 3.777 MHz and, while I fought the static level with a modified Windom, Tom and several of the 3777 regulars told of their transition to using special antennas, dedicated to receive mode, which had brought them an impressive degree of relief from the low-band static nemesis. Tom has named this class of wire receiving antennas *snakes* because they either lie on their bellies on the ground or (more often) are buried just below the earth's surface. Employment of the *snake* has spread from the 75-meter to 160-meter community, and their numbers are now considerable.

Several accounts of this antenna agree that attributes of the *snake* are quite significant in this practical communications context. At present, they are 'optimized' by trial-and-error, and all the users I have spoken with have expressed a desire to have a computer-based analysis tool for this antenna type which will produce accurate and reliable performance predictions.

The experimenters are now using coaxial cable sections, with various characteristic impedance values, lengths, and terminations. It appears, however, that the logical beginning point for analysis is with rudimentary center-fed and end-fed buried insulated wire elements, terminated with either an open circuit or a matched load. The paper which follows presents the component equations which describe these initial cases of interest. Only the buried antenna case is treated, as a wire precisely at the air-earth interface is both a more difficult and avoidable case. The equations are well-suited to computer implementation, and numerical results will be presented in a later paper.

Wire antennas of this generic class have been known for many decades. However, a comprehensive scientific explanation of their performance in this specific application context remains incomplete. The paper which follows provides essential model details necessary for interested individuals to pursue this topic as an academic investigation without the need for access to advanced versions of NEC.

Submission of measured data, NEC-3I models, static burst characterizations, etc., is invited as the overall problem is analyzed in progressive steps. Interested parties and prospective authors (on this or other subjects) should address correspondence to the following address:

Perry Wheless
P.O. Box 11134
Tuscaloosa, AL USA 35486

Components of an Analytical Model for *Snake* Antennas

W. Perry Wheless, Jr. and Larry T. Wurtz
Department of Electrical Engineering
University of Alabama
Tuscaloosa, AL 35487
e-mail wwheless@ua1vm.ua.edu

25 May 1997

Abstract

Several variations of buried wire antennas, here called the *snake* type, have been popularized as receiving antennas by experimentalists at frequencies near 1.9 and 3.8 MHz in recent years. The *snake* has been found empirically to reduce static levels far more than desired incoming radio signals at these frequencies, improving overall communications link performance. This paper presents the governing equations which comprise an analytical model for the most fundamental *snake* forms. Radiation patterns and other numerical results will be presented in a later paper.

1. Introduction

Naturally occurring static has been historically problematic for practical MF and HF communicators. Static levels especially affect operations below approximately 7 MHz, and seasonally higher levels prevail from late Spring, through the summer months, and into early or mid-Fall. This phenomenon seriously afflicts the 80 and 160-meter amateur radio bands during the stormy warm-weather months.

Recently, buried wire elements have been popularized by experimentalists for receiving antennas at these frequencies. These buried receiving antennas are referred to here as members of the *snake* antenna class, and they are now in relatively widespread use in the amateur bands about 1.9 and 3.8 MHz. Empirical results have clearly established that *snake* antennas attenuate static far more than desired incoming radio signals at these frequencies. For example, **improvement** in signal-to-static level by switching from a typical above-ground antenna

to a *snake* is frequently greater than 20 dB! The improvement is generally quite significant.

2. *Snake* Modeling

Both present and potential users of the *snake* desire a computer-based modeling capability for optimizing antenna details to their individual requirements.

The earliest version of the Numerical Electromagnetics Code (NEC) which has provisions for reliable analysis of buried, insulated wires is NEC-3I [1]. It is practical, therefore, to employ NEC for modeling this particular antenna type. NEC-2 remains the kernel of most common availability, however, and NEC-2 is not equipped to solve this class of buried wire problems. Therefore, a reasonably accurate analytical model suitable for personal computer (PC) implementation becomes a desirable objective.

The subject receiving antennas of interest are simple single-element buried antennas. A more ambitious buried antenna analytic modeling program was described in 1989 [2]. The Communications System Division of Eyring, Inc., developed and marketed a series of buried antennas, including multi-element array configurations, before the Division was deactivated. Eyring holds several patents in this area, including U.S. Patents 4,743,917, 4,750,001, 4,809,010, and 4,825,224. The fundamental governing equations presented in this paper are available, or directly follow, from the scientific literature, and the intent is to stimulate academic study of this class of antennas by individuals. The reader should utilize results of the component equations presented here for personal education and experimentation only, and avoid other uses which could infringe on the existing U.S. patents held by Eyring, Inc.

3. Cases of Interest

It is assumed that the buried wire is straight, and aligned along the x-axis as illustrated in Figure 1. ϕ denotes azimuth angle, measured CCW from the +x axis. θ denotes elevation angle, with $\theta = 0$ representing the air-earth interface plane, taken to be (locally) horizontal. The vertical E-field component is taken by definition to be E_θ and, similarly, the horizontal component is taken to be E_ϕ. The total, or mixed polarization, E-field is then given by $\sqrt{E_\theta^2 + E_\phi^2}$.

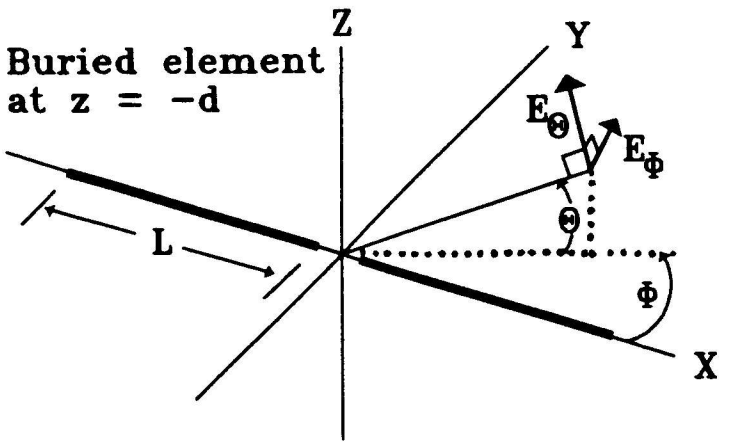

Figure 1. Basic *snake* antenna geometry.

There are two deployments of interest here - unidirectional and bidirectional - as illustrated in Figure 2.

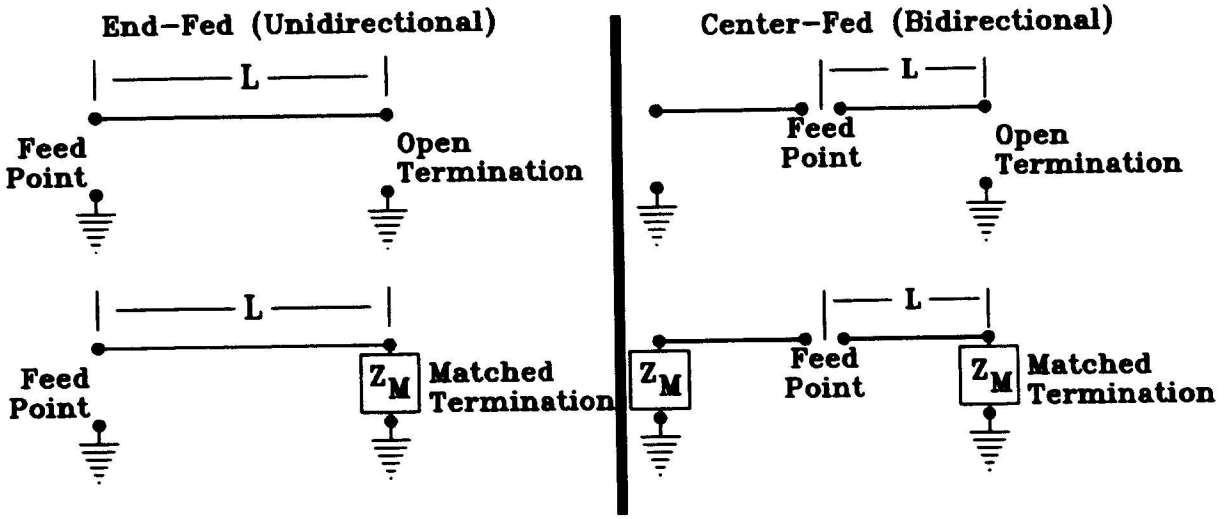

Figure 2. Unidirectional and bidirectional deployments.

For skywave pattern calculations, both E_θ and E_ϕ are relevant. For groundwave, however, only E_θ need be considered. Hence, a total of twelve cases are treated in this report:

CASE	FIELD	COMPONENT	FEED	TERMINATION
1	sky	E_θ	center	open
2	sky	E_ϕ	center	open
3	sky	E_θ	center	matched
4	sky	E_ϕ	center	matched
5	sky	E_θ	end	open
6	sky	E_ϕ	end	open
7	sky	E_θ	end	matched
8	sky	E_ϕ	end	matched
9	ground	E_θ	center	open
10	ground	E_θ	center	matched
11	ground	E_θ	end	open
12	ground	E_θ	end	matched

4. Input Impedance

The antenna element wire is assumed to be a perfect conductor. Also, it is assumed that

$$\left|\frac{\hat{\epsilon}_2}{\hat{\epsilon}_i}\right| \geq 1.2 \tag{4.1}$$

where the complex ground permittivity is $\hat{\epsilon}_2 = \epsilon_{r2} - j\dfrac{\sigma_2}{\omega\epsilon_0}$ and $\hat{\epsilon}_i$ is the similar complex permittivity of the antenna wire insulation. ϵ_{r2} and ϵ_{ri} are the respective dielectric constants, and the conductivities σ_2, σ_i have units of S/m. Region 1 is air, and region 2 is earth, denoted with subscripts.

Input impedance Z_i for cases 1, 2, and 9 (center fed, with open termination) [Reference: King and Smith, p. 509 (4.16)] is

$$Z_i = j2Z_{AC}\left[\frac{1 + jtan\,(\beta\ell)\,tanh\,(\alpha\ell)}{-tan\,(\beta\ell) + jtanh\,(\alpha\ell)}\right] \tag{4.2}$$

where β is the phase constant, in radians/m, and α is the attenuation constant, in Np/m, in the complex propagation constant $\gamma = \beta - j\alpha$ (see below). An end-fed element has length ℓ, so the overall length of a center-fed *snake* is 2ℓ. Factor Z_{AC} is computed from [Reference: King and Smith, p. 510 (4.22)]

$$Z_{AC} = 60\frac{\gamma}{k_1}\left[\frac{ln\left(\frac{b}{a}\right)}{\hat{\epsilon}_i} + \frac{H_0^{(2)}(k_2 b)}{\hat{\epsilon}_2 (k_2 b) H_1^{(2)}(k_2 b)}\right] \tag{4.3}$$

with a and b denoting, respectively, the antenna wire radius and wire insulation radius, both in meters. The propagation constant γ is from

$$\gamma = k_1\sqrt{\hat{\epsilon}_2}\left[\frac{H_0^{(2)}(k_2 b) + H_0^{(2)}(2k_2|-d|) + (k_2 b)\, ln\left(\frac{b}{a}\right) H_1^{(2)}(k_2 b)}{H_0^{(2)}(k_2 b) + \frac{\hat{\epsilon}_2}{\hat{\epsilon}_i}(k_2 b)\, ln\left(\frac{b}{a}\right) H_1^{(2)}(k_2 b)}\right], \tag{4.4}$$

[Reference: King and Smith, p. 509 (4.19), p. 510 (4.21), and R.W.P. King, p. 1 (1 – 6)] in which d (a positive number) is the depth of the *snake* antenna element below the air-earth interface, in meters.

For cases 5, 6, and 11 (end fed with open termination) the input impedance expression becomes [Reference: King and Smith, p. 509 (4.16)]

$$Z_i = jZ_{AC}\left[\frac{1 + jtan(\beta\ell)\, tanh(\alpha\ell)}{-tan(\beta\ell) + jtanh(\alpha\ell)}\right]. \tag{4.5}$$

For cases 7, 8, and 12 (end fed with matched termination)

$$Z_i = Z_{AC} \tag{4.6}$$

[Reference: King and Smith, p. 514 (6.2)] and, by the same reference, cases 3,4, and 10 (center fed with matched termination) are governed by

$$Z_i = 2Z_{AC}. \tag{4.7}$$

5. Antenna Power Gain $\mathbf{G}(\Theta, \Phi)$

After [5], an approach well-suited to computer implementation is to calculate the skywave and groundwave power gains, as functions of elevation angle θ and azimuth angle ϕ, from a cascade of appropriate multiplicative factors:

$$G(\theta, \phi) = F_1 F_2 F_3 F_4 F_5. \tag{5.1}$$

Factor F_1 depends on the antenna input resistance, and makes the computed gain relative to isotropic. F_2 is the Fresnel transmission coefficient in the skywave case, and interface loss factor in general. F_3 is the pattern factor for a Hertzian current

element. Factor F_4 is from integration of currents along the length of the antenna element. Finally, factor F_5 accounts for depth attenuation associated with the buried antenna element.

The governing equations are presented in the following subsections. Important **note:** the Lavrov and Knyazev reference uses α for the phase constant and β for the attenuation constant, which is opposite to the prevailing U.S. convention.

5.1. Factor F_1 (Scale Factor)

There are two relevant forms for this factor. First, for cases 1-8 (skywave radiation)

$$F_1 = \frac{30}{Re\,(Z_i)} = \frac{30}{R_i} \tag{5.2}$$

[Reference: Lavrov and Knyazev, V. 3.10] and, by the same reference plus Hasserjian and Guy, p. 229 (17), for cases 9-12 (groundwave) the appropriate factor is

$$F_1 = \frac{120}{R_i}. \tag{5.3}$$

5.2. Factor F_2 (Interface Loss Factor)

Three forms of F_2 apply to the various cases of interest here. For cases 1, 3, 5, and 7 (skywave E_θ) [Reference: Lavrov and Knyazev, I. 1.20, V. 3.13, 3.21, 3.23]

$$F_2 = \left| 1 - \frac{\hat{\epsilon}_2 sin\theta - \sqrt{\hat{\epsilon}_2 - cos^2\theta}}{\hat{\epsilon}_2 sin\theta + \sqrt{\hat{\epsilon}_2 - cos^2\theta}} \right|^2 . \tag{5.4}$$

The form applicable to cases 2, 4, 6, and 8 (skywave E_ϕ) is

$$F_2 = \left| 1 + \frac{sin\theta - \sqrt{\hat{\epsilon}_2 - cos^2\theta}}{sin\theta + \sqrt{\hat{\epsilon}_2 - cos^2\theta}} \right|^2 \tag{5.5}$$

[Reference: Lavrov and Knyazev, I. 1.21, V. 3.14, 3.22, 3.24].

For groundwave E_θ calculations (cases 9-12), this factor becomes

$$F_2 = \left| \frac{\frac{k_1^2}{k_2^2}\left(1 - \frac{k_1^2}{k_2^2}\right)}{\frac{k_1^2}{k_2^2}\left(1 - \frac{k_1^2}{k_2^2}\right) + 1} \right| \tag{5.6}$$

[Reference: Lavrov and Knyazev, I. 2.20 and V. 3.12, 3.16-3.20].

5.3. Factor F_3 (Hertzian current element pattern)

This factor for skywave E_θ (cases 1, 3, 5, and 7) is

$$F_3 = sin^2\theta cos^2\phi \tag{5.7}$$

[Reference: Lavrov and Knyazev, V. 3.13, 3.21, 3.23]. For skywave E_ϕ calculation (cases 2, 4, 6, and 8), this becomes

$$F_3 = sin^2\phi \tag{5.8}$$

[Reference: Lavrov and Knyazev, V. 3.14, 3.22, 3.24]. For remaining cases 8-12, all for groundwave E_θ [Reference: Lavrov and Knyazev, V. 3.12, 3.18-3.20] :

$$F_3 = cos^2\phi. \tag{5.9}$$

5.4. Factor F_4 (Integrated Pattern Factor)

Factor F_4 is the most tedious to document and program. Again, four variations are required to cover all the cases of interest. Straightaway, then, let us begin with the proper form for cases 1, 2, and 9 (center fed, open termination):

$$F_4 = 8\left[\frac{\frac{\alpha^2}{k_1^2}+\frac{\beta^2}{k_1^2}}{\left(\frac{\beta^2}{k_1^2}-\frac{\alpha^2}{k_1^2}-cos^2\theta cos^2\phi\right)^2+4\frac{\alpha^2\beta^2}{k_1^4}}\right]\left[\frac{A_4^2+B_4^2}{cosh\,(2\alpha\ell)-cos\,(2\beta\ell)}\right] \tag{5.10}$$

where

$$\begin{aligned} A_4 &= cos(k_1\ell cos\theta cos\phi) - cos\,(\beta\ell)\,cosh\,(\alpha\ell) \\ B_4 &= sin\,(\beta\ell)\,sinh\,(\alpha\ell) \end{aligned}$$

[Reference: Lavrov and Knyazev, V. 3.21]. For cases 3, 4, and 10 (center fed, matched termination) [Reference: Lavrov and Knyazev, IV. 1.8, V. 1.26, V. 3.10-3.14, V. 3.16-3.24],

$$F_4 = 4\left[\frac{\frac{\alpha^2}{k_1^2}+\frac{\beta^2}{k_1^2}}{\left(\frac{\beta^2}{k_1^2}-\frac{\alpha^2}{k_1^2}-cos^2\theta cos^2\phi\right)^2+4\frac{\alpha^2\beta^2}{k_1^4}}\right]\left[A_6^2+B_6^2\right] \tag{5.11}$$

with

$$A_6 = \begin{cases} e^{-\alpha\ell}\{cos(\beta\ell)\, cos(k_1\ell cos\theta cos\phi) + \dfrac{k_1 cos\theta cos\phi}{\alpha^2+\beta^2} sin(k_1\ell cos\theta cos\phi) \times \\ [\beta sin(\beta\ell) - \alpha cos(\beta\ell)]\} - 1 \end{cases}$$

$$B_6 = \begin{cases} e^{-\alpha\ell}\{sin(\beta\ell)\, cos(k_1\ell cos\theta cos\phi) + \dfrac{k_1 cos\theta cos\phi}{\alpha^2+\beta^2} sin(k_1\ell cos\theta cos\phi) \times \\ [\beta cos(\beta\ell) + \alpha sin(\beta\ell)]\} \end{cases}$$

The third variation of F_4 applies to cases 5, 6, and 11 (end fed, open termination):

$$F_4 = 2\left[\frac{\frac{1}{k_1^2}}{\left(\frac{\beta^2}{k_1^2} - \frac{\alpha^2}{k_1^2} - cos^2\theta cos^2\phi\right)^2 + 4\frac{\alpha^2\beta^2}{k_1^4}}\right]\left[\frac{A_7^2 + B_7^2}{cosh(2\alpha\ell) - cos(2\beta\ell)}\right] \tag{5.12}$$

with

$$A_7 = \begin{cases} \beta[cos(k_1\ell cos\theta cos\phi) - cos(\beta\ell)\, cosh(\alpha\ell)] + \alpha[sin(k_1\ell cos\theta cos\phi) \\ -sin(\beta\ell)\, sinh(\alpha\ell)] - k_1 cos\theta cos\phi cos(\beta\ell)\, sinh(\alpha\ell) \end{cases}$$

$$B_7 = \begin{cases} \beta[sin(k_1\ell cos\theta cos\phi) - sin(\beta\ell)\, sinh(\alpha\ell)] - \alpha[cos(k_1\ell cos\theta cos\phi) \\ +cos(\beta\ell)\, cosh(\alpha\ell)] - k_1 cos\theta cos\phi sin(\beta\ell)\, cosh(\alpha\ell) \end{cases}$$

in accord with [Reference: Lavrov and Knyazev, IV. 1.8, V. 1.26, V. 3.10-3.14, V. 3.16-3.24].

Finally, for cases 7, 8, and 12 (end fed with matched termination),

$$F_4 = \frac{\left[e^{-\alpha\ell}cos(\beta\ell - k_1\ell cos\theta cos\phi) - 1\right]^2 + \left[e^{-\alpha\ell}sin(\beta\ell - k_1\ell cos\theta cos\phi)\right]^2}{\left(\frac{\beta}{k_1} - cos\theta cos\phi\right)^2 + \frac{\alpha^2}{k_1^2}} \tag{5.13}$$

[Reference: Lavrov and Knyazev, V. 3.23].

5.5. Factor F_5 (Depth Attenuation Factor)

A common factor for depth attenuation applies to all twelve cases of interest, as they are all buried elements [Reference: Lavrov and Knyazev, V. 3.12-3.15] :

$$F_5 = e^{-2k_1|-d|\cdot Imag\sqrt{\hat{\epsilon}_2 - cos^2\theta}}.$$

6. Concluding Remarks

It should be noted that exact formulation of the governing equations for the buried *snake* antenna is exceedingly difficult. Therefore, the analytical model component equations are approximations developed by the given references for propagation constant, characteristic impedance, input impedance, and power gain radiation patterns. Approximations, as always, are predicated on an allowable range of input parameter values, and interested readers are directed to the references for more details regarding validity restrictions.

Ancillary equations describing ground parameter dependence on frequency and groundwave field strength will become relevant in future developments of this subject, but are omitted here in the interest of conserving space.

Computed impedances and patterns will appear in a later paper. Radio experimenters and owners of NEC-3I (and later) NEC codes are invited to participate in making *snake* antenna design a reliable process for all prospective users of this antenna type by submission of their measured data and CEM results.

7. Acknowledgments

The contributions of David Faust and the Communications Division of Eyring, Inc., to the content of this paper are gratefully acknowledged. Their extensive earlier work may allow devotees of the 80 and 160-meter amateur bands, and other low-frequency practical communicators, to lessen the persistent toll of static (QRN) on their ears in the future!

Buried wires have been known as a generic class of antennas for many years, but this specific communications application merits a name for convenient reference. The authors thank Tom McLees, W5FV, for his contribution of the *snake* moniker.

References

[1] G.J. Burke and A.J. Poggio, *Numerical Electromagnetics Code (NEC) - Method of Moments*, Naval Ocean Systems Center Technical Document 116, January 1981.

[2] R.B. Gilchrist, P.O. Berrett, B. Grose, M.B. King, and D.L. Faust, "A buried antenna analytic modeling program - PAT6," presented at the 5^{th} *Annual Review of Progress in Applied Computational Electromagnetics*, Monterey, CA, 1989 (Abstract only published in the *Proceedings*, p. 373).

[3] R.W.P. King and G.S. Smith, *Antennas in Matter*, MIT Press, Cambridge, MA, 1982.

[4] R.W.P. King, "Antennas in material media near boundaries with application to communication and geophysical exploration, Part II: The terminated insulated antenna," *IEEE Transactions on Antennas and Propagation*, vol. AP-34, no. 4, pp. 490-496, April 1986.

[5] M.B. King, R.B. Gilchrist, and D.L. Faust, *Eyring Low Profile and Buried Antenna Modeling Program*, Eyring (preliminary) Document 300-0085A, June 1991.

[6] G.A. Lavrov and A.S. Knyazev, *Near Earth and Buried Antennas*, Sovetskoye Radio, Moscow, 1965 (translated by the Joint Publications Research Service, U.S. Department of Commerce, Washington, D.C.).

[7] G. Hasserjian and A.W. Guy, "Low frequency subsurface antennas," *IEEE Transactions on Antennas and Propagation*, vol. AP-11, no. 5, pp. 225-231, May 1963.

Tutorial Article

Professor William T. Smith, Rodney D. Slone, and Dr. Sudip K. Das have contributed "Recent progress in reduced-order modeling of electrical interconnects using asymptotic waveform evaluation and Pade' approximation via the Lanczos process" for this issue of the newsletter.

Dr. William T. Smith is an associate professor in the Department of Electrical Engineering at the University of Kentucky. He received his BSEE from the University of Kentucky in 1980. From 1981 to 1984, he worked as an RF engineer for Harris Corporation in Melbourne, Florida. He earned his MSEE and PhDEE degrees from Virginia Tech in 1986 and 1990, respectively. He was employed by the Satellite Communications Group while at Virginia Tech. Dr. Smith joined the faculty at UK in 1990. During the summers of 1991 and 1992, Dr. Smith was a NASA/ASEE Summer Faculty Fellow at NASA Langley Research Center in Hampton, Virginia. His research interests lie in the areas of electromagnetic compatibility and antennas. He is a member of IEEE and ASEE, and is an associate member of URSI.

Rodney Daryl Slone was born on January 13, 1975 in Martin, Floyd County, KY. He graduated from the June Buchanan High School in 1993. He finished a BSEE with a double major in Mathematics at the University of Kentucky in 1996. As an undergraduate, he was a National Merit Scholar, a National Science Scholar, a Robert C. Byrd Scholar and received scholarships from the University of Kentucky. He was supported by the National Science Foundation during the summer of 1995 to research vibrating transmission lines. He was supported by fellowships from the University of Kentucky to pursue a Master's Degree in Electrical Engineering. Mr. Slone's areas of interest are computational electromagnetics, numerical analysis and electromagnetic compatibility. He is a member of IEEE (AP, EMC, and MTT Societies) and has served as a member of the EMC-S TC-9 (Computational EMC). He also served as a technical paper reviewer for the 1996 IEEE International Symposium on EMC.

Dr. Sudip K. Das (S'93-M'95) was born in Calcutta, India. He received the degree of Bachelor of Technology in Electronics and Electrical Communication Engineering from the Indian Institute of Technology, Kharagpur, India in 1990. He obtained his M.S. and Ph.D degrees in Electrical Engineering from the University of Kentucky, Lexington, in 1992 and 1995, respectively. His graduate education and research were funded by graduate assistantships and research assistantships sponsored by the University of Kentucky and Ford Motor Company. From 1990 to 1995 he conducted research in the areas of lossy bus structures, crosstalk and numerical modeling of high speed interconnects. In 1995 he joined Sun Microsystems as an EMC engineer. His current research interests include analysis and numerical modeling of various EMI problems in low cost computer platforms and high-end servers. He is also working on developing Sun's internal EMC guidelines. Dr. Das has published and presented several papers in international conferences. He is also a member of Eta Kappa Nu.

Recent Progress in Reduced–Order Modeling of Electrical Interconnects Using Asymptotic Waveform Evaluation and Padé Approximation Via the Lanczos Process

William T. Smith
Dept. of Electrical Engineering
University of Kentucky
Lexington, Kentucky

Rodney D. Slone
Dept. of Electrical Engineering
University of Kentucky
Lexington, Kentucky

Sudip K. Das
Sun Microsystems Computer Corp.
Mountain View, California

Abstract

There has been a great deal of interest in the EM community to use reduced–order modeling to dramatically improve computational efficiency. The EM research primarily falls under the broad umbrella of Model–Based Parameter Estimation (MBPE). Since the late 80's and early 90's, there has been a parallel effort ongoing in the circuits CAD/CAE area for design of integrated circuits and multi–chip modules. Increased clock speeds have forced designers to move to more advanced modeling approaches involving, for example, quasi–TEM multiconductor transmission line analysis and now full–wave techniques. The approaches developed in the EM area (MBPE) and the techniques from the circuits area are very similar and sometimes overlap. Recently some researchers have been formulating EM analysis techniques based on papers published in the circuits community. This tutorial is primarily a survey of the techniques developed in the circuits area involving interconnect modeling with references to some of the recent EM applications. The two methods reviewed here are Asymptotic Waveform Evaluation (AWE) and Padé approximation Via the Lanczos process (PVL). These are two ways to formulate Padé approximants of a system response by matching the moments of the approximant to the actual response. AWE and PVL are compared and some exemplary results are shown to illustrate the types of problems they have been used to analyze.

1. Introduction

Signal simulations for high–speed printed circuit boards, multi–chip modules and peripheral cables present challenging problems for development of CAE tools. The inhomogeneity and high density of electrical interconnects inherently require large systems of equations to accurately represent the circuits. Nonlinear devices and frequency dependent parameters such as conductor loss add to the complexity of the circuit models. At higher frequencies, the interconnects may be electrically large compared to a wavelength which necessitates inclusion of signal retardation. In addition, the high clock speeds coupled with fast rise and fall times impose the need for wideband solutions ranging in frequency from DC to several GHz.

Conventional differential equation solvers will, in most cases, require a great deal of CPU time if presented with a complex circuit model. Prohibitively long simulation times will render a CAE tool useless to a designer. Speeding up simulations motivated the need for finding alternative approximate solution techniques that could still provide reasonably accurate results. The need for accurate yet efficient solution algorithms served as part of the motivation for the development of Asymptotic Waveform Evaluation (AWE) in which a low order approximation of the system response is formulated [4]. The name indicates that as the order of the approximation is increased, the approximate response begins to "asymptotically" approach that of the actual system response [5].

The AWE formulation provides straightforward efficient circuit analysis in either the time or frequency domains. AWE simulations are often orders of magnitude faster than conventional circuit solvers. In AWE analysis, the transfer functions are expanded into series and moment matching is used to approximate the circuit models with lower–order transfer functions. The responses of transfer functions for circuits depend on the systems' poles and residues. AWE extracts the dominant poles and associated residues using Padé approximations. One of the most important benefits of a Padé approximant is its ability to define a convergent function beyond the radius of convergence for the power series [8]. An example of the series convergence for moment matching analysis of electrical interconnects is given in [19]. In electrical engineering, this means that the Padé approximation of a transfer function will be more broadband than a series solution of the response. With high speed clocks and fast signal transients, this broadband characteristic is especially beneficial. Moment matching has previously been used in circuit analysis and similar techniques have also been used to evaluate the response of full–wave electromagnetic models (for example, see [20,21,22,23,24,25]).

The Padé approximation is essentially decomposed into partial fractions, yielding the poles and residues of an approximate system response. This decomposition allows for a straightforward transformation to the time domain. Using AWE, the transfer functions of system models for electrical interconnects are approximated by matching the first $2q$–1 moments of exact solutions to lower q–order models [4,6,7].

Calculation of the poles and residues in AWE is inherently a challenging computational problem. The circuit parameters encountered in interconnect analysis range in value from pF to kohm which causes ill–conditioning of the system matrices. The Padé approximation requires several digits of accuracy for pole calculation. Maintaining the accuracy requires using techniques such as complex frequency hopping [10] and scaling [12].

Overcoming some of the computational difficulties encountered in AWE served in part as motivation for the development of the Padé Via Lanczos (PVL) algorithm [18]. In PVL analysis, the moment matching is not explicitly performed. The poles and residues are formed by extracting quantities generated by a PVL algorithm. PVL is capable of accurately extracting several more poles per expansion point than AWE. Each pole extracted with either PVL or AWE has a similar computational cost [18].

In this paper, general formulations for AWE and PVL are presented. Section 2 presents some of the basics of Padé approximants as they apply to interconnect simulations. This serves as the lead in to discussion of AWE and PVL. The pole/residue calculation for AWE is discussed in Section 3. Several recent applications of AWE are listed along with a basic AWE formulation which closely follows the discussion in Section 2. The accuracy and efficiency of AWE are illustrated through examples from previous works. The recent applications of PVL to interconnect analysis are discussed in Section 4 along with a version of the PVL algorithm typically used for circuit simulation. The formulation of the Padé approximation using Lanczos quantities is then derived. The stability and accuracy of the PVL algorithm when computing several poles and residues are illustrated, again, with examples from previous works. Summary and conclusions are presented in Section 5.

2. Padé Approximants

The key to reducing system models is to extract the dominant poles and associated residues of the response. In AWE and PVL analysis, this is accomplished by forming Padé approximants. A large body of work can be found relating to theories and applications of Padé approximations. A very good reference on Padé approximants is [8]. In [10], a summary of Padé approximant calculations and properties as they pertain to electrical interconnect analysis is presented. The following general discussion of Padé approximants is in large part taken from both [8] and [10]. To be consistent with the applications in electrical engineering, the functions will be variables of the Laplace complex frequency s.

A Padé approximant is a rational approximation of a power series. Given a power series

$$F(s) = \sum_{k=0}^{\infty} c_k s^k \quad , \tag{1}$$

the Padé approximant for that power series is defined as

$$\hat{F}(s) = [L/M] = \frac{a_0 + a_1 s + a_2 s^2 + \ldots + a_L s^L}{b_0 + b_1 s + b_2 s^2 + \ldots + b_M s^M} \tag{2}$$

where the $[L/M]$ notation from [8] is used to define the orders of the polynomials. Typically, the choice of $b_0 = 1$ is made to remove an arbitrary constant of proportionality between the numerator and denominator coefficients. In general, L is usually less than or equal to M. In the electrical interconnect analysis, it is common to generate Padé approximants in which the denominator is a polynomial of one order higher than the numerator, i.e., $[q-1/q]$. However, the orders of the polynomials may differ depending on the application. The remaining discussion in this paper is based on a $[q-1/q]$ approximation in which there is no direct feed–through from the input to the output.

The $2q$ unknown coefficients are determined by equating (1) and (2) giving

$$F(s) = \sum_{k=0}^{\infty} c_k s^k = \frac{a_0 + a_1 s + a_2 s^2 + \ldots + a_{q-1} s^{q-1}}{1 + b_1 s + b_2 s^2 + \ldots + b_q s^q} + O\left(s^{2q}\right) \tag{3}$$

Equation (3) shows the approximation (2) to have an error on the order of $O\left(s^{2q}\right)$. The unknown a_i's and b_j's are determined by matching (2) to the moments of (1). Since there are $2q$ unknown coefficients, the Padé approximation should match the series (1) out to the s^{2q-1}–term [8].

Cross–multiplying (1) and (2) gives

$$\begin{aligned}(1 + b_1 s + b_2 s^2 + \ldots + b_q s^q)\,(c_0 + c_1 s + c_2 s^2 + \ldots + c_{2q-1} s^{2q-1}) \\ = a_0 + a_1 s + a_2 s^2 + \ldots + a_{q-1} s^{q-1}\end{aligned} \tag{4}$$

Equating the like–power terms for s^q through s^{2q-1} gives a system of q equations for determining the unknown b_j's

$$\begin{bmatrix} c_0 & c_1 & c_2 & \cdots & c_{q-1} \\ c_1 & c_2 & c_3 & \cdots & c_q \\ c_2 & c_3 & c_4 & \cdots & c_{q+1} \\ \vdots & \vdots & \vdots & & \vdots \\ c_{q-1} & c_q & c_{q+1} & \cdots & c_{2q-2} \end{bmatrix} \begin{bmatrix} b_q \\ b_{q-1} \\ b_{q-2} \\ \vdots \\ b_1 \end{bmatrix} = - \begin{bmatrix} c_q \\ c_{q+1} \\ c_{q+2} \\ \vdots \\ c_{2q-1} \end{bmatrix} \tag{5}$$

The a_i's are determined by equating the like–power terms of s^0 through s^{q-1}

$$\begin{aligned} a_0 &= c_0 \\ a_1 &= c_1 + b_1 c_0 \\ a_2 &= c_2 + b_1 c_1 + b_2 c_0 \\ a_3 &= c_3 + b_1 c_2 + b_2 c_1 + b_3 c_0 \\ &\vdots \\ a_{q-1} &= c_{q-1} + \sum_{i=1}^{q-1} b_i \, c_{q-i-1} \end{aligned} \tag{6}$$

In AWE analysis, the rational form of $\hat{F}(s)$ from (2) is factored using partial fraction expansion. The partial fraction expansion allows for straightforward evaluation of the system response in either the time or frequency domains through use of the Laplace transform [10]. For unique roots of the denominator, (2) may be rewritten as

$$\hat{F}(s) = \sum_{j=1}^{q} \frac{\hat{k}_j}{s - \hat{p}_j} \tag{7}$$

where the $\hat{p}_j$ are the approximate system poles and the $\hat{k}_j$ are the corresponding residues. The AWE calculation of the poles and residues is discussed in Section 3. Using a PVL algorithm, the approximate poles and residues are generated from quantities associated with the Lanczos iteration without explicit formulation of (2) using moment matching. The PVL calculation of the poles and residues is covered in Section 4. Using the inverse Laplace transform, the time–domain function corresponding to (7) is

$$\hat{f}(t) = \sum_{j=1}^{q} \hat{k}_j \, e^{\hat{p}_j t} \tag{8}$$

Equations (7) and (8) correspond to the impulse response of a system. The responses to other singularity functions of interest are shown in Table I. For linear systems, an arbitrary input waveform may be decomposed into a sum of these singularity functions and the output will be a superposition of these responses as suggested in [10]. The k_∞–terms allow for direct coupling between the input and output.

Caution must be emphasized in the numerical analysis associated with Padé approximants. The accuracy of the pole calculations depends very strongly upon highly accurate calculation of the moments c_j. When using AWE, there are many issues which must be addressed to ensure the accuracy of the lower order model. These issues are outlined in Section 3. The PVL algorithm overcomes many of these issues at a similar computational cost [18].

3. Asymptotic Waveform Evaluation (AWE)

AWE Applications

AWE is a method of approximating a large network possibly consisting of hundreds of poles with a smaller set of approximate poles and residues [10]. The motivation behind the development of AWE was to formulate a method which can produce a simplified solution of a complex interconnect network and obtain the transient response using considerably less CPU time than conventional circuit simulators. Though

TABLE I

SYSTEM RESPONSES TO SINGULARITY FUNCTIONS

Input function	Response	
$(t \rightarrow s)$	$h(t)$	$H(s)$
Impulse $\delta(t) \rightarrow 1$	$k_\infty \delta(t) + \sum_{j=1}^{q} k_j e^{p_j t}$	$k_\infty + \sum_{j=1}^{q} \frac{k_j}{s - p_j}$
Step $u(t) \rightarrow \frac{1}{s}$	$k_\infty u(t) + \sum_{j=1}^{q} \frac{k_j}{p_j} \left(e^{p_j t} - u(t)\right)$	$\frac{k_\infty}{s} + \sum_{j=1}^{q} \frac{k_j}{p_j} \left(\frac{1}{s - p_j} - \frac{1}{s}\right)$
Ramp $t\,u(t) \rightarrow \frac{1}{s^2}$	$k_\infty t\,u(t) + \sum_{j=1}^{q} \frac{k_j}{p_j} \left(\frac{e^{p_j t}}{p_j} \frac{u(t)}{p_j} - t\,u(t)\right)$	$\frac{k_\infty}{s^2} + \sum_{j=1}^{q} \left(\frac{k_j}{p_j^2} \frac{1}{s - p_j} - \frac{k_j}{s p_j^2} - \frac{k_j}{s^2 p_j}\right)$
Exponential $(\alpha \neq p_j)$ $e^{\alpha t} \rightarrow \frac{1}{s - \alpha}$	$k_\infty e^{\alpha t} + \sum_{j=1}^{q} \left(\frac{k_j}{\alpha - p_j} e^{\alpha t} - \frac{k_j}{\alpha - p_j} e^{p_j t}\right)$	$\frac{k_\infty}{s - \alpha} + \sum_{j=1}^{q} \left(\frac{k_j/(\alpha - p_j)}{s - \alpha} - \frac{k_j/(\alpha - p_j)}{s - p_j}\right)$

circuits may contain large numbers of poles and residues, all poles and residues do not contribute equally over a particular frequency range. The transient response is primarily controlled by the dominant poles and associated residues. AWE extracts these dominant poles and residues and hence constructs a low order transfer function which can approximate the original circuit response within reasonable accuracy.

AWE was originally proposed by Pillage and Rohrer [4]. It was developed as a method for obtaining transient response and line delay of a network consisting of linearized lumped elements. Since that first paper, a substantial body of work has been developed using AWE. The work can be broadly classified into two groups. The first group consists of efforts concerned with implementation of AWE in solving either lumped or full wave circuit simulations. The second group is mainly involved with the numerical/computational aspects of AWE.

Under the first group, some of the early works include AWE simulation of RC trees and transmission lines. Modeling interconnects in multi–chip modules (MCM) is one of the main impetus behind the rapid development of AWE. When the interconnect is electrically short relative to a wavelength, lumped circuit analysis may be used [4,10,14]. With increasing clock speeds, the distributive nature of the interconnects becomes dominant and can be accounted for by analyzing the interconnect using transmission line analysis [6,7,10,14,33]. Accurate AWE modeling of the terminations and sources is also essential for simulating the interconnect networks. AWE has been used to model non–linear terminations [7,9,34] and switching transistors[35]. Since time delay and edge shape are very critical for high speed clocks, it is often necessary

to consider the frequency dependent nature of the transmission lines and their eigendecomposition. AWE has been successfully applied to analyze lossless and lossy coupled transmission lines [6,7,11,33,36], and nonuniform transmission lines [37]. AWE has also been applied to simulate the susceptibility of transmission lines to incident field coupling [38].

With significant clock harmonics well above 1 GHz, transmission line modeling can prove to be insufficient. For example, multiconductor transmission line (MTL) analysis is incapable of predicting common–mode type currents and is only valid in cases where quasi–TEM propagation is the dominant mode for the signals. In these cases, the interconnects can be analyzed with Partial Element Equivalent Circuits (PEEC) or other full–wave methods. Large networks modeled using retarded PEEC (rPEEC) can be analyzed with AWE [40,41]. One characteristic of most PEEC circuit models is that they are very large in size and hence can be numerically intensive. In order to simulate PEEC circuits or any similar large circuit, it is often computationally efficient to partition the model or represent the circuit with multi–port networks using measured data describing one or more of the ports [44]. Recently, other applications of full–wave AWE analysis of Maxwell's equations have been demonstrated. Problems are solved using techniques such as FEM [43,52], FDTD[42] and also spectral domain methods [39].

The second broad group of work in AWE concerns the computational/numerical aspects. The linear network equations describing the interconnect network are expanded in terms of a Taylor series in the frequency domain. The coefficients of the expansions are known as moments. These moments are matched to low order transfer functions [10] through the use of Padé [8] approximations. Typically, the expansion is initially performed about $s = 0$ (DC) although this is not possible in some EM applications. The poles and residues from this initial series are accurate in the neighborhood of the expansion point. The first step towards achieving improved accuracy was attempted through optimal pole selection [15,16]. This limitation was lifted through formulation of complex frequency hopping (CFH) [10,17]. Using the CFH technique with AWE, it is possible to approximate the dominant poles and residues up to any pre–defined maximum frequency through generating moments from series expanded for $s \neq 0$. Recently new algorithms like Padé Via Lanczos algorithm [18] and the Arnoldi algorithm [53] have been used to accurately compute the poles. The PVL algorithm is discussed in Section 4.

AWE Circuit Formulation

An electrical network can be described as a lumped linear network or distributed network or combination of both using the modified nodal analysis (MNA) technique [13]. The system model can be analyzed using

$$YV = I = \left(C\frac{d}{dt} + G\right)V \tag{9}$$

for a circuit with only lumped circuits and PEEC elements. C and G are the matrices describing the admittance parameters for the circuit. For interconnect networks that include lumped circuits, PEEC models or possibly transmission lines, each set of transmission lines can be treated as a subnetwork. The system matrix description from (9) can be augmented to include the distributed components. For an impulse excitation, the system matrix including the subnetwork representation of MTL's is given by (following [10])

$$C\frac{dV(t)}{dt} + G\,V(t) + \sum_{k=1}^{N_s} D_k\, i_k(t) - b\,\delta(t) = 0 \tag{10}$$

where $V(t)$ is a vector of length N containing the node voltages and independent voltage sources, current sources and linear inductor currents; C and G are N x N lumped network matrices; b is a vector of length N depending on the voltage sources and current sources; D_k is a selector matrix that maps the currents $i_k(t)$ entering a linear subnetwork into the space of the network; and N_s is the number of linear subnetworks (MTL's). If subnetworks are not present in a circuit, the summation (third term) from (10) is omitted.

When a subnetwork is a multiconductor transmission line, the D_k selection matrix contains references for currents entering and leaving the transmission lines. For an MTL with K conductors, one reference conductor and length d, the terminal voltages and currents can be related using [10]

$$\begin{bmatrix} V(d,s) \\ I(d,s) \end{bmatrix} = e^{(D+sE)d}\begin{bmatrix} V(0,s) \\ I(0,s) \end{bmatrix} = T(s)\begin{bmatrix} V(0,s) \\ I(0,s) \end{bmatrix} \tag{11}$$

where

$$D = \begin{bmatrix} 0 & -R \\ -G & 0 \end{bmatrix} \qquad E = \begin{bmatrix} 0 & -C \\ -L & 0 \end{bmatrix} \tag{12}$$

R, G are the K x K per–unit–length (PUL) resistance and conductance matrices, respectively, and L, C are the K x K PUL inductance and capacitance matrices, respectively. The "0" represents a submatrix containing zeros. The $T(s)$ is the transmission line parameter matrix. For the n^{th} subnetwork, (11) can be restated in terms of the near–end and far–end voltages and currents[14]

$$T_n(s)\begin{bmatrix} V_{NE,n} \\ I_{NE,n} \end{bmatrix} - \begin{bmatrix} V_{FE,n} \\ I_{FE,n} \end{bmatrix} = 0 \tag{13}$$

The Laplace–domain form of (10) and (13) can be combined in a single matrix system of equations $Y(s)X(s) = E_S$. One such system of equations is given by [36]

$$\left[\begin{array}{c|c|ccccccc|c} \multicolumn{2}{c|}{\text{Circuit parameters involving terminations, sources and lumped circuits (no connection to MTLs; } V_{NC},\, I_{NC} \text{ only)}} & \multicolumn{8}{c}{\text{Circuit parameters involving terminations, sources and lumped circuits only (connection to MTLs; } V_{FE,n},\, I_{FE,n},\, V_{NE,n},\, I_{NE,n})} & \\ \hline 0 & -1 & T_1 & 0 & 0 & 0 & \cdots & 0 & 0 & \\ 0 & 0 & 0 & -1 & T_2 & 0 & \cdots & 0 & 0 & \\ \vdots & \vdots & \vdots & \vdots & \vdots & \vdots & & \vdots & \vdots & \\ 0 & 0 & 0 & 0 & 0 & 0 & \cdots & -1 & T_{Ns} & \end{array}\right] \left[\begin{array}{c} V_{NC} \\ I_{NC} \\ V_{FE,1} \\ I_{FE,1} \\ V_{NE,1} \\ I_{NE,1} \\ \vdots \\ V_{FE,Ns} \\ I_{FE,Ns} \\ V_{NE,Ns} \\ I_{NE,Ns} \end{array}\right] = \left[\begin{array}{c} b \\ 0 \\ 0 \\ 0 \\ \vdots \\ 0 \\ 0 \end{array}\right] \tag{14}$$

The matrix $\boldsymbol{Y}$ is organized into two major blocks. The upper block contains the parameters for all lumped circuit elements. If the circuit has only lumped elements and PEEC models, the system matrix from (14) reduces to the upper left block. If MTLs are present, the lower block is populated with the transmission line parameter matrices from (11). The upper right block defines the connection of the MTL nodes with the lumped parameters and sources. The "$\boldsymbol{0}$" submatrices contain all zero elements. The "$-\boldsymbol{I}$" submatrices are identity matrices multiplied by –1. The top block in the vector of unknowns $\boldsymbol{X}$ contains all voltages and currents $\boldsymbol{V}_{NC}, \boldsymbol{I}_{NC}$ that have *No Common* connection or nodes with any of the MTLs. In the event that MTLs are present, the remaining unknowns in the vector are organized into successive far–end voltage and current vectors $\boldsymbol{V}_{FE,n}$, $\boldsymbol{I}_{FE,n}$ and near–end voltage and current vectors $\boldsymbol{V}_{NE,n}$, $\boldsymbol{I}_{NE,n}$ for the N_s multiconductor transmission line networks. The vector of knowns $\boldsymbol{E}_S$ is given by the sources attached to lumped circuits or transmission lines $\boldsymbol{b}$ from (10) supplemented by a column of zeros.

Approximating the System Response Using Asymptotic Waveform Evaluation

Equation (14) can be expanded in a Maclaurin series [10]

$$\left(\boldsymbol{Y}_{[0]} + s\boldsymbol{Y}_{[1]} + s^2\boldsymbol{Y}_{[2]} + \cdots\right)\left(\boldsymbol{X}_{[0]} + s\boldsymbol{X}_{[1]} + s^2\boldsymbol{X}_{[2]} + \cdots\right) = \boldsymbol{E}_s \tag{15}$$

Equating terms of like powers of s gives a recursive solution for the moments

$$\boldsymbol{Y}_{[0]}\boldsymbol{X}_{[0]} = \boldsymbol{E}_s \tag{16}$$

$$\boldsymbol{Y}_{[0]}\boldsymbol{X}_{[n]} = -\sum_{r=1}^{n} \boldsymbol{Y}_{[r]}\boldsymbol{X}_{[n-r]} \tag{17}$$

where

$$\boldsymbol{Y}_{[n]} = \frac{\left[\frac{\partial^n}{\partial s^n}\boldsymbol{Y}_{(s)}\right]_{s=0}}{n!} \tag{18}$$

For a linear network containing lumped and distributed elements, the moments are given by [10]

$$\begin{aligned} \boldsymbol{M}_{[0]} &= \boldsymbol{Y}_{[0]}^{-1}\boldsymbol{E}_s \\ \boldsymbol{M}_{[1]} &= \boldsymbol{Y}_{[0]}^{-1}\left[-\boldsymbol{Y}_{[1]}\boldsymbol{Y}_{[0]}^{-1}\boldsymbol{E}_s\right] \\ \boldsymbol{M}_{[n]} &= \boldsymbol{Y}_{[0]}^{-1}\left[-\sum_{r=1}^{n}\boldsymbol{Y}_{[r]}\boldsymbol{M}_{[n-r]}\right] \end{aligned} \tag{19}$$

where the moments $\boldsymbol{M}_{[n]}$ correspond to the series terms $\boldsymbol{X}_{[n]}$. For networks involving only lumped elements, the higher moments are given by

$$\boldsymbol{M}_{[n]} = \boldsymbol{Y}_{[0]}^{-1}\left[-\boldsymbol{Y}_{[1]}\boldsymbol{M}_{[n-1]}\right] \tag{20}$$

as $\boldsymbol{Y}_{[r]} = 0$ for $r \geq 2$.

Using asymptotic waveform evaluation, the transient response of the MNA circuit model for the electrical interconnect is approximated by matching the first $2q$–1 moments of the exact solution to a lower q–order model [4,6,7]. A brief summary of the AWE formulation as is presented below.

The Laplace solution can be approximated from the first few lower order moments through use of the Padé approximation [8]. From the jth row in the moment matrix $\boldsymbol{M}$, the lower order moments at node j are given by

$$m_0 = \left[\boldsymbol{M}_{[0]}\right]_j \qquad m_1 = \left[\boldsymbol{M}_{[1]}\right]_j \qquad m_n = \left[\boldsymbol{M}_{[n]}\right]_j \tag{21}$$

Let the lower order solution for node j be given by $\left[X^*(s)\right]_j$ which corresponds to $\hat{F}(s)$ from (2). The m_n's correspond to the c_k's from (1). The Padé approximant for the impulse response is then found using (2) through (6). Other methods could be used to find a rational approximation to the transfer function(for example, see [54]). The poles of the denominator polynomial from (2) are found using a root solver. The residues may be computed using [6]

$$\begin{bmatrix} p_1^{-1} & p_2^{-1} & \cdots & p_q^{-1} \\ p_1^{-2} & p_2^{-2} & \cdots & p_q^{-2} \\ \vdots & \vdots & \vdots & \vdots \\ p_1^{-q} & p_2^{-q} & \cdots & p_q^{-q} \end{bmatrix} \begin{bmatrix} \hat{k}_1 \\ \hat{k}_2 \\ \vdots \\ \hat{k}_q \end{bmatrix} = - \begin{bmatrix} m_0 \\ m_1 \\ \vdots \\ m_{q-1} \end{bmatrix} \tag{22}$$

for an $[q-1/q]$ Padé approximant.

Varying L and M from (2) makes it possible to have many sets of poles and residues. Each of these sets could be used to approximate the transfer function with a different Padé approximant. Criteria for selecting the set of optimal poles that give the best approximation are given in [15,16]. The skew of a set of poles is a measure of the scaled difference between a given moment and its approximation. The optimal poles and residues correspond to the set with minimum skew.

The coefficients of the numerator polynomial from (2) can be computed using the moments and the b_j coefficients. However, the Padé approximation can generate erroneous right half plane poles. To avoid including the spurious poles, the poles and residues are calculated without first formulating the numerator polynomial. The transfer function is then rebuilt by including only the legitimate left half plane pole terms. The time–domain response can be computed directly from the legitimate poles and residues (without reconstructing the approximate frequency response) using (8).

The accuracy of the AWE approximation primarily depends on the order of the approximation q and the accuracy of the pole calculations at the point of expansion. In the original formulation for AWE, the moments are generated from expansion at $s = 0$ (Maclaurin series) or from $s = \infty$ (Laurent series). The accuracy of the transfer function at any point in the complex s–plane is inversely related to its distance from the point of expansion. The inaccuracy can be minimized by generating the moments at different points in the complex plane using complex frequency hopping (CFH) [10,17]. For AWE implemented with CFH, the sets of poles and residues obtained from the different expansion points can be combined for a more accurate approximation of the transfer function. For most electrical interconnect networks, however, the majority of the dominant poles are found at lower frequencies near $s = 0$ [17]. CFH is discussed in more detail in the next subsection.

Complex Frequency Hopping (CFH)

Complex frequency hopping is a multi–expansion point moment matching technique which can extract dominant poles of a linear network up to any pre–defined maximum frequency [17]. Using CFH, Taylor series are generated for different expansion points in the complex s–plane. The points of expansion are referred to as "hops" and the poles computed for each of these series expansions are selected through an error checking mechanism. The poles are combined to give a single transfer function which is more accurate than a single expansion–point moment matching for $s = 0$. CFH is especially useful in networks containing significant high frequency poles.

The first step in applying CFH is to determine the "hopping" points for Taylor series expansion. The cpu usage is proportional to the number of hops chosen. A binary search strategy for finding the optimum number of hops is given in [17]. The simplest approach is to perform a single hop. The poles are determined based on moments computed at $s = 0$ and a single point ($s \neq 0$). Choosing an arbitrary complex frequency point

$$s_0 = \alpha + j\beta \ , \tag{23}$$

a Taylor series approximation at the point is performed by applying a real frequency shift by substituting $\sigma = s - s_0$ [10]. This is equivalent to shifting the origin of the complex plane to $\sigma = 0$. As a result of this shift, the modified MNA equations for a network containing only lumped circuit elements (9) generate the following recursion for calculation of the moments (following [10])

$$(\boldsymbol{G} + (\alpha + j\beta)\boldsymbol{C})\boldsymbol{V}_{[0]} = \boldsymbol{I} \tag{24}$$

$$(\boldsymbol{G} + (\alpha + j\beta)\boldsymbol{C})\boldsymbol{V}_{[i]} = -\boldsymbol{C}\boldsymbol{V}_{[i-1]} \ , \ i > 0 \tag{25}$$

After applying the frequency shift, all the generated moments are complex. Applying the same shift to interconnect networks containing transmission lines, (11) becomes [10]

$$\begin{bmatrix} \boldsymbol{V}(d,s) \\ \boldsymbol{I}(d,s) \end{bmatrix} = e^{(\boldsymbol{D}' + s\boldsymbol{E}')d} \begin{bmatrix} \boldsymbol{V}(0,s) \\ \boldsymbol{I}(0,s) \end{bmatrix} \tag{26}$$

where

$$\begin{aligned} \boldsymbol{D}' &= \boldsymbol{D} + (\alpha + j\beta)\boldsymbol{E} \\ \boldsymbol{E}' &= \boldsymbol{E} \end{aligned} \tag{27}$$

The pole selection process for CFH is now presented. The discussion follows [10]. At each hopping frequency, the complex moments are obtained from the new set of shifted MNA matrix equations. The poles and residues are computed for each hopping frequency by applying the Padé approximation for the generated set of moments. The poles obtained at a hop are in the shifted reference frame ($\sigma = 0$) and they can be shifted or scaled back with respect to the origin ($s = 0$) from the hopping frequency by substituting $s = \sigma + s_0$. The poles generated at a particular hopping frequency are accurate with respect to the actual poles in the neighborhood of the point of expansion. The accuracy decreases with the increase in distance between the approximate pole and the point of expansion. If one expansion point is close to another expansion point, the

same poles will be detected by both hops. Two poles are said to be collocated if their values are the same or within an error tolerance for two adjacent hops. These common poles are confirmed to be accurate and are selected along with their residues. The distance between a confirmed pole and its point of expansion is the radius of accuracy for that particular hop. The poles obtained from a particular hop which are within the radius of accuracy are marked as accurate poles along with their residues. The poles which are not confirmed by at least two hops or which are outside the radius of accuracy are discarded as inaccurate poles. For interconnect networks with a high operating frequency, the distributed nature of the interconnect becomes more pronounced. As a result more hops are necessary to accurately evaluate the network response.

In order to search for the high frequency poles, the hops are confined to the upper left half of the complex plane. Searching only in the upper left half plane is sufficient since stable systems have poles with negative real parts or complex conjugate pairs with negative real parts. The contributions of the poles which have large, negative real parts are often insignificant in the time–domain transient response. Hence, in order to efficiently approximate the network response, the pole search points or hops should be confined primarily to the imaginary axis. Therefore the MNA matrices are shifted by hops of the form $s_0 = j\beta$. In order to find all of the poles, an infinite number of hops would have to be used. However, from the significant frequency content of the input waveform, the highest frequency for which the poles need to be computed can be determined. Performing hops beyond this highest frequency does not significantly increase the accuracy but adds to the cpu cost.

The procedure for determining the poles at each hop is similar to the method discussed above. The poles are selected through optimal pole selection at each hop. The residues at each hop are extracted from the moments using [10]

$$\begin{bmatrix} \hat{p}_1^{-L-2} & \hat{p}_2^{-L-2} & \cdots & \hat{p}_M^{-L-2} \\ \hat{p}_1^{-L-3} & \hat{p}_2^{-L-3} & \cdots & \hat{p}_M^{-L-3} \\ \vdots & \vdots & \vdots & \vdots \\ \hat{p}_1^{-L-M-1} & \hat{p}_2^{-L-M-1} & \cdots & \hat{p}_M^{-L-M-1} \end{bmatrix} \begin{bmatrix} \hat{k}_1 \\ \hat{k}_2 \\ \vdots \\ \hat{k}_M \end{bmatrix} = - \begin{bmatrix} m_{L+1} \\ m_{L+2} \\ \vdots \\ m_{L+M} \end{bmatrix} \tag{28}$$

Therefore, through use of a multi–point moment matching technique, CFH ensures accuracy over a broad frequency range. CFH uses multiple expansion points and applies the Padé approximation at each of these hops or frequencies of interest. The cpu usage for each hop is approximately equal to one single frequency point analysis [17]. In contrast, to evaluate a full FFT (Fast Fourier Transform), thousands of frequency points could be necessary. AWE simulation using CFH typically requires about 2–10 hops and thus minimizes the cpu usage to a large extent [17].

AWE Examples

The examples illustrate the types of problems addressed with AWE interconnect analysis and the accuracy of the simulations. The first example is taken from [17]. In [17], an interconnect with two multiconductor transmission line networks was analyzed (see Fig. 1). Complex frequency hopping was used to produce the AWE solution. The problem illustrates the sensitivity of the solution to the number of poles

computed (see Fig. 2). The short time transients require more poles to extract the detail from the high frequency signal content.

The second example is taken from [7]. In [7], Bracken, et al., presented a method for partitioning the interconnect into multiport macromodels and showed how to implement AWE with the general method of characteristics. The advantage of the technique is that AWE can be used to evaluate the linear parts of the circuits while other methods can be used to evaluate the nonlinear responses. In this example, admittance macromodels are used in the simulation of a logic gate driving a system with two sets of lossy transmission lines. The circuit is shown in Fig. 3. Crosstalk data from the 4–conductor MTL is shown in Fig. 4.

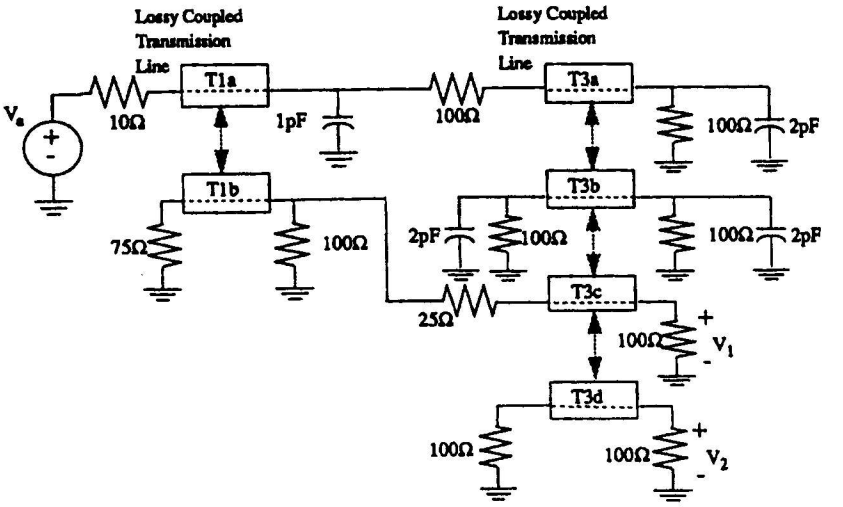

Figure 1. Interconnect circuit with two lossy multiconductor transmission line networks (Reproduced from [17], © 1995 IEEE).

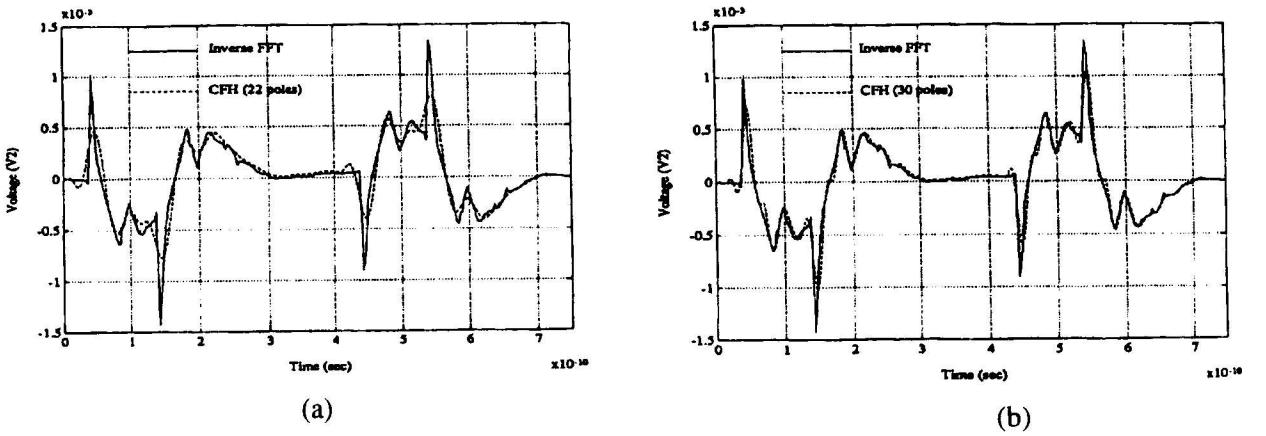

(a) (b)

Figure 2. Far–end crosstalk voltage V_2 for (a) 22 poles and 4 hops; (b) 30 poles and 6 hops (Reproduced from [17], © 1995 IEEE).

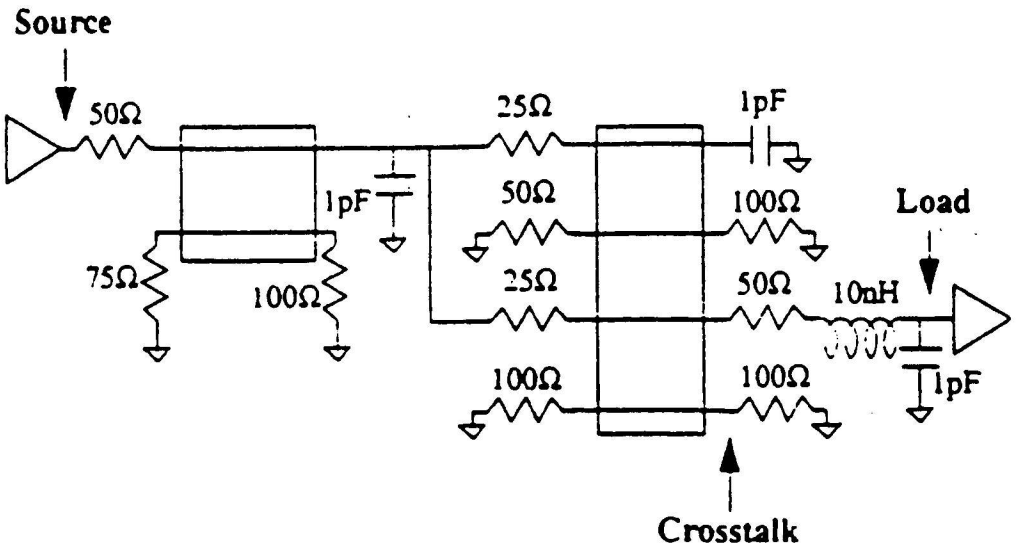

Figure 3. Circuit used to illustrate the admittance macromodeling approach for AWE analysis from (Reproduced from [7], © 1992 IEEE).

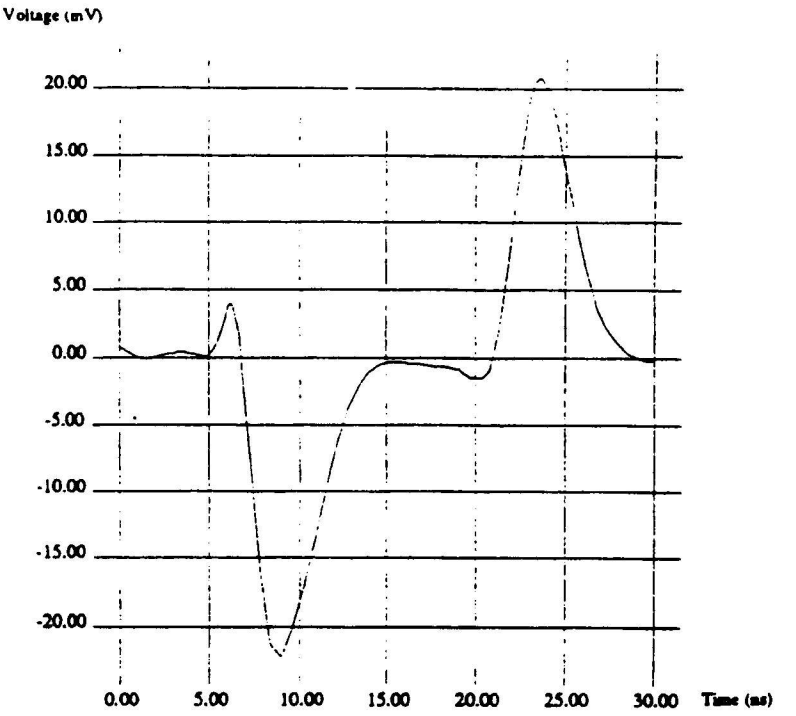

Figure 4. Far–end crosstalk data predicted for the loaded line shown in Fig. 3 (Reproduced from [7], © 1992 IEEE).

4. Padé Via the Lanczos Process (PVL)

PVL Applications

Recently, the Padé Via Lanczos (PVL) algorithm has been applied for analysis of electrical interconnects. PVL has been shown to be capable of producing accurate approximations of the impulse responses and transfer functions of systems over broad frequency ranges. In most cases, techniques such as scaling and multiple expansion points are not required. In [18,27,49], the link between AWE, the Padé approximation and PVL was derived. In those papers, it was demonstrated that PVL is an efficient and numerically stable technique for calculating the poles and residues of a system. The PVL techniques essentially calculate orthogonal bases for Krylov subspaces that are used for the approximation of the original system. This approximation is the projection of the original problem onto a smaller subspace where the projection is orthogonal to the other subspace. In addition, in [18], the PVL algorithm was applied to lumped–type circuit models including PEEC [1,2,3]. Good agreement was found between PVL and exact solutions in several examples. A bound on the pole approximation error was also shown. However, no bound for error of the approximate system response was given. In [30], an adaptive block Lanczos algorithm was applied for solution of multiconductor transmission line (MTL) problems. In that work, a least square fitting procedure with frequency partitioning was used to obtain high order approximations of the MTL parameters [30]. In a more recent work [28], the PVL algorithm was applied to MTL problems by using Chebyshev polynomials to represent the spatial variation of the transmission–line voltages and currents. Modified nodal analysis stamps were developed for the resulting system model. Therefore, the formulation from [28] can be used with existing PVL algorithms. The Chebyshev method was applied to both digital interconnects and microwave circuits. In [27] and [26], a matrix based derivation for the order of approximation of the PVL technique was developed. This derivation resulted in a computationally inexpensive error bound for the system response. This error bound was implemented as a non–heuristic stopping criterion for the Padé Via Lanczos algorithm With an Error Bound (PVL–WEB) [27] and some modeling issues related to the PVL technique were discussed in [32].

Some of the more recent applications of PVL pertain to full–wave EM modeling. In [46] and [50], the spatial derivatives in Maxwell's Equations were discretized using Yee's lattice and the time variation was accounted for by working in the Laplace domain. In [46], the PVL technique was applied and the standard Lanczos algorithm was used. By using PVL, a broadband response was efficiently calculated.. In [50], a modified Lanczos algorithm was implemented for computing the transient response of the fields in inhomogeneous media. The solution was extremely accurate for all time less than a specified value t_{max}. In [48], an efficient, low frequency solution to Maxwell's equations was developed using the Spectral Lanczos Decomposition Method (SLDM) where Krylov subspaces were generated using inverse powers of the Maxwell operator. The SLDM was developed in [47]. The SLDM could completely remove numerical spurious modes. The Lanczos process can sometimes produce spurious unstable poles in the right half plane. In [53], the Arnoldi algorithm was used instead of the Lanczos algorithm to compute the Krylov subspace. The resulting reduced order models have no unstable right half plane poles. The Arnoldi algorithm, however, requires a long term recurrence instead of the short term recurrence used with the Lanczos algorithm.

Therefore, the Arnoldi algorithm will require more floating point operations. More importantly, the increased data storage requirements of the Arnoldi algorithm could also require disk swapping for large problems. Since the residues associated with any spurious unstable poles in the Lanczos algorithm are usually very small, the unstable poles can be discarded without loss of accuracy and the use of the more data intensive Arnoldi algorithm is usually not required. In [45], both AWE and the Lanczos based ALPS [51] procedure were used to obtain a broadband response of an electromagnetic system. A reduced order model of the system was computed using a rational fitting procedure, and an equivalent model for transient circuit analysis was formed.

PVL Technique

In this section, the basics of the PVL algorithm will be presented. First, the origin of the matrices involved in the solution will be discussed. Next, a version of the PVL algorithm that has been widely accepted for solving the resulting linear systems will be reviewed. The connection between the PVL algorithm and the governing equations of the Lanczos process will then be shown.

Typically, the system matrices used with the PVL algorithm are modified nodal analysis (MNA) matrices [13]. These MNA matrices are derived from the state variable equations of the system [18] or from other methods such as shown in [28]. In either case, the transfer function is given by

$$H(s) = l^H (G + sC)^{-1} b \tag{29}$$

where $s = j2\pi f$ for f the frequency, l^H is an N–vector that selects the output of interest, b is the excitation N–vector to the network, C and G are N by N matrices that represent the contribution of memory and memoryless elements, and the superscript "H" denotes a complex conjugate transpose. Next set

$$s = s_0 + \sigma \tag{30}$$

where s_0 is the point of expansion in the s plane. Substituting (30) into (29) gives

$$H(s) = l^H (G + s_0 C + \sigma C)^{-1} b \tag{31}$$

$$H(s) = l^H \left((G + s_0 C)\,(I + \sigma (G + s_0 C)^{-1} C)\right)^{-1} b \tag{32}$$

$$H(s) = l^H (I + \sigma (G + s_0 C)^{-1} C)^{-1} (G + s_0 C)^{-1} b \ . \tag{33}$$

Defining

$$A = -(G + s_0 C)^{-1} C, \quad r = (G + s_0 C)^{-1} b \tag{34}$$

and using (34) in (33), the transfer function is rewritten as

$$H(s_0 + \sigma) = l^H (I - \sigma A)^{-1} r \, . \tag{35}$$

In [18], matrix equations are given that define a version of the Lanczos process. These equations are by far the predominant version used in the Electrical Engineering community. An equivalent formulation which explicitly shows the complex nature of the equations is now presented [31]. These equations are valid for $n = 1,2,...,q$ where q is the final step in the iteration. The equations are

$$A V_n = V_n T_n + v_{n+1} \rho_{n+1} e_n^T \tag{36}$$

$$A^H W_n = W_n \tilde{T}_n + w_{n+1} \eta_{n+1} e_n^T \tag{37}$$

where T_n and $\tilde{T}_n$ are the tridiagonal matrices

$$T_n = \begin{bmatrix} \alpha_1 & \beta_2 & & \\ \rho_2 & \alpha_2 & \ddots & \\ & \ddots & \ddots & \beta_n \\ & & \rho_n & \alpha_n \end{bmatrix} \qquad \tilde{T}_n = \begin{bmatrix} \tilde{\alpha}_1 & \gamma_2 & & \\ \eta_2 & \tilde{\alpha}_2 & \ddots & \\ & \ddots & \ddots & \gamma_n \\ & & \eta_n & \tilde{\alpha}_n \end{bmatrix} \tag{38}$$

$V_n = [v_1\, v_2 \ldots v_n]$ and $W_n = [w_1\, w_2 \ldots w_n]$ are matrices of the Lanczos vectors which satisfy the bi–orthogonality property

$$W_n^H V_n = D_n = \text{diag}\,(\delta_1, \delta_2, \cdots, \delta_n) \tag{39}$$

and $\|v_n\|_2 = \|w_n\|_2 = 1$. The superscript "$T$" denotes an unconjugated transpose. Premultiply (36) by W_n^H

$$W_n^H A\, V_n = W_n^H V_n T_n + W_n^H v_{n+1} \rho_{n+1} e_n^T \tag{40}$$

and noting that $W_n^H v_{n+1} = 0$ and using (39) gives

$$W_n^H A\, V_n = D_n T_n\,. \tag{41}$$

Now premultiply (37) by V_n^H to obtain

$$V_n^H A^H W_n = V_n^H W_n \tilde{T}_n + V_n^H w_{n+1} \eta_{n+1} e_n^T\,. \tag{42}$$

Taking the complex conjugate transpose and simplifying,

$$W_n^H A\, V_n = \tilde{T}_n^H W_n^H V_n \tag{43}$$

or

$$W_n^H A\, V_n = \tilde{T}_n^H D_n\,. \tag{44}$$

Finally, equating (41) and (44), it is shown that T_n and $\tilde{T}_n$ are related by

$$\tilde{T}_n^H = D_n T_n D_n^{-1}\,. \tag{45}$$

From (36) and (37) and the definition for the matrices T_n and $\tilde{T}_n$ note that

$$A v_n = v_{n-1}\beta_n + v_n \alpha_n + v_{n+1}\rho_{n+1} \tag{46}$$

$$A^H w_n = w_{n-1}\gamma_n + w_n \tilde{\alpha}_n + w_{n+1}\eta_{n+1} \tag{47}$$

with $v_0 = w_0 = 0$.

The Lanczos process is derived from the above equations as follows: Pre–multiply (46) by w_n^H and (47) by v_n^H:

$$w_n^H A v_n = w_n^H v_{n-1}\beta_n + w_n^H v_n \alpha_n + w_n^H v_{n+1}\rho_{n+1} \tag{48}$$

$$v_n^H A^H w_n = v_n^H w_{n-1}\gamma_n + v_n^H w_n \tilde{\alpha}_n + v_n^H w_{n+1}\eta_{n+1}\,. \tag{49}$$

From (39), $w_n^H v_{n+1} = w_n^H v_{n-1} = v_n^H w_{n-1} = v_n^H w_{n+1} = 0$ and

$$\delta_n = w_n^H v_n \tag{50}$$

The equations reduce to

$$\alpha_n = w_n^H A v_n (\delta_n)^{-1} \tag{51}$$

and

$$\tilde{\alpha}_n = \left(v_n^H A^H w_n\right)\left(v_n^H w_n\right)^{-1}\,. \tag{52}$$

But notice $\tilde{\alpha}_n$ is just

$$\tilde{\alpha}_n = \left(w_n^H A v_n\right)^H \left(\left(w_n^H v_n\right)^H\right)^{-1} = \alpha_n^* . \tag{53}$$

To find βn and γ_n consider (45) in expanded form

$$\begin{bmatrix} \alpha_1 & \eta_2^* & & \\ \gamma_2^* & \alpha_2 & \ddots & \\ & \ddots & \ddots & \eta_n^* \\ & & \gamma_n^* & \alpha_n \end{bmatrix} = \begin{bmatrix} \delta_1 & & & \\ & \delta_2 & \ddots & \\ & & & \delta_n \end{bmatrix} \begin{bmatrix} \alpha_1 & \beta_2 & & \\ \rho_2 & \alpha_2 & \ddots & \\ & \ddots & \ddots & \beta_n \\ & & \rho_n & \alpha_n \end{bmatrix} \begin{bmatrix} 1/\delta_1 & & & \\ & 1/\delta_2 & \ddots & \\ & & & 1/\delta_n \end{bmatrix} \tag{54}$$

so $\eta_n^* = \delta_{n-1}\beta_n/\delta_n$ and $\gamma_n^* = \delta_n \rho_n/\delta_{n-1}$. Therefore $\delta_{n-1}/\delta_n = \rho_n/\gamma_n^*$ and hence

$$\eta_n^* = \rho_n \beta_n / \gamma_n^* . \tag{55}$$

Pre–multiply (47) by v_{n+1}^H to obtain

$$v_{n+1}^H A^H w_n = v_{n+1}^H w_{n-1}\gamma_n + v_{n+1}^H w_n \alpha_n^* + v_{n+1}^H w_{n+1}\eta_{n+1} . \tag{56}$$

Using (39), this results in

$$v_{n+1}^H A^H w_n = v_{n+1}^H w_{n+1}\eta_{n+1} = \delta_{n+1}^* \eta_{n+1} . \tag{57}$$

Downshift this index by 1 so

$$v_n^H A^H w_{n-1} = v_n^H w_n \eta_n = \delta_n^* \eta_n . \tag{58}$$

Now complex conjugate transpose (46) and postmultiply by w_{n-1} to obtain

$$v_n^H A^H w_{n-1} = v_{n-1}^H w_{n-1}\beta_n^* + v_n^H w_{n-1}\alpha_n^* + v_{n+1}^H w_{n-1}\rho_{n+1}^* \tag{59}$$

which results in

$$v_n^H A^H w_{n-1} = \delta_{n-1}^* \beta_n^* . \tag{60}$$

Combine (58) and (60) to get (61) and (55) and (61) to get (62)

$$\beta_n = \delta_n \eta_n^* / \delta_{n-1} \tag{61}$$

$$\gamma_n^* = \rho_n \delta_n / \delta_{n-1} . \tag{62}$$

To find ϱ_n and η_n, consider (46) and (47) and rewrite as

$$v_{n+1}\rho_{n+1} = Av_n - v_{n-1}\beta_n - v_n\alpha_n \tag{63}$$

$$w_{n+1}\eta_{n+1} = A^H w_n - w_{n-1}\gamma_n - w_n\alpha_n^* . \tag{64}$$

Choose the following from (63) and (64)

$$\rho_{n+1} = \| Av_n - v_{n-1}\beta_n - v_n\alpha_n \|_2 , \tag{65}$$

$$v_{n+1} = (Av_n - v_{n-1}\beta_n - v_n\alpha_n)(\rho_{n+1})^{-1} , \tag{66}$$

$$\eta_{n+1} = \| A^H w_n - w_{n-1}\gamma_n - w_n\alpha_n^* \|_2 , \tag{67}$$

$$w_{n+1} = (A^H w_n - w_{n-1}\gamma_n - w_n\alpha_n^*)(\eta_{n+1})^{-1} . \tag{68}$$

Equations (50), (51) and (61) through (68) give rise to the following algorithm:

Algorithm 1: q steps of the Lanczos process.

$\rho_1 \leftarrow \| r \|_2, \ \eta_1 \leftarrow \| l \|_2, \ w_0 \leftarrow 0, \ v_0 \leftarrow 0, \ \delta_0 \leftarrow 1, \ n \leftarrow 0.$

$v_1 \leftarrow r\,(\rho_1)^{-1}, \ w_1 \leftarrow l\,(\eta_1)^{-1}.$

for $n = 1, 2, \ldots, q$ do

$f \leftarrow A v_n .$

$\delta_n \leftarrow w_n^H v_n, \ \alpha_n \leftarrow w_n^H f \delta_n^{-1}.$

$\beta_n \leftarrow \delta_n \eta_n^* / \delta_{n-1}, \ \gamma_n \leftarrow (\delta_n \rho_n / \delta_{n-1})^*.$

$f \leftarrow f - v_n \alpha_n - v_{n-1} \beta_n, \ \rho_{n+1} \leftarrow \| f \|_2 .$

$v_{n+1} \leftarrow f \rho_{n+1}^{-1}.$

$f \leftarrow A^H w_n - w_n \alpha_n^* - w_{n-1} \gamma_n, \ \eta_{n+1} \leftarrow \| f \|_2 .$

$w_{n+1} \leftarrow f \eta_{n+1}^{-1} .$

endfor

The reduced transfer function is defined to be (following [18])

$$H_q(s_0 + \sigma) = \left(l^H r\right) e_1^T (I - \sigma T_q)^{-1} e_1 \tag{69}$$

which is used as the approximation to $H(s_0 + \sigma)$ in (35). In recent works, the accuracy of the PVL iteration was demonstrated by comparing various q–order models with other accurate but much less efficient solution approaches. From these comparisons, the approximate number of iterations required for a specific type of problem was determined. Recently, a new matrix based derivation of the PVL technique has been proposed [27], [26]. This derivation is not only able to show the order of the approximation of the PVL algorithm, but more importantly it provides a computationally inexpensive error bound for the approximation. This error bound has been used as a stopping criterion for the Lanczos process [26], [31] and is called PVL–WEB. By using PVL–WEB, the need for a heuristic scheme to terminate the Lanczos process is eliminated. Some of the implementation issues associated with PVL–WEB are discussed in [27] and [26].

Calculating the Poles and Residues

After the Lanczos process has been terminated, the dominant poles and associated residues of the system can be computed and used to visualize the characteristics of the system. The poles and residues can also be used to determine the circuit response to the inputs from Table I. The poles and residues are derived using quantities generated as a part of the Lanczos process. When the process has terminated after the q^{th} iteration, the tridiagonal matrix (38) can be factored as

$$T_q = S_q \Lambda_q S_q^{-1} \tag{70}$$

where Λ_q is a diagonal matrix of eigenvalues and S_q is a matrix of eigenvectors. Using (70) in (69) and

factoring gives

$$\begin{aligned} H_q(s_0 + \sigma) &= \left(l^H r\right) e_1^T \left(I - \sigma S_q \Lambda_q S_q^{-1} \right)^{-1} e_1 \\ &= \left(l^H r\right) e_1^T \left(S_q \left(I - \sigma \Lambda_q \right) S_q^{-1} \right)^{-1} e_1 \\ &= \left(l^H r\right) e_1^T S_q \left(I - \sigma \Lambda_q \right)^{-1} S_q^{-1} e_1 \end{aligned} \tag{71}$$

Define $\mu = S_q^T e_1$ and $\nu = S_q^{-1} e_1$ where again the superscript "T" denotes the unconjugated transpose. The quantity $\left(I - \sigma \Lambda_q \right)^{-1}$ is a diagonal matrix, i.e., diag $\left((1 - \sigma\lambda_1)^{-1}, (1 - \sigma\lambda_2)^{-1}, \ldots, (1 - \sigma\lambda_q)^{-1} \right)$. Equation (71) becomes

$$H_q(s_0 + \sigma) = \left(l^H r\right) \mu^T \text{diag} \left((1 - \sigma\lambda_1)^{-1}, (1 - \sigma\lambda_2)^{-1}, \ldots, (1 - \sigma\lambda_q)^{-1} \right) \nu \tag{72}$$

Multiplying the diagonal matrix by ν and expanding gives

$$H_q(s_0 + \sigma) = \left(l^H r\right) \left[\mu_1 \mu_2 \ldots \mu_q\right] \begin{bmatrix} \dfrac{\nu_1}{1 - \sigma\lambda_1} \\ \dfrac{\nu_2}{1 - \sigma\lambda_2} \\ \vdots \\ \dfrac{\nu_q}{1 - \sigma\lambda_q} \end{bmatrix} \tag{73}$$

Carrying out the vector multiplication in (73) results in

$$\begin{aligned} H_q(s_0 + \sigma) &= \sum_{j=1}^{q} \frac{\left(l^H r\right) \mu_j \nu_j}{1 - \sigma\lambda_j} \\ &= \sum_{j=1}^{q} \frac{-\left(l^H r\right) \mu_j \nu_j / \lambda_j}{\sigma - 1/\lambda_j} \\ &= \sum_{j=1}^{q} \frac{-\left(l^H r\right) \mu_j \nu_j / \lambda_j}{s - (1/\lambda_j + s_0)} \end{aligned} \tag{74}$$

Define $k_j = -\left(l^H r\right) \mu_j \nu_j / \lambda_j$ and $p_j = 1/\lambda_j + s_0$. Using these in (74) gives

$$H_q(s) = \sum_{j=1}^{q} \frac{k_j}{s - p_j} \tag{75}$$

which is the Padé approximation for the impulse response from (7) using the Lanczos quantities.

The above definitions for the poles p_j and residues k_j give rise to Algorithm 2 (following [18]):

Algorithm 2: Computing the poles and residues.

Compute the eigendecomposition $T_q = S_q \operatorname{diag}(\lambda_1, \lambda_2, ..., \lambda_q) S_q^{-1}$.

set $\mu = S_q^T e_1$, $\nu = S_q^{-1} e_1$ and $k_\infty = 0$.

for $j = 1, 2, \ldots, q$ do

  if $\lambda_j \neq 0$ then

    $p_j = \frac{1}{\lambda_j} + s_0$ and $k_j = -\left(l^H r\right) \mu_j \nu_j / \lambda_j$

  else

    $k_\infty = k_\infty + \left(l^H r\right) \mu_j \nu_j$

  endif

endfor

Relationship between AWE and PVL

In [18,49], the derivation of the approximation for PVL is linked to the moment matching techniques of AWE. For the PVL algorithm, the order of approximation of the reduced transfer function $H_q(s_0 + \sigma)$ to the transfer function $H(s_0 + \sigma)$ is $2q - 1$. This is the same order of approximation that the AWE algorithm produces. For the PVL algorithm, it is straightforward to derive the order of approximation up to $2q - 2$. However, the proof for the approximation of order $2q - 1$ is rather involved [29]. In a more recent study [27], a straightforward matrix–based derivation up to and including the $2q-1$ order of approximation is presented.

PVL Examples

These examples illustrate the types of problems addressed with PVL interconnect analysis and the accuracy of the simulations. The first example is taken from [18]. In Fig. 5, the voltage gain of a filter was simulated. In the figure, the increasing accuracy with increasing numbers of PVL iterations (increasing numbers of poles) is shown. Figure 6 shows the frequency response for a three–dimensional electromagnetic problem modeled using PEEC. After $q = 60$ iterations, the PVL response was able to accurately simulate the exact solution out to 5 GHz.

The next example is from [28]. A mathematical model developed for dispersive MTL's was used for the simulation [28]. In Fig. 7, the circuit for a low–pass filter realized using transmission lines is shown. The cut–off frequency of the device is 4 GHz and the transmission lines are $\frac{\lambda}{8}$ in length at cut–off. The frequency response of the filter is shown in Fig. 8. The algorithm was run for $q = 70$ iterations and the PVL simulation demonstrated excellent agreement with the exact solution beyond 50 GHz.

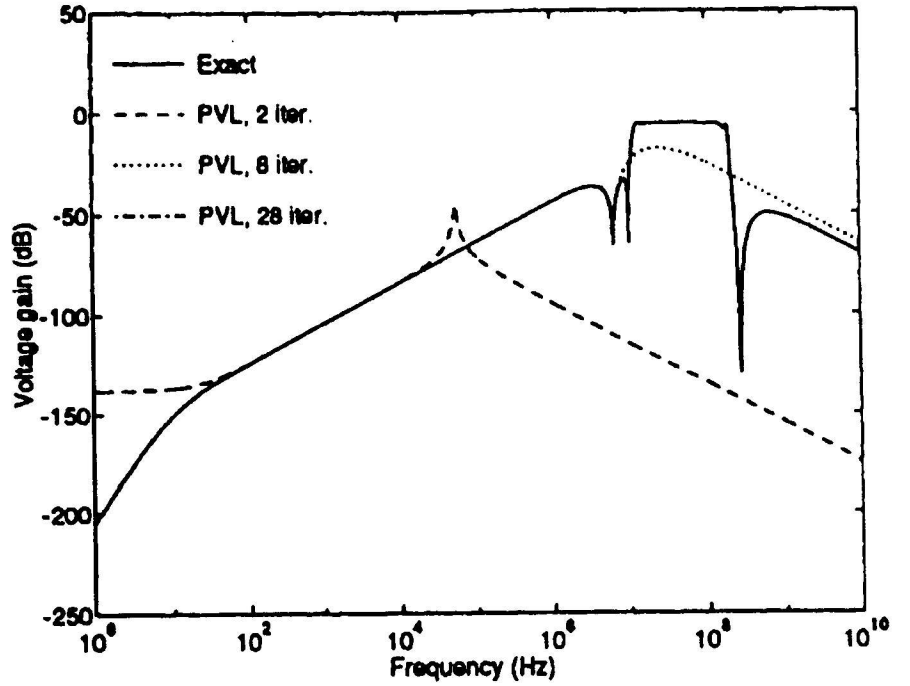

Figure 5. Filter response illustrating the increasing bandwidth and accuracy for increasing numbers of PVL iterations (Reproduced from [18], © 1995 IEEE).

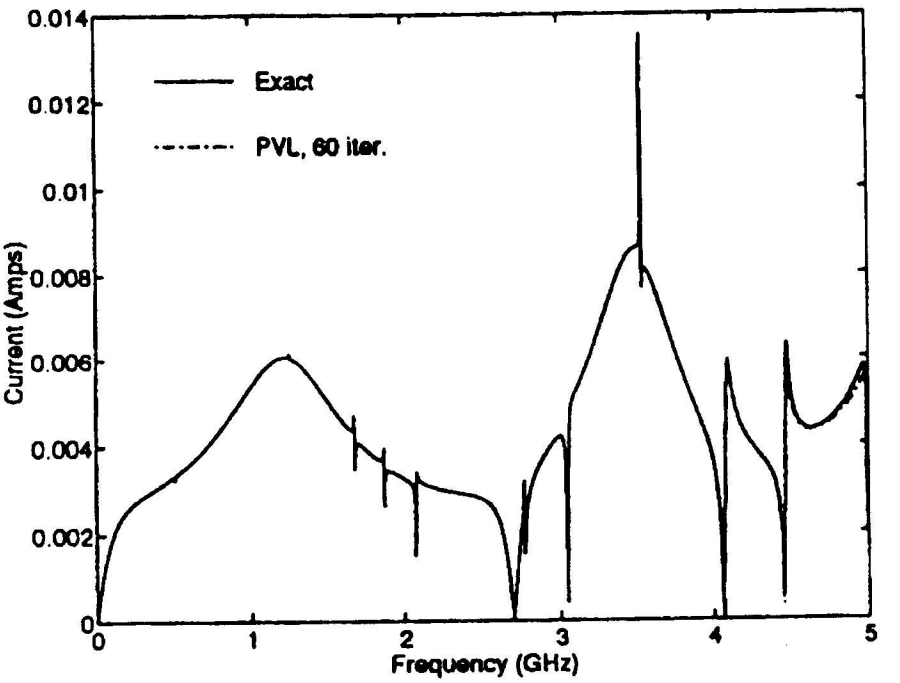

Figure 6. Three–dimensional EM simulation using PVL (Reproduced from [18], © 1995 IEEE).

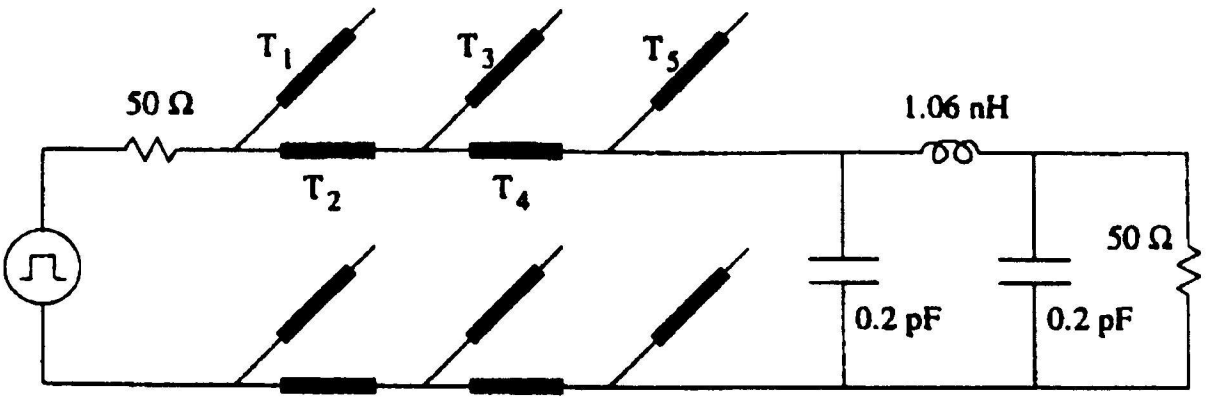

Figure 7. Low–pass transmission line filter (Reproduced from [28], © 1996 IEEE).

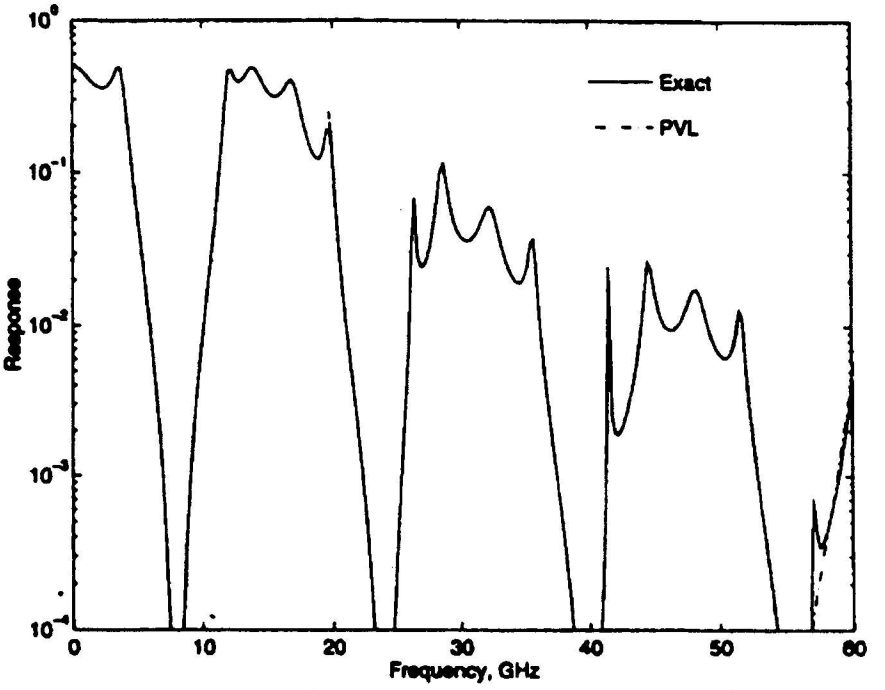

Figure 8. Frequency response for the filter from Fig. 7 (Reproduced from [28], © 1996 IEEE).

5. Summary

Reduced–order modeling has been demonstrated to be an efficient accurate method for dramatically reducing the simulation times associated with large circuit models by a few orders of magnitude or more. Asymptotic waveform evaluation (AWE) and Padé via the Lanczos process (PVL) are two recently developed approaches which formulate Padé approximants of circuits modeled in the Laplace domain. In addition to computational efficiency, it is straightforward to compute either time–domain or frequency–domain responses.

Using AWE, a reduced–order model is formulated following a more classical approach to generate the Padé approximants. Rational polynomials are formulated and factored using partial fraction expansion to generate the desired forms of the Padé approximants. The AWE method is able to predict poles in the vicinity of an expansion point but suffers in accuracy for poles removed from the expansion point due the Padé approximation's sensitivity to numerical precision. This limitation was overcome by generating poles for sets of expansion points using complex frequency hopping (CFH). CFH allows accurate pole and residue calculation for an arbitrary number of poles and zeros.

Using PVL, the rational polynomials of Padé approximants are not explicitly formulated. The reduced–order models are generated by extracting the poles and residues from quantities associated with the Lanczos iteration. The PVL method overcomes many of the numerical difficulties of a classical Padé approximation approach and is able to accurately predict several more poles per expansion point than AWE. In most cases, only a single expansion point is required for a PVL iteration.

Both AWE and PVL have been successfully applied to several interconnect problems of interest to the electrical engineering community. At this time, AWE has been applied to a wider variety of problems, partly due to the method being somewhat more mature. In addition, the moment generation methods of AWE provide more flexibility in the system matrix description/formulation. Currently, most of the PVL applications require a system matrix structure of the form " $G + sC$ ". This restriction will most likely be relaxed as the work in PVL advances.

6. References

1. A. E. Ruehli, "Equivalent Circuit Models for Three–Dimensional Multiconductor Systems," *IEEE Trans. Microwave Theory Tech.*, vol. 22, no. 3, pp. 216–221, March, 1974.

2. A. E. Ruehli, "Inductance Calculations in a Complex Integrated Circuit Environment," *IBM J. Res. Develop.*, pp. 470–481, September, 1972.

3. A. E. Ruehli, P. A. Brennan, "Efficient Capacitance Calculations for Three Dimensional Multiconductor Systems," *IEEE Trans. Microwave Theory Tech.*, vol. 21, no. 2, pp. 76–82, February, 1973.

4. L. T. Pillage, R. A. Rohrer, "Asymptotic Waveform Evaluation for Timing Analysis," *IEEE Trans. Computer Aided–Design*, vol. 9, no. 4, pp. 352–366, April, 1990.

5. V. Raghavan, R. A. Rohrer, L. T. Pillage, J. Y Lee, J. E. Bracken, M. M. Alaybeyi, "AWE–Inspired," *Proceedings of the IEEE 1993 Custom Integrated Circuits Conference*, San Diego, California, pp. 18.1.1–18.1.8, May, 1993.

6. T. K. Tang, M. S. Nakhla, "Analysis of High–Speed VLSI Interconnects Using the Asymptotic Waveform Evaluation Technique," *IEEE Trans. Computer–Aided Design*, vol. 11, no. 3, pp. 341–352, March, 1992.

7. J. E. Bracken, V. Raghavan, R. A. Rohrer, "Interconnect Simulation with Asymptotic Waveform Evaluation (AWE)," *IEEE Trans. Circuits and Systems*, vol. 39, pp. 869–878, November, 1992.

8. G. A. Baker, Jr., P. Graves–Morris, *Padé Approximants, Part I: Basic Theory*, Addison–Wesley Publishing Company, Reading, Massachusetts, 1981.

9. D. Xie, M. S. Nakhla, "Delay and Crosstalk Simulation of High–Speed VLSI Interconnects with Nonlinear Terminations," *IEEE Trans. Computer Aided Design*, vol. 12, pp. 1198–1211, November, 1993.

10. E. Chiprout, M. S. Nakhla, Asymptotic Waveform Evaluation and Moment Matching for Interconnect Analysis, Kluwer Academic Publishers, Boston, 1994.

11. R. Khazaka, E. Chiprout, M. S. Nakhla, Q. J. Zhang, "Analysis of High–Speed Interconnects with Frequency Dependent Parameters," *11 th International Zurich Symposium and Technical Exhibition on Electromagnetic Compatibility*, March, 1995, pp203–208.

12. J. Vlach, K. Singhal, Computer Methods for Circuit Analysis and Design, Van Nostrand Reinhold, New York, 1983.

13. C. W. Ho, A. E. Ruehli, P. A. Brennan, "The Modified Nodal Approach to Network Analysis," *IEEE Trans. Circuits Syst.*, vol. CAS–22, pp. 504–509, June, 1975.

14. W. T. Smith, S.K. Das, "Application of Asymptotic Waveform Evaluation for EMC Analysis of Electrical Interconnects" *1995 IEEE International Symposium on Electromagnetic Compatibility*, Atlanta, 1995.

15. E. Chiprout, M. S. Nakhla, "Generalized Moment–Matching Methods for Transient Analysis of Interconnect Networks," *29th ACM/IEEE Design Automation Conference*, Anaheim, pp. 201–206, June, 1992.

16. E. Chiprout, M. S. Nakhla, "Optimal Pole Selection in Asymptotic Waveform Evaluation," *Proceedings of the IEEE International Symposium on Circuits and Systems*, San Diego, pp. 1961–1964, May, 1992.

17. E. Chiprout, M. S. Nakhla, "Analysis of Interconnect Networks Using Complex Frequency Hopping (CFH)," *IEEE Trans. Computer–Aided Design of Integrated Circuits and Systems*, vol. 14, no. 2, pp. 186–200, February, 1995.

18. P. Feldmann, R. W. Freund, "Efficient linear circuit analysis by Padé approximation via the Lanczos process," *IEEE Trans. on Computer–Aided Design of Integrated Circuits and Systems*, vol. 14, no. 5, pp. 639–649, May, 1995.

19. Z. Bai, A. Orlandi, W. T. Smith, "Moment Matching Method for Numerical Solution of MTL Equations in Interconnect Analysis," accepted for publication in the *Journal of Computational and Applied Mathemetics*.

20. F. M Tesche, "On the Analysis of Scattering and Antenna Problems Using the Singularity Expansion Technique," *IEEE Trans. on Ant. and Prop.*, vol AP–21, no. 1, pp. 53–62, 1973.

21. J. N. Brittingham, E. K. Miller, J. L. Willows, "Pole Extraction from Real–Frequency Information," *Proc. IEEE*, vol. 68, no. 2, pp. 263–273, February, 1980.

22. G. J. Burke, E. K. Miller, S. Chakrabarti, K. Demarest, "Using Model–Based Parameter Estimation to Increase the Efficiency of Computing Electromagnetic Transfer Functions," *IEEE Trans. Magn.*, vol. 25, no. 4, pp. 2807–2809, July, 1989.

23. E. K. Miller, "Model–Based Parameter Estimation in Electromagnetics: I – Background and Theoretical Development," *Applied Computational Electromagnetics Society Newsletter*, vol. 10, no. 3, 1995.

24. E. K. Miller, "Model–Based Parameter Estimation in Electromagnetics: II – Applications to EM Observables," *Applied Computational Electromagnetics Society Newsletter*, vol. 11, no. 1, pp. 35–56, 1996.

25. E. K. Miller, "Model–Based Parameter Estimation in Electromagnetics: III – Applications to EM Integral Equations," *Applied Computational Electromagnetics Society Journal*, vol. 10, no. 1, pp. 9–29, 1995.

26. Z. Bai, R. D. Slone, W. T. Smith, Q. Ye, "Error Bound for Reduced System Model by Padé Approximation Via the Lanczos Process," submitted for review to *IEEE Trans. Computer–Aided Design*, March, 1997.

27. Z. Bai and Qiang Ye, "Error Estimation of the Padé Approximation of Transfer Function Via the Lanczos Process," to be published.

28. M. Celik and A. C. Cangellaris, "Simulation of Dispersive Multiconductor Transmission Lines by Padé Approximation via the Lanczos Process," *IEEE Trans. on Microwave Theory and Techniques*, vol. 44, no. 12, pp. 2525–2535, Dec. 1996.

29. W. B. Gragg, "Matrix interpretations and applications of the continued fraction algorithm", *Rocky Mountain J. Math.*, vol. 4, pp. 213–225, 1994.

30. T. V. Nguyen, J. Li, Z. Bai, "Dispersive Coupled Transmission Line Simulation Using an Adaptive Block Lanczos Algorithm," *Proceedings of IEEE Conference on Custom Integrated Circuits*, 1996.

31. R. D. Slone, "A Computationally Efficient Method for Solving Electromagnetic Interconnect Problems: The Padé Approximation Via the Lanczos Process With an Error Bound," Master's Thesis, University of Kentucky, Lexington, KY, 1997.

32. R. D. Slone, W. T. Smith and Z. Bai, "Using Partial Element Equivalent Circuit Full Wave Analysis and Padé Via Lanczos to Numerically Simulate EMC Problems," *1997 IEEE International Symposium on Electromagnetic Compatibility Digest*, August, 1997.

33. T. K. Tang, M. S. Nakhla and R. Griffith, "Analysis of lossy multiconductor transmission lines using the Asymptotic Waveform Evaluation Technique," *IEEE Trans. Computer–Aided Design of Integrated Circuits and Systems*, vol. 10, November 1991.

34. E. Chiprout, M. S. Nakhla, "Fast nonlinear waveform estimation of large distributed networks" In *Proc. of the IEEE Int. Microwave Symposium*, (MTT–S), pp. 1341–1344, June 1992.

35. R. J. Trihy and R. A. Rohrer, "Simulating Sigma–Delta Modulators in AWEswit," In *Proc. of the IEEE 1993 Custom Integrated Circuits Conf.*, pp. 141–144, 1993.

36. S. K. Das, W. T. Smith, "Application of Asymptotic Waveform Evaluation for Analysis of Skin Effect in Lossy Interconnects," *IEEE Trans. EMC*, vol. 39, no.2, pp. 138–146, May, 1997.

37. S. L. Manney, M. S. Nakhla, Q. J. Zhang, "Transient Analysis of nonuniform transmission lines using Asymptotic Waveform Evaluation," 23rd European Microwave Conference, September 1993.

38. S. K. Das, W. T. Smith, "Incident Field Coupling Analysis of Multiconductor Transmission Lines Using Asymptotic Waveform Evaluation," *1996 IEEE International Symposium on Electromagnetic Compatibility*, Santa Clara, California, 1996.

39. R. Achar, M.S. Nakhla, Q.J. Zhang, "Addressing High Frequency Effects in VLSI Interconnects with Full Wave Model and CFH," *Proc. IEEE/ACM Int. Conf. Computer Aided Design*, pp 53–56, San Jose, CA, Nov. 1995.

40. E. Chiprout, H. Heeb, M. S. Nakhla, A. E. Ruehli, "Simultaneous 3–D Retarded Interconnect Models Using Complex Frequency Hopping (CFH)," *IEEE Int. Conf. on Computer Aided Design*, pp. 66–72, November, 1993.

41. H. Heeb, A. E. Ruehli, J. E. Bracken, R. A. Rohrer, "Three Dimensional Circuit Oriented Electromagnetic Modeling for VLSI Interconnects," *Proc. of IEEE Int. Conf. on Computer Design*, pp. 218–221, 1992.

42. M. Li, Q.–J. Zhang, M. Nakhla, "Finite Difference solution of EM fields by asymptotic waveform techniques," *IEE Proc.–Microw. Antennas Propag.*, vol. I43, no. 6, pp. 512–520, December, 1996.

43. J. Gong, J.L. Volakis "AWE Implementation for electromagnetic FEM analysis," *Electronics Letters*, no. 24, pp. 2216–2217, Nov. 21, 1996.

44. G. Zheng, Q.J. Zhang, M.S. Nakhla, R. Achar, "An Efficient Approach for Moment Matching Simulation of Linear Subnetworks with Measured or Tabulated Data," *IEEE Int Conf. Computer Aided Design*, San Jose, CA, pp 20–23, November, 1996

45. J. E. Bracken and Z. J. Cendes, "Transient Analysis via Electromagnetic Fast–Sweep Methods and Circuit Models," *13th Annual Review of Progress in Applied Computational Electromagnetics*, Monterey, California, pp. 172–179, March, 1997.

46. A. C. Cangellaris and L. Zhao, "Reduced–Order Modeling of Electromagnetic Systems with Padé Via Lanczos Approximations," *13th Annual Review of Progress in Applied Computational Electromagnetics*, Monterey, California, pp. 148–155, 1997.

47. V. Druskin and L. Knizhnerman, "Spectral approach to solving three–dimensional Maxwell's diffusion equations in the time and frequency domains," *Radio Science*, vol. 29, no. 4, pp. 937–953, 1994.

48. V. Druskin, P. Lee and L. Knizhnerman, "Solution of Maxwell Equations Using Krylov Subspace From Inverse Powers Of Stiffness Matrix," *13th Annual Review of Progress in Applied Computational Electromagnetics*, Monterey, California, pp. 1001–1008, 1997.

49. K. Gallivan, E. Grimme and P. Van Dooren, "Asymptotic Waveform Evaluation via a Lanczos Method," *Appl. Math. Lett.*, vol. 7, no. 5, pp. 75–80, 1994.

50. R. F. Remis and P. M. van den Berg, "Computation of Transient Electromagnetic Wavefields in Inhomogeneous Media Using a Modified Lanczos Algorithm," *13th Annual Review of Progress in Applied Computational Electromagnetics*, Monterey, California, pp. 132–139, 1997.

51. D. K. Sun, "ALPS — an adaptive Lanczos–Padé approximation for the spectral solution of mixed–potential integral equations," *USNC/URSI Radio Sci. Mtg. Digest*, Baltimore, Maryland, p. 30, July 1996.

52. M. A. Kolbehdari, M. Srinivasan, M. S. Nakhla, Q. Zhang, R. Achar, "Simultaneous Time and Frequency Domain Solutions of EM Problems Using Finite Element and CFH Techniques," *IEEE Trans. Microwave Theory Tech.*, vol. 44, no. 9, pp. 1526–1534, September, 1996.

53. L. M. Silveira, M. Kamon, I. Elfadel, J. White, "A Coordinate–Transformed Arnoldi Algorithm for Generating Guaranteed Stable Reduced–Order Models of RLC Circuits," *IEEE/ACM Digest of Technical Papers*, IEEE/ACM International Conference on Computer Aided Design, San Jose, California, pp. 288–294, November, 1996.

54. M. D'Amore, M. S. Sarto, "Time–Domain Analysis of Field–Excited Transmission Line Systems by Using Model–Based Parameter Estimation," *1994 IEEE International Symposium on Electromagnetic Compatibility*, Chicago, Illinois, pp. 258–263, August, 1994.

INDEX TO COMPUTER CODE REFERENCES FOR VOL. 11 (1996) OF THE ACES JOURNAL AND THE ACES NEWSLETTER

This computer code index is updated annually and published in the second issue of the ACES Newsletter.

LEGEND:

AJ	ACES Journal
AN	ACES Newsletter
SI	Special Issue
*	Pre- or postprocessor for another computational electromagnetics code
**	Administrative reference only: no technical discussion (This designation and index do not include bibliographic references)
Page no.	The first page of each paper in which the indicated code is discussed

NOTE: The inclusion of any computer code in this index does not guarantee that the code is available to the general ACES membership. Where the authors do not give their code a specific name, the computational method used is cited in the index. The codes in this index may not all be general purpose codes with extensive user-orientated features - some may only be suitable for specific applications. While every effort has been made to be as accurate and comprehensive as possible, it is perhaps inevitable that there will be errors and/or omissions. I apologise in advance for any inconvenience or embarrassment caused by these.

Duncan C Baker, Editor-in-Chief, ACES Journal.
3 December 1996.

COMPUTER CODE	JOURNAL OR NEWSLETTER ISSUE AND PAGE NO.	
ABC	AN No. 1,	20
	AJ No. 2,	14
AI/ES	AN No. 2,	28*
Applied Mathematics	AJ No. 1,	SI
Benchmarks	AN No. 1,	14
BIE	AJ No. 1 (SI),	32
Charge simulation	AJ No. 3,	16
DRAW	AJ No. 2,	4
EM Wave Problems	AN No. 2,	60**
	AJ No. 1 (SI),	8
EM Scattering	AJ No. 1 (SI),	17
EFIE	AJ No. 2,	4
FDM	AN No. 2,	21
FDTD	AN No. 1,	61**, 37
	AJ No. 1 (SI),	90
	AJ No. 2,	55
	AJ No. 3,	62
FE/BE	AJ No. 2,	40
FEM	AJ No. 2,	14
FEMAX	AJ No. 2,	24
FERM	AJ No. 2,	4
FIT	AJ No. 1 (SI),	70
Gaussian Quadrature	AN No. 2,	50
GEOM	AJ No. 2,	4
GMRES	AJ No. 1 (SI),	63
Gradient associated CD	AJ No. 3,	82
ICEMES	AN No. 2,	28
Improved circuit theory	AJ No. 3,	44
Legendre Polynomials	AJ No. 1 (SI),	85
Low Freq. Diffraction	AJ No. 1 (SI),	47
MATHMATICA	AJ No. 1 (SI),	47
MBPE	AN No. 1,	35
MFIE	AJ No. 2,	66
MFIT	AJ No. 2,	66
MININEC	AN No. 1,	64
MM	AJ No. 2,	32
MPM	AJ No. 3,	4
NEC	AN No. 1,	12, 14
	AN No. 2,	18
	AJ No. 2,	4
	AJ No. 3,	9
NECVU	AN No. 2,	13
NLS	AN No. 2,	20
Parallel Computing	AN No. 3,	25**
PDE	AN No. 2,	21
RCS	AJ No. 1 (SI),	63
	AJ No. 3,	25
RFEC	AJ No. 2,	72
Scalar potential FD	AJ No. 3,	63, 72
Scattering	AJ No. 1 (SI),	57

ABSTRACTS OF ACES JOURNAL PAPERS

VOLUME 11, 1996

This compilation of abstracts is updated annually and normally published in the second issue of the *ACES Newsletter*. The material was scanned in using a digital scanner and converted to text using a program for character recognition. I extend the sincere thanks and appreciation of the *ACES Journal* to Ms. Alet van Zyl who undertook this task. The document was proofread only once. As Editor-in-Chief, I accept full responsibility for any errors and/or omissions which appear in the text. I apologize in advance for any inconvenience or embarrassment caused by these.

Duncan C. Baker, Editor-in-Chief, *ACES Journal*.
3 December 1996.

THE COMPUTATION OF LINEAR DISPERSIVE ELECTROMAGNETIC WAVES

Peter G. Petropoulos

Numerical solutions of the equations describing electromagnetic pulse propagation in geometrically complex Debye-dispersive dielectrics are used in the development of safety standards for human exposure to non-ionizing radiation. Debye dispersion is a relaxation process, a phenomenon which occurs when the underlying material is forced into non-equilibrium due to the passing waves. This relaxation is typically stiff in applications, and the system of equations is then singularly perturbed. Such systems are notoriously expensive to solve with standard numerical methods. We review previous work related to the numerical solution of such problems, and consider a representative numerical scheme in order to elucidate the nature of the challenge posed to Computational Electromagnetics by the stiffness. Further. an analysis of the stiffness leads us to propose a scheme that seems "natural" for the problem at hand. **[Vol. 11, No. 1 (1996), pp 8-16, Special issue on Applied Mathematics: Meeting the challenges presented by computational electromagnetics]**

CALCULATION OF ELECTROMAGNETIC SCATTERING VIA VARIATIONS AND ANALYTIC CONTINUATION

Oscar P. Bruno and Fernando Reitich

In this paper we review a numerical method we introduced recently for the solution of problems of electromagnetic scattering. Based on variations of the boundaries of the scatterers and analytic continuation, our approach yields algorithms which are applicable to a wide variety of scattering configurations. We discuss some recent applications of this method to scattering by diffraction gratings and by large two-dimensional bounded bodies, and we present results of new applications to three-dimensional gratings containing corners and edges. In many cases of practical interest our algorithms give numerical results which are several orders of magnitude more accurate than those given by classical methods. **[Vol. 11, No. 1 (1996), pp 17-31, Special issue on Applied Mathematics: Meeting the challenges presented by computational electromagnetics]**

ERROR CONTROL IN NUMERICAL SOLUTIONS OF BOUNDARY INTEGRAL EQUATIONS

G . C . HSIAO and R. E . KLEINMAN

A method of estimating the error committed in numerical solutions of integral equations is presented. It is shown how the error can be computed in spaces other than L^2, why this is reasonable and sometimes necessary. The appropriate function spaces are also shown to lead to bounded condition numbers even for first kind equations. **[Vol. 11, No. 1 (1996), pp 32-36, Special issue on Applied Mathematics: Meeting the challenges presented by computational electromagnetics]**

SUB-GRIDDING FDTD SCHEMES

Peter Monk

Local meshing or sub-gridding has been advocated by a

number of authors as a way of increasing the spatial resolution of the finite difference time domain method (FDTD). In this paper we show how to use supraconvergence to analyze the error in a simple sub-gridding strategy in two dimensions. We also analyze the spurious reflection that occurs at an interface between two grids for the standard FDTD scheme, for simple subgridding method and for another subgridding scheme employing linear interpolation. The overall order of convergence of the reflection coefficients is the same for all the methods, but the linear scheme has a lower amplitude spurious transmitted mode compared to the simple subgridding scheme. **[Vol. 11, No. 1 (1996), pp 37-46, Special issue on Applied Mathematics: Meeting the challenges presented by computational electromagnetics]**

CALCULATIONS IN *MATHEMATICA* ON LOW-FREQUENCY DIFFRACTION BY A CIRCULAR DISK

J. Boersma and M. J. H. Anthonissen

This paper is devoted to the symbolic calculation of the scattering coefficient in diffraction by a circular disk, by the use of *Mathematica*. Three diffraction problems are considered: scalar diffraction by an acoustically soft disk, scalar diffraction by an acoustically hard disk, and electromagnetic diffraction by a perfectly conducting disk. In the low-frequency approximation, the solutions of these problems are in the form of expansions in powers of ka, where a is the radius of the disk and k is the wave number. The emphasis is on the low-frequency expansion for the scattering coefficient, of which several terms are determined exactly with the help of *Mathematica*. **[Vol. 11, No. 1 (1996), pp 47-56, Special issue on Applied Mathematics: Meeting the challenges presented by computational electromagnetics]**

SCATTERING BY LARGE STRUCTURES WITH PERIODIC SURFACES: A PROTOTYPE PROBLEM

G.A. Kriegsmann

A hybrid method which uses both numerical and asymptotic techniques is described and applied to the scattering of an electromagnetic wave off a large corrugated circular cylinder. The radius of the cylinder is large compared to the wavelength of the incident radiation, but the corrugation height and period are of the same order as the wavelength. This problem is a prototype of a more general situation where the surface of a target is covered with a periodic coating. The method of attack essentially blends boundary layer theory, which describes the local scattering behavior of the surface, and the theory of geometrical optics which gives a global description of the scattering. Although the hybrid method is only developed here for this simple model, its applicability for other targets is clear. **[Vol. 11, No. 1 (1996), pp 57-62, Special issue on Applied Mathematics: Meeting the challenges presented by computational electromagnetics]**

MONO-STATIC RCS COMPUTATION WITH A BLOCK GMRES ITERATIVE SOLVER

William E. Boyse and Andrew A. Seidl

We present a new method of computing mono-static radar cross sections using a preconditioned Block GMRES iterative algorithm. The convergence properties of this algorithm are analyzed using RCS error, equation residual error and solution error. It is found that this method is nearly an order of magnitude faster than direct methods (LINPACK) for realistic method of moment problems. **[Vol. 11, No. 1 (1996), pp 63-69, Special issue on Applied Mathematics: Meeting the challenges presented by computational electromagnetics]**

MODERN KRYLOV SUBSPACE METHODS IN ELECTROMAGNETIC FIELD COMPUTATION USING THE FINITE INTEGRATION THEORY

Markus Clemens, Rolf Schuhmann, Ursula van Rienen and Thomas Weiland

A theoretical basis for numerical electromagnetics, the so-called Finite Integration Theory, is described. Based upon Maxwell's equations in their integral form, it results in a set of matrix equations, each of which is a discrete analogue of its original analytical equation. Applications of this discretization process are described here in the context of the numerical simulation of electroquasistatic problems and of time-harmonic field computations including a new type of waveguide boundary condition, which is presented here for the first time. In both fields the process of mathematical modelling and discretization yields large systems of complex linear equations which have to be solved numerically. For this task several modern Krylov subspace methods are presented such as BiCG, CGS and their more recent stabilized variants CGS2, BiCGSTAB(I) and TFQMR. They

are applied in connection with efficient preconditioning methods. The **applicability** of these modern methods is shown for a number of examples for both problem types. **[Vol. 11, No. 1 (1996), pp 70-84, Special issue on Applied Mathematics: Meeting the challenges presented by computational electromagnetics]**

CALCULATION OF ASSOCIATED LEGENDRE POLYNOMIALS WITH NON-INTEGER DEGREE

Keith D. Trott

The exact eigenfunction solution for the electromagnetic scattering from a perfectly conducting cone (or any other sectoral body of revolution with a tip) requires the solution in the form of spherical harmonics. The solution for the θ variation of these harmonics is the associated Legendre polynomial. The boundary conditions for the cone generate associated Legendre polynomials with non-integer degree found for a specific cone angle. This paper will discuss the derivation used to calculate the associated Legendre polynomial, the determination of the eigenvalues, the incomplete normalization integral, and a validation technique. **[Vol. 11, No. 1 (1996), pp 85-89, Special issue on Applied Mathematics: Meeting the challenges presented by computational electromagnetics]**

FINITE DIFFERENCE METHODS FOR THE NONLINEAR EQUATIONS OF PERTURBED GEOMETRICAL OPTICS

E. Fatemi, B. Engquist and S. Osher

Finite difference methods are developed to solve the nonlinear partial differential equations approximating solutions of the Helmholtz equation in high frequency regime. Numerical methods are developed for solving the geometrical optics approximation, the classical asymptotic expansion, and a new perturbed geometrical optics system. We propose a perturbed geometrical optics system to recover diffraction phenomena that are lost in geometrical optics approximations. We discuss techniques we have developed for recovering multivalued solutions and we present numerical examples computed with finite difference approximations of the above systems. **[Vol. 11, No. 1 (1996), pp 90-98, Special issue on Applied Mathematics: Meeting the challenges presented by computational electromagnetics]**

ANALYSIS OF THE FINITE ELEMENT RADIATION MODEL CODE FOR ANTENNA MODELING

Marcos C. Medina, Constantine A. Balanis, Jian Peng and Panayiotis A. Tirkc

The Finite Element Radiation Model (FERM) code is applied to examine radiation patterns and input impedance of various antenna configurations on complex helicopters. This paper addresses the strengths and weaknesses of the FERM code when applied in antenna analysis and is compared with other national codes, such as the Numerical Electromagnetics Code (NEC). In addition, guidelines are outlined for various applications of the code. **[Vol. 11, No. 2 (1996), pp 4-13]**

ACCURACY OF THE FINITE ELEMENT METHOD WITH SECOND ORDER ABSORBING BOUNDARY CONDITIONS FOR THE SOLUTION OF APERTURE RADIATION PROBLEMS

John Silvestro, Xingchao Yuan and Zoltan Cendes

The Finite Element Method with second order Absorbing Boundary Condition is a recently developed computational technique that finds use in antenna design and Electromagnetic Compatibility simulation. To determine the accuracy of this new procedure, the problem of aperture radiation was studied. The near zone and aperture fields of a waveguide antenna computed using the Finite Element Method are compared with published data and results found using other simulation techniques. These comparisons show that the new method is accurate even when the ABC boundary conforms to the problem geometry and is placed as near as $\lambda/2\pi$ to the aperture. **[Vol. 11, No. 2 (1996), pp 14-23]**

THE FEMAX FINITE-ELEMENT PACKAGE FOR COMPUTING THREE-DIMENSIONAL ELECTROMAGNETIC FIELDS

Gerrit Mur

The structure and the properties of the FEMAX package are discussed. The FEMAX finite-element package is an efficient and highly accurate package especially designed for computing three-dimensional transient as well as time-harmonic electromagnetic fields in arbitrarily inhomogeneous, (an)isotropic media. The most unique features of the FEMAX package are that 1) the electric field strength is computed directly, i.e. without the

intermediate use of (vector) potentials, 2) when inhomogeneities are encountered in the domain of computation, the package automatically chooses edge elements to ensure that all local continuity conditions can be met, nodal elements are used elsewhere, and 3) that the electromagnetic compatibility relations are taken into account in the formulation of the finite-element method used, thus avoiding spurious solutions. These features are included in the package in such a way that optimum results are obtained both in regard to computational efficiency (storage and time) and in regard to the desired accuracy. **[Vol. 11, No. 2 (1996), pp 24-31]**

A MOMENT METHOD FORMULATION FOR THE ANALYSIS OF WIRE ANTENNAS ATTACHED TO ARBITRARY CONDUCTING BODIES DEFINED BY PARAMETRIC SURFACES

F. Rivas, L. Valle and M.F. Catedra

A Moment Method (MM) technique for the analysis of wire antennas on board resonant-sized bodies modelled with parametric surfaces is presented. The approach may have useful applications for the study of the behaviour of wire antennas on board complex conducting structures like aircrafts. The current is represented by curved rooftop functions on the body, piecewise linear functions on the wires and a new junction function in the attachment region between the body and the antenna. The
bodies are precisely defined by means of a small number of NURBS surfaces (Non Uniform Rational B-Splines) and Bézier patches (BP). In addition the new junction function that can be defined over any BP allows the antenna to be attached to any part of the body. Radiation patterns and input impedance calculations for several geometries are presented to show the accuracy of the method. The results are successfully validated when comparisons with measurements or results from other methods are carried out. **[Vol. 11, No. 2 (1996), pp 32-39]**

A POSTERIORI ERROR ESTIMATES FOR TWO-DIMENSIONAL ELECTROMAGNETIC FIELD COMPUTATIONS: BOUNDARY ELEMENTS AND FINITE ELEMENTS

F.J.C. Meyer and D.B. Davidson

A brief summary of the variational boundary-value problem formulation of the 2D finite element/boundary element (FE/BE) method is presented. From this a posteriori error estimates and error indicators for the FE/BE method are developed and applied to electromagnetic scattering and radiation problems. The results obtained indicate that these error estimates and indicators can be obtained within negligible computational times and can be used successfully to obtain valuable a posteriori accuracy and convergence information regarding the reliability of the FE/BE method solutions. **[Vol. 11, No. 2 (1996), pp 40-54]**

MODELLING OF AN ARBITRARILY-ORIENTED MOBILE TELEPHONE HANDSET IN THE FINITE-DIFFERENCE TIME-DOMAIN FIELD COMPUTATION METHOD

P.S. Excell, P. Olley and N.N. Jackson

The implementation of a generic mobile telephone handset model in the Finite Difference Time Domain (FDTD) method for computation of electromagnetic field distributions is described. The handset can be rotated about the principal FDTD axes to achieve any orientation. The 'thin wire' technique is used to model the antenna in a way that ensures that its correct electrical length is maintained despite the 'staircasing' effect of the FDTD grid. Computed predictions from the model agree with near-field measurements on a physical realisation of the handset, and accurate near and far fields are calculated for arbitrary orientations of the handset. It is concluded that this wire rotation technique has broad application to problems involving components that are required to move in relation to fixed structures. **[Vol. 11, No. 2 (1996), pp 55-65]**

A MAGNETIC FIELD ITERATIVE TECHNIQUE FOR IMPROVING HIGH FREQUENCY PREDICTION METHODS

Daniel D. Reuster, Gary A. Thiele and Paul W. Eloe

A Magnetic Field Iterative Technique (MFIT) is developed as a technique for improving the results from high frequency based prediction methods. The technique combines the accuracy of low frequency methods with the speed of high frequency methods to develop a contraction mapping based, iterative solver, which is directly parallelizable on current massively parallel processing machines. In this paper, the MFIT is developed from a Magnetic Field Integral Equation (MFIE) and its contraction discussed. Results obtained mapping properties are using the technique and convergence properties are three dimensional perfect illustrations of the technique's presented for both two

and electrically conducting (PEC) targets. **[Vol. 11, No. 2 (1996), pp 66-71]**

MODELING OF REMOTE FIELD EDDY CURRENT TRANSIENT PHENOMENA

M. Raugi, N. Ida

An integral formulation is presented and used for the analysis of the Remote Field Eddy Current (RFEC) transient phenomena. The model presented allows simple and accurate modeling of RFEC systems in the presence of axisymmetric defects. The method has been validated first by comparison of the computed results with results obtained with an analytical model. Then the method was used to show that the Remote Field effect is mainly due to a direct induction effect rather than propagation effects. The Remote Field effect phenomena are usually analysed using a steady state domain. However, the results obtained here have shown that detection of defects is not due to a steady state phenomenon, but depends mainly on the transient signal. **[Vol. 11, No. 2 (1996), pp 72-75]**

SOLUTION OF LAPLACE'S EQUATION USING MULTIPLE PATHS METHOD (MPM) t

J. Rashed-Mohassel and M. Fasih

A probabilistic method called the multiple paths method (MPM) is presented to solve the potential equation. Unlike other probabilistic techniques there is no need for the generation of a grid resulting in less computation time and simplicity. The method is based on the calculation of the probability of absorption of a particle at a point on the boundary. The random walk is along a "path" which is a line passing through the starting point, where the potential is to be determined. The results show good agreement with other probabilistic methods and numerical techniques. **[Vol. 11, No. 3 (1996), pp 4-8]**

A NEW DESIGN METHOD FOR LOW SIDELOBE LEVEL LOG-PERIODIC DIPOLE ANTENNAS

James K. Breakall and Rafael A. Rodriguez Solis

A new design procedure for log-periodic dipole arrays is presented in this paper. In this method, either the scale factor or the number of dipole elements is selected, after the boom length, and the operating frequency region are specified. The procedure is applied iteratively, in conjunction to the Numerical Electromagnetic Code, to produce a design with low sidelobe levels. With this new procedure, the antenna designer has more control over the boom length; in older techniques, the boom length and the element spacing were dependent on previous calculations, which frequently resulted on unreasonable values

Results for several designs are presented, showing the peak gain to peak-sidelobe level ratio, and the antenna gain as a function of frequency, for different scale factors and boom lengths, for a frequency range of 13 to 30 MHz. **[Vol. 11, No. 3 (1996), pp 9-15]**

NUMERICAL EVALUATION OF SINGULAR INTEGRANDS IN THE APPLICATION OF THE CHARGE SIMULATION METHOD WITH DISTRIBUTED CHARGE DENSITY

Ermanno Cardelli and Loris Faina

As it is well known the Charge Simulation Method is a numerical method for the computation of the electric field in three-dimensional problems, based on the concept of the substitution of the electrodic geometry with a series of elementary charge suitably arranged. In this paper we will show a possible, useful way to overpass the difficulties arising in the numerical computations on the integral expression of the electric potential in the contour points where the boundary conditions are imposed, when distributed surface charges are used in the simulation. The numerical approach presented here allows us to evaluate with accuracy the potential coefficients on the metallic surfaces, avoiding the presence of oscillatory numerical solutions in the computation of the electric potential and of the electric field strength around the electrodes, that generally occurs when discrete charges are used in the simulation. **[Vol. 11, No. 3 (1996), pp 16-24]**

MEASURED RCS POLAR CONTOUR MAPS FOR CODE VALIDATION

C.L. Larose and C.W. Trueman

Measured radar cross-section (RCS) data as a function of the angle of incidence and of the frequency over a wide range provide an excellent basis for code validation. This paper examines the RCS of six targets measured as a function of the angle of incidence of the plane wave, and of the frequency, through and beyond the resonance range of target size. The RCS is presented as a function of frequency and incidence angle using a color contour map in a polar format, with the radius

proportional to the frequency. Such polar contour maps exhibit striking patterns to the underlying scattering mechanisms and target geometry. The RCS as a function of incidence angle and frequency is available from the authors for an extensive collection of targets. **[Vol. 11, No. 3 (1996), pp 25-43]**

AN EFFICIENT METHOD OF ANALYSIS OF CO-PLANAR DIPOLE ARRAY ANTENNAS

A. I. Imoro, N. Inagaki and N. Kikuma

Generalized impedance formulas for non-uniform array configurations based on the improved Circuit Theory (ICT) are presented for the first time in an English text. To further enhance the ICT as an accurate and fast method for evaluations, a new and more com pact closed-form formula is derived to replace a function requiring time intensive numerical integration during the implementation of the of the ICT algorithm in co-planar dipole array antenna evaluations. The resulting ICT computational scheme reduces the required CPU time by a factor of two and has the same order of accuracy as the conventional MoM. The new ICT implementation would be of considerable use as a Computer Aided Design (CAD) tool of co-planar dipole array antennas. **[Vol. 11, No. 3 (1996), pp 44-54]**

AN ALGORITHM FOR SOLUTION OF THE INVERSE ELECTROMAGNETIC LIQUID METAL CONFINEMENT PROBLEM

G.J. Bendzsak

The design of an electromagnetic levitation system for large amounts of liquid metal requires the solution of an inverse field problem. The objective is to calculate the electromagnetic pressure distribution which corresponds to a specific metallo-static head. This paper describes an algorithm for the design of coil systems which will produce the desired pressure distribution. The technique is illustrated by the design of a torroidal levitation system. **[Vol. 11, No. 3 (1996), pp 55-62]**

COMPARISON OF MAGNETICALLY INDUCED ELF FIELDS IN HUMANS COMPUTED BY FDTD AND SCALAR POTENTIAL FD CODES

Trevor W. Dawson, Jan De Moerloose and Maria A. Stuchly

This paper presents a detailed numerical comparison of the magnetically-induced extremely low-frequency - electric field and current density within an anatomically realistic model of the full human body, as computed using two different numerical techniques.

The first technique is a recently-described full-wave quasi-static finite-difference time-domain (FDTD) method. The use of a time-ramped excitation involving pairs of oppositely-directed plane waves allows for the calculation of decoupled magnetic and electric induction in complex heterogeneous bodies, in relatively short (5 ns) simulation times.

The second method is an implementation of Stevenson's method applied for isolated conducting bodies. With the lowest-order external magnetic field represented by a vector potential, the lowest-order internal electric field can be represented by a scalar conduction potential, and the magnetically-induced contribution can be calculated in isolation.

Both methods have an underlying similarity in their finite-difference approach, but are nevertheless very distinct. Each code was used to calculate the fields, induced by three orthogonal uniform magnetic fields, in a 7.2 mm-resolution human full-body model. Three-dimensional correlation coefficients of better than 99.9998% were observed between current densities computed by the two methods. Individual edge electric fields typically agree to 3 significant digits. **[Vol. 11, No. 3 (1996), pp 63-71]**

ANALYTIC VALIDATION OF A THREE-DIMENSIONAL SOLAR-POTENTIAL FINITE-DIFFERENCE CODE FOR LOW-FREQUENCY MAGNETIC INDUCTION

Trevor W. Dawson and Maria A. Stuchly

This paper presents a detailed comparison of numerical and analytical calculations of the low-frequency electric and current density fields, induced by an applied uniform axial magnetic field, in an equatorially stratified sphere having the conductivity distribution $\sigma(\phi)=\sigma_0 e^{-\lambda \cos(\varphi_-)}$ with $p \in \{1,2\}$ and $\gamma > 0$. As shown by the analytic solution, the resulting induced fields are fully three-dimensional, and the model therefore serves as a rigorous test of numerical codes

The numerical method is a scalar-potential finite-difference scheme based on Stevenson's method for isolated conducting bodies. This computer code was recently shown to provide excellent agreement with

results computed independently by a modified Finite-Difference Time-Domain method. Nevertheless, both codes share some underlying similarities, such as their common use of parallelepiped material voxels to represent the conductivity distribution, and of an edge-based staggered to model the electric fields. Therefore, it is of value to compare the numerical results with analytic ones

The analytic model has a freely adjustable contrast parameter, and supports both π and 2π-periodic conductivity distributions. Numerical and analytical results are compared for several configurations. Full three-dimensional volumetric correlation coefficients are typically of the order of 99% or better. As might be expected, the main differences occur at the surface of the sphere, where the true circumferential fields are most poorly approximated by the staircasing approximation inherent the numerical approximation. **[Vol. 11, No. 3 (1996), pp 72-81]**

THE GRADIENT ASSOCIATED CONJUGATE DIRECTION METHOD

Min Zhang

A new conjugate direction (CD) based method, GaCD by name, is addressed with its full derivations. Comparison with some commonly used CD methods is made, concluding that the GaCD method is among the best of them, in terms of an assessment number. A practical example is presented in which a waveguide-microstrip transition section is optimized with respect to its transmission parameter S21. The measurement of the transition agrees very well with the numerical results. **[Vol. 11, No. 3 (1996), pp 82-96]**

VIEWS OF THE 13TH ANNUAL REVIEW
at
THE ANNUAL AWARDS BANQUET

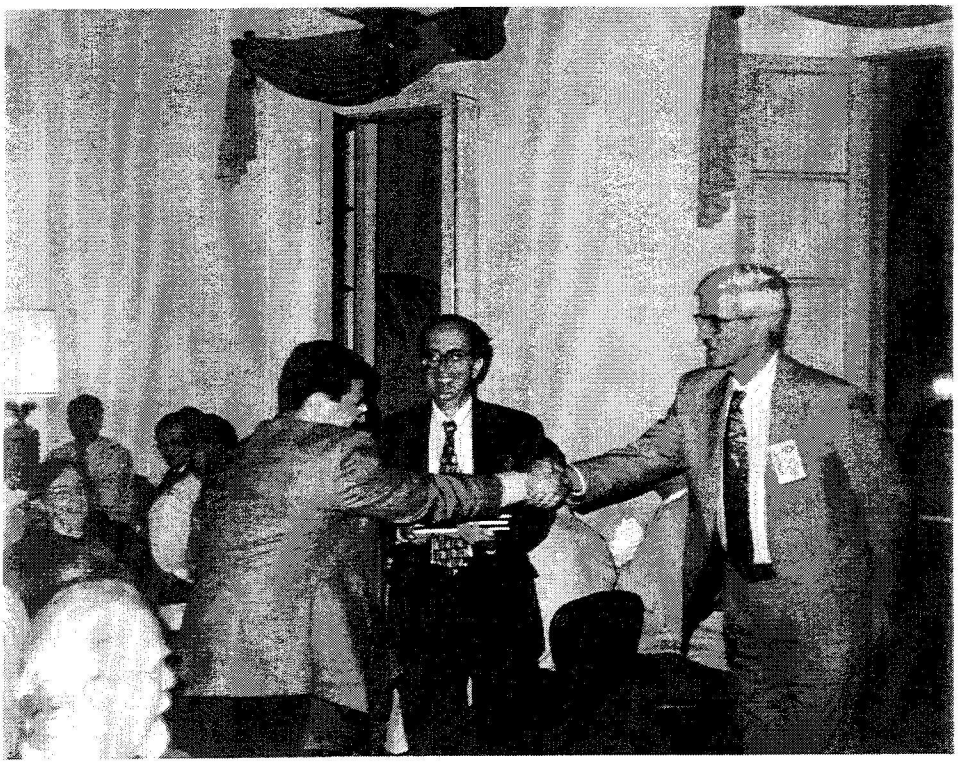

Atef Elsherbeni, U of Mississippi, accepting the "Valued Service Award" for Richard Gordon, U of Mississippi, from John Brauer and Hal Sabbagh

Andrew Efanov, Motorola, IL, and others

VIEWS OF THE 13TH ANNUAL REVIEW
at
THE ANNUAL AWARDS BANQUET

Ross Speciale, Research & Development, CA., and Bob Bevensee, Boma Enterprises, CA.

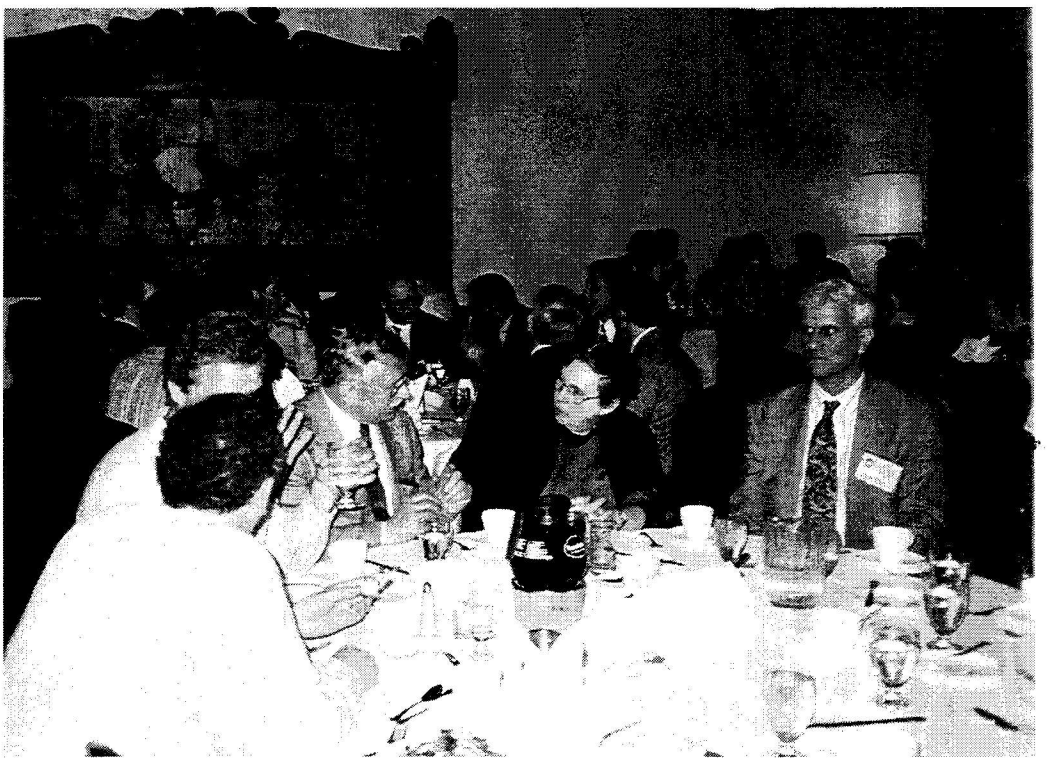

Stan Kubina, U of Concordia, Canada, Past President, Pat Foster, MAS, UK, ACES Vice President and Hal Sabbagh, ACES President, Sabbagh Associates, IN, and others

VIEWS OF THE 13TH ANNUAL REVIEW
at
THE ANNUAL AWARDS BANQUET

Manuel Catedra, U of Cantabria, Spain, Atef Elsherbeni, U of Miss., Brian Zook, SW Research, TX., and others

John Shaeffer, Marietta Scientific, GA., Malcolm Packer, Harris Corp. NY., and others

VIEWS OF THE 13TH ANNUAL REVIEW
at
THE ANNUAL AWARDS BANQUET

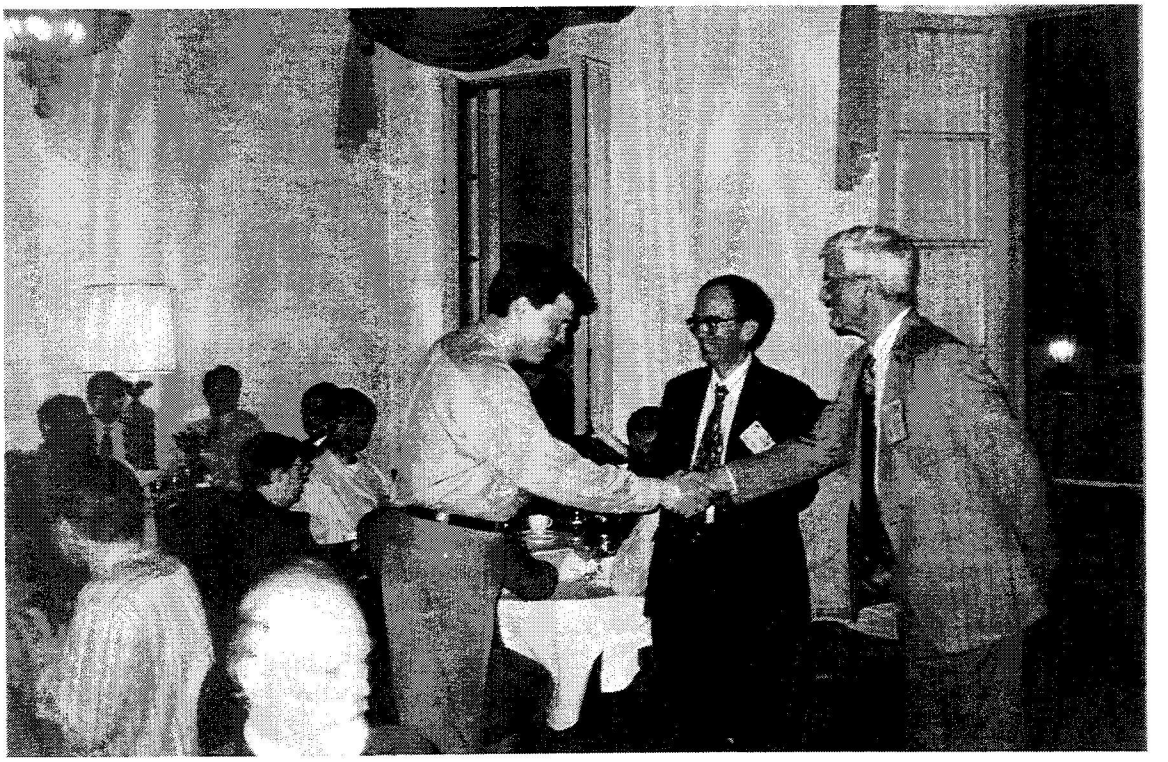

Keith Whites, Univ of Ky, accepting " Mainstay Award".

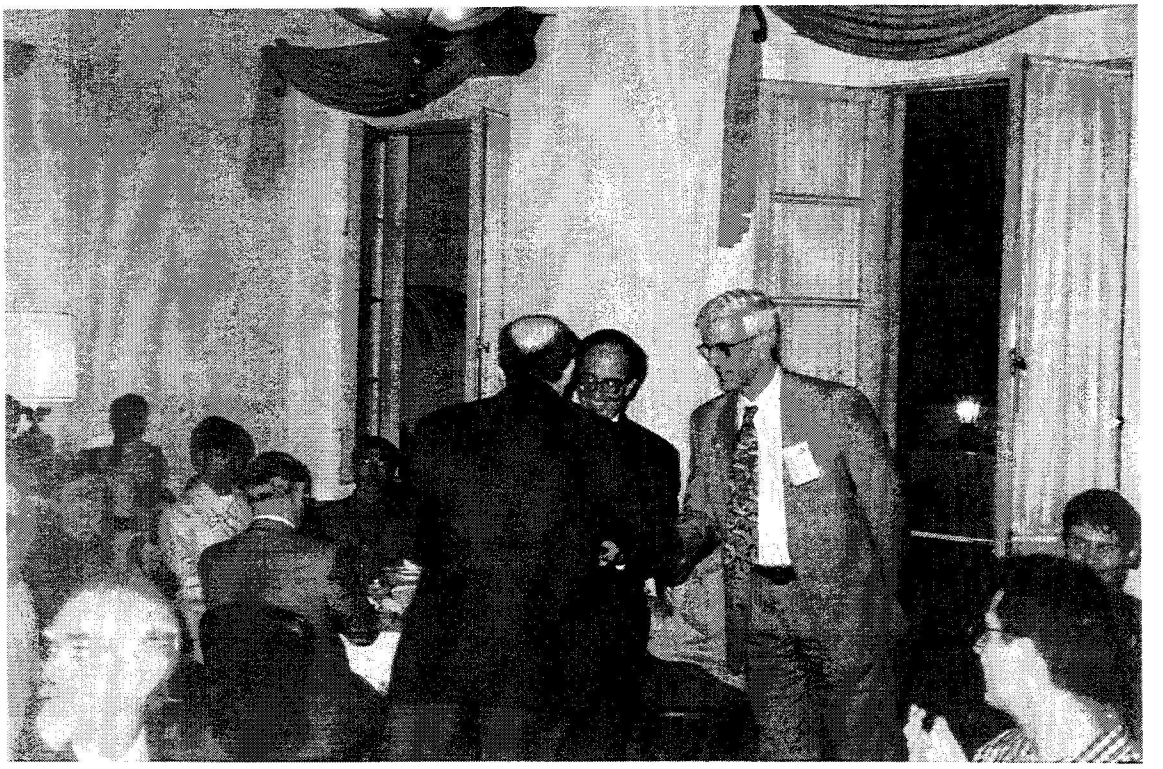

Manuel Catedra accepting the "Exemplary Service Award" for Joao Pedro Bastos, U. Santa Catarina, Brazil

THE APPLIED COMPUTATIONAL ELECTROMAGNETIC SOCIETY

CALL FOR PAPERS

The 14th Annual Review of Progress

in Applied Computational Electromagnetics

March 16-20, 1998

Naval Postgraduate School, Monterey, California

"Share Your Knowledge and Expertise with Your Colleagues"

The Annual ACES Symposium is an ideal opportunity to participate in a large gathering of EM analysis enthusiasts. The purpose of the Symposium is to bring analysts together to share information and experience about the practical application of EM analysis using computational methods. The symposium offerings include technical presentations, demonstrations, vendor booths and short courses. All aspects of electromagnetic computational analysis are represented. Contact Jianming Jin for details.

Technical Program Chairman
Jianming Jin
ECE Department
University of Illinois
1406 W. Green Street
Urbana, IL 61801-2991
Phone: (217) 244-0756
Fax: (217) 333-5962
Email:j-jin1@uiuc.edu

Symposium Administrator
Richard W. Adler
ECE Dept/Code EC/AB
Naval Postgraduate School
833 Dyer Road, Room 437
Monterey, CA 93943-5121
Phone: (408) 646-1111
Fax: (408) 649-0300
Email:rwa@ibm.net

Symposium Co-Chairman
Michael A. Jensen
ECE Dept., 459 CB
Brigham Young University
Provo, UT 84602
Phone: (801) 378-5736
Fax: (801) 378-6586
Email:jensen@ee.byu.edu

Symposium Co-Chairman
Randy L. Haupt
EE Dept., 260
University of Nevada
Reno, NV 89557-0153
Phone: 702-784-6927
Fax: 702-784-6627
Email:haupt@ee.unr.edu

The ACES Symposium is a highly influential outlet for promoting awareness of recent technical contributions to the advancement of computational electromagnetics. Attendance and professional program paper participation from non-ACES members and from outside North America are encouraged and welcome.

Early Registration Fees; (approximate*)	**ACES MEMBERS**	**$255**
	NON-MEMBER	**$295**
	STUDENT/RETIRED/UMEMPLOYED	**$115 (no proceedings)**
	STUDENT/RETIRED/UNEMPLOYED	**$150 (includes proceedings)**

*The exact fee will be announced later. Each conference registration is entitled to publish two papers in the proceedings free of charge. Excess pages over a paper limit of 8 will be charged $15/page.

1998 ACES Symposium
Sponsored by: ACES, NPS, DOE/LLNL, U of KY, U of IL, BYU, DOD, SIAM, NCCOSC and AMTA
in cooperation with: The IEEE Antennas and Propagation Society, the IEEE Electromagnetic Compatibility Society and USNC/URSI

THE APPLIED COMPUTATIONAL ELECTROMAGNETIC SOCIETY

CALL FOR PAPERS

The 14th Annual Review of Progress in Applied Computational Electromagnetics

Papers may address general issues in applied computational electromagnetics, or may focus on specific applications, techniques, codes, or computational issues of potential interest to the Applied Computational Electromagnetics Society membership. Area and topics include:

- Code validation
- Code performance analysis
- Computational studies of basic physics
- Examples of practical code application
- New codes, algorithms, code enhancements, and code fixes
- Computer Hardware Issues
- Partial list of applications:

antennas	wave propagation
radar imaging	radar cross section
shielding	bioelectromagnetics
EMP, EMI/EMC	visualization
dielectric & magnetic materials	inverse scattering
microwave components	MIMIC technology
fiberoptics	remote sensing & geophysics
communications systems	propagation through plasmas
eddy currents	non-destructive evaluation

- Partial list of techniques:

frequency-domain & time-domain techniques	
integral equation & differential equation techniques	
finite difference & finite element analysis	
diffraction theories	physical optics
modal expansions	perturbation methods
hybrid methods	moment methods

+ + + NEW + + + INSTRUCTIONS FOR AUTHORS AND TIMETABLE + + + NEW + + +

November 25, 1997: Submission deadline. Submit four copies of a full-length, camera-ready paper to the Technical Program Chairman. Please supply the following data for the corresponding author: name, address, email address, FAX, and phone numbers. See below for instructions for the format of paper.

December 20, 1997: Authors notified of acceptance.

PAPER FORMATTING REQUIREMENTS

The recommended paper length is 6 pages, with 8 pages as a maximum, including figures. The paper should be camera-ready (good resolution, clearly readable when reduced to the final print of 6 x 9 inch paper). The paper should be printed on 8-1/2 x 11 inch papers with 13/16 side margins, 1-1/16 inch top margin, and 1 inch on the bottom. On the first page, place title 1-1/2 inches from top with author and affiliation beneath the title. Single spaced type using 10 or 12 point front size, entire text should be justified (flush left and flush right). No typed page numbers, but number your pages lightly in pencil on the back of each page.

SHORT COURSES

Short courses will be offered in conjunction with the Symposium covering numerical techniques, computational methods, surveys of EM analysis and code usage instruction. It is anticipated that short courses will be conducted principally on Monday March 16 and Friday March 20. Fee for a short course is expected to be approximately $90 per person for a half-day course and $140 for a full-day course, if booked before March 3, 1998. Full details of 1998 Symposium will be available by November 1997. Short Course Attendance is not covered by the Symposium Registration Fee!

EXHIBITS

Vendor booths and demonstrations will feature commercial products, computer hardware and software demonstrations, and small company capabilities.

WINNERS OF THE BEST STUDENT PAPER AWARD

A paper by Eric A. Jones and William T. Joines, Department of Electrical and Computer Engineering at Duke University, "Improved Computational Efficiency by Using Sub-regions in FDTD Simulations" won the Best Student Paper Award at the 13th Annual Review of Progress in Applied Computational Electromagnetics, at the Naval Postgraduate School, in Monterey, CA.

Prizes consisted of (1) free Annual Review Attendance for 1988; One free short course during the 1997 Annual Review and a $200 check.

Since the winning paper was announced after the 13th Review ended, we wish to thank Eric and William at this time for submitting a high quality Paper to our 13th Review, and congratulate them for winning this award.

"ADVANCED MODELING IN APPLIED COMPUTATIONAL ELECTROMAGNETICS"

THE PENN STATE/ACES SHORT COURSES/HANDS-ON WORKSHOPS AT

THE PENN STATE UNIVERSITY CONFERENCE CENTER,

STATE COLLEGE, PA

22-24 SEPTEMBER 1997

OFFERINGS: Three days of short courses and hands-on-workshops which treat modeling in the frequency domain (Method of Moments - MOM), time domain (Finite Difference Time Domain - FDTD), Transmission Line Modeling - TLM, applications of MATHCAD and MATLAB in the frequency and time domains, representation of fields and geometries for modeling, wavelets, and modeling of propagation and interference in communication systems.

TYPICAL TOPICS:

What's New In NEC-MoM? - A hands-on workshop with coverage from the origins of NEC to NEC-4, NEC-WIN-PRO, GNEC and beyond - (Two-day workshop)

Advanced Topics in FDTD - (Three-day short course)

Applied CEM using MATHCAD, MATLAB, and FORTRAN 90 (Three-day hands-on workshop)

The TLM Method and its Applications - (Two-day short course)

Practical Genetic Algorithms - (One-day short course)

Isoparametric, Curvilinear Modelling for CEM - (Three day: Two-day short course, with one-day hands-on workshop)

SELECTED TOPICS IN CEM

- Using Model Based Parameter Estimation to Improve the Efficiency and Effectiveness of Computational Electromagnetics - (Half-day short course)
- Verification and Validation of Computational Software - (Half-day short course)
- A Survey of the Foundation and Applications of the Various Kinds of CEM Models - (Half-day short-course)
- An Exploration of Radiation Physics - (Half-day short course)

A Complete Theory of Antennas as Transmitters, Receivers, and Scatterers - (Two-day short course)

Modeling Interference in Wireless Communications - (Three-day short course)

Using GEMACS for the Analysis of Electromagnetic Systems - (Three-day: two-day short course, with one-day hands-on workshop)

Efficient Ray-Tracing Techniques for Mobile Communications - (One-day short course)

Fast Solvers of Maxwell's Integral Equations - (Two-day short course)

Wavelets: Theory, Algorithms and Applications - (One-day short course)

CALL 1-800-PSU-TODAY for more information or contact Richard W. Adler, ACES Executive Officer, 833 Dyer Road/Room 437, Code EC/AB Naval Postgraduate School, Monterey, CA 93943-5121, USA. Telephone: 408-656-2352; Fax: 408-649-0300; E-mail: rwa@ibm.net

TEAM WORKSHOP IN RIO DE JANEIRO

The global TEAM (Testing Electromagnetic Analysis Methods) workshop in the sixth round of workshops will take place immediately following Compumag Rio. Information about schedule and location of the workshop will be communicated to those who respond to this mailing as well as with the final Compumag program. This will also be available at http:/www.cpdee.ufmg.br/compumag97/team.html.

The first TEAM workshop in the 6th round of TEAM workshops was held immediately after the CEFC conference in Okayama, Japan, on March 20-21, 1996. The second TEAM workshop was held in Graz, on September 26, 1996, following the IGTE Symposium. The third workshop was held in Wuhan, following the ICEF Conference, on October 17, 1996.

The currently active problems are:

Problem 13: 3-D Nonlinear Magnetostatic Model
Problem 15: Rectangular slot in a thick plate: A problem in Non-destructive Testing
Problem 17: The Jumping Ring Experiment
Problem 18: Canonical Problems: Waveguide Loaded Cavity
Problem 19: Microwave field in a loaded cavity resonator
Problem 20: 3-D Static Force Model
Problem 21: An Engineering Oriented Loss Model
Problem 22: Optimization of Superconducting Magnetic Energy Storage (SMES) Arrangement
Problem 23: Force Calculations in Permanent Magnets
Problem 24: Nonlinear Time-Transient Rotating Test Rig
Problem 25: Optimization of Die Press Model

Although these problems are considered active, all other problems published by the workshop may be presented.

Problem definitions and additional information may be obtained from the following sources:

1. ida@uakron.edu - hard copies of all problems, information about past workshops, information on the Rio workshop, etc.
2. http://www-igte.tu-graz.ac.at/team - information on problem 22.
3. http://ics.ascn3.uakron.edu/compumag.html - Information on TEAM workshops and downloadable problem 23.

An effort is underway to hall all current and completed TEAM problems on the web. At the present time only problems 22 and 23 are available on the web.

Dr. Nathan Ida
Department of Electrical Engineering
The University of Akron
Akron, OH. 44325-3904
Tel: 300-972-6525
Fax: 330-972-6487
email: nida@uakron.edu

Renato Cardosa Mesquita
Departamento de Engenharia Eletrica
Universidade Federal de Minas Gerais-Brasil
Av. Antonio Carlos 6627, Caixa Postal 209
30161-970, Belo Horizonte, MG
http://www.cpdee.ufmg.br/-renato
renato@cpdee.ufmg.br / r.mesquita@ieee,org
Fax: 55 31 499-4810
Fone: 55 31 499-4838
telnet://moo.cpdee.ufmg.br:7777

ADVERTISING RATES

	FEE	PRINTED SIZE
Full page	$200.	7.5" x 10.0"
1/2 page	$100.	7.5" x 4.7" or 3.5" x 10.0"
1/4 page	$ 50	3.5" x 4.7"

All ads must be camera ready copy.

Ad deadlines are same as Newsletter copy deadlines.

Place ads with Ray Perez, Newsletter Editor, Martin Marietta Astronautics, MS 58700, PO Box 179, Denver, CO 80201, USA. The editor reserves the right to reject ads.

DEADLINE FOR THE SUBMISSION OF ARTICLES

Issue	Copy Deadline
March	January 13
July	May 25
November	September 25

For further information on the ***ACES JOURNAL,*** contact Prof. Duncan Baker.

For the ***ACES NEWSLETTER*** send copy to Ray Perez in the following formats:

1. A hardcopy.
2. Camera ready hardcopy of any figures.
3. If possible also send text on a floppy disk. We can read any version of MICROSOFT-WORD and ASCII files on both IBM and Macintosh disks. On IBM disks we can also read WORDPERFECT, WORDSTAR , and LATEX files. If any software other than MICROSOFT WORD has been used on Macintosh Disks, contact the Managing Editor, Richard W. Adler **before** submitting a diskette. If it is not possible to send a Macintosh disk then the hardcopy should be in Courier font **only,** for scanning purposes.

ACES MEMBERSHIP - NEWSLETTER & JOURNAL SUBSCRIPTION FORM

please print

LAST NAME _____ FIRST NAME _____ MIDDLE INITIAL _____

COMPANY/ORGANIZATION/UNIVERSITY _____ DEPARTMENT/MAIL STATION _____

PLEASE LIST THE ADDRESS YOU WANT USED FOR PUBLICATIONS

MAILING ADDRESS _____

CITY _____ PROVINCE/STATE _____ COUNTRY _____ ZIP/POSTAL CODE _____

TELEPHONE _____ FAX _____ AMATEUR RADIO CALL SIGN _____

E-MAIL ADDRESS _____ E-MAIL ADDRESS CAN BE INCLUDED IN ACES DATABASE ☐ YES ☐ NO

PERMISSION IS GRANTED TO HAVE MY NAME PLACED ON MAILING LISTS WHICH MAY BE SOLD ☐ YES ☐ NO

CURRENT SUBSCRIPTION PRICES

AREA	INDIVIDUAL SURFACE MAIL	INDIVIDUAL AIRMAIL	ORGANIZATIONAL (AIRMAIL ONLY)
U.S. & CANADA	( ) $ 65	( ) $ 65	( ) $115
MEXICO, CENTRAL & SOUTH AMERICA	( ) $ 68	( ) $ 70	( ) $115
EUROPE, FORMER USSR TURKEY, SCANDINAVIA	( ) $ 68	( ) $ 78	( ) $115
ASIA, AFRICA, MIDDLE EAST & PACIFIC RIM	( ) $ 68	( ) $ 85	( ) $115

FULL-TIME STUDENT/RETIRED/UNEMPLOYED RATE IS $25 FOR ALL COUNTRIES

CREDIT CARD USERS

IF YOU ARE PAYING BY CREDIT CARD & CARD *IS* YOUR OWN, YOU MUST, (1) PRINT AND SIGN YOUR NAME BELOW; (2) MAKE SURE YOUR COMPLETE ADDRESS IS LISTED ABOVE. * IF THE CARD YOU ARE USING IS *NOT* YOUR CARD, THE CARD HOLDER MUST, (3) PRINT AND SIGN HIS/HER NAME AND, (4) ENTER HIS/HER COMPLETE ADDRESS BELOW.

PRINT FIRST AND LAST NAME OF CARD HOLDER _____ SIGNATURE OF CARD HOLDER _____

MAILING ADDRESS _____

MAILING ADDRESS (cont) _____

METHOD OF PAYMENT

- ☐ A bank check for the total amount is enclosed.(1)
- ☐ Traveler's checks for the total amount are enclosed.(2)
- ☐ International Money Order is enclosed.(3)
- ☐ Charge to: ☐ MasterCard ☐ Visa. ☐ Discover ☐ Amex.(4)

Card No. | | | | | | | | | | | | | | | | |

Card Exp. Date: Mo. _____ **Year** _____

MAKE CHECKS PAYABLE TO "ACES" and send to: RICHARD W. ADLER, EXEC. OFFICER, NAVAL POSTGRADUATE SCHOOL, ECE DEPT., CODE EC/AB, 833 DYER ROAD, ROOM 437, MONTEREY, CA 93943-5121

Visit us on line at: www.emclab.umr.edu/aces

Non-USA participants: Prices are in U.S. dollars. All currencies must be converted to U.S. dollars, payable by banks with U.S. affiliates. (1) **Bank Checks**, (2) **Traveler's Checks** (in U.S. $$); **(3) International Money Order** drawn in U.S. funds, payable in U.S.; (4) **Credit Cards:** Visa, Master Card, Discover Card, and Amex.

Total Remittance (U.S. Dollars Only) $_____